

**INSTALLATION OF A ND:YAG LASER
FACILITY AND INITIAL SINGLE
PULSE LASER DRILLING OF
SOME ADVANCED
MATERIALS**

By

JOHNNIE LEE HIXSON

Bachelor of Science

Oklahoma State University


Stillwater, Oklahoma

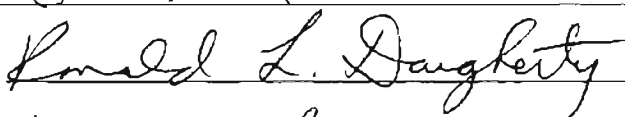
1992

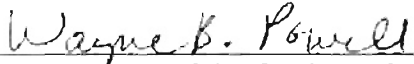
Submitted to the Faculty of the Graduate College of the
Oklahoma State University
in partial fulfillment of
the requirements for
the Degree of
MASTER OF SCIENCE
DECEMBER, 1998

**INSTALLATION OF A ND:YAG LASER
FACILITY AND INITIAL SINGLE
PULSE LASER DRILLING OF
SOME ADVANCED
MATERIALS**

Thesis Approved



B. E. Davis Thesis Advisor




Dean of the Graduate College

ACKNOWLEDGEMENTS

First and foremost I want to thank my professor Dr. Ranga Komanduri for his guidance, input, and patience and for allowing me to explore and conduct research in many diverse areas of advanced materials and manufacturing processes. I would also like to thank Professors C. E. Price and R. Dougherty for agreeing to serve in my thesis committee. Sincere thanks are due to my colleagues, Rob Stewart, Dave Stokes, Malika Kamarjugadda, Rajesh Iyer, Sujatha Iyengar, and Professor. Hou, who interacted with me and made my experience at the Mechanical and Aerospace Engineering Research Labs (MAERL) all the more rich. I also want to thank Mr. Ameeth Palla and Mr. Beera Veera Ravinder for assistance with the experimental work and Mr. Jerry Dale, Lab Manager at MAERL for his assistance and support in the operational support.

SUMMARY

In this investigation, a Nd:YAG laser (maximum nominal pulse energy: 90 joules per pulse @ 4.00 ms pulse width) (maximum power: 400 watts nominal) was used to study the interaction of the laser on various advanced cutting tool materials during drilling. This project began with the acquisition and installation of the Controls Laser's Nd:YAG laser at the Mechanical Aerospace Engineering Research Laboratory of the Oklahoma State University. This was followed by the alignment of the optical path of the laser beam. Peripheral safety equipment was acquired and installed. A 3-axis CNC motion control system was integrated with the laser system to provide motion control and firing of the laser from a more modern, p.c. based system. A review of literature was conducted in the general area of lasers and laser materials processing with the focus on Nd:YAG laser in particular. It was found that much of the research has been conducted with the CO₂ laser and a comparatively limited amount with Nd:YAG laser. Calibration studies were performed to characterize the operating characteristics of the laser using a laser power probe before conducting experiments since, upon review of the literature and reference material, it was noted that factors such as usage and alignment can affect the performance. Subsequently, initial single pulse laser drilling experiments were conducted at four voltage levels (700 V, 1050V, 1350 V and 1700V) and three pulse durations (0.65 ms, 1.50 ms, and 4.00 ms) on a range of advanced tool materials (Al₂O₃, Al₂O₃-TiC, SiC whisker reinforced Al₂O₃-ZrO₂, Si₃N₄, SiAlON, TiC-TiN cermet with Ni-Mo binder, WC-6%Co, WC-6%Co +TiN coating, and polycrystalline cubic boron nitride) which covers the whole spectrum of advanced tool materials. The primary purpose of the single pulse laser drilling tests is to obtain experimental data of the cross sections of the material removed from various tool materials by the laser beam to correlate with the analytical thermal modeling currently underway at O.S.U. by Hou and Komanduri. The cross sections of the holes drilled were examined using an optical microscope with a sample holder with micrometer adjustments to obtain dimensional data and a scanning electron microscope to obtain micrographs.

TABLE OF CONTENTS

Chapter	Page
INSTALLATION OF A ND:YAG LASER FACILITY AND INITIAL SINGLE PULSE LASER DRILLING OF SOME ADVANCED MATERIALS	i
ACKNOWLEDGEMENTS.....	ii
SUMMARY	iii
TABLE OF CONTENTS	iv
LIST OF TABLES	vi
LIST OF FIGURES.....	vii
CHAPTER I INTRODUCTION	1
Brief history of lasers	2
Requirements of a Laser System for use in Laser Beam Machining.....	5
Description of one of the major laser technologies: The Nd:YAG laser.....	8
Nd:YAG Lasers.....	16
Nd:YAG Laser Optics	17
Nd:YAG Laser in Machining	18
Advanced Materials Suitable for Laser Machining	18
CHAPTER II BASICS OF LASERS	20
Laser Parameters	20
Properties of the laser light.....	20
Lens Focal Length and Position	22
Beam Characteristics	22
Laser Power and Pulsing	27
Parameters of lasers and laser beam machining	28
CHAPTER 3 LITERATURE REVIEW.....	35
Introduction	35
Experimental Studies.....	36
Theoretical Work on Laser Drilling and Cutting.....	54
Modeling as heat source on surface.....	54
Modeling from Fundamentals:	61
In situ Measurements during Laser Processing	62
CHAPTER 4 PROBLEM STATEMENT	68
CHAPTER 5 DESCRIPTION OF THE ND: YAG LASER SYSTEM AND OPERATING PROCEDURE.....	70
I. Elements of the Laser System.....	74
II. System Preparation	82
III. System Operating Instructions.....	82
IV. Shut Down Instructions	84
CHAPTER 6 ALIGNMENT OF THE ND:YAG LASER OPTICAL SYSTEM.....	87
CHAPTER 7 METHODOLOGY	91
Test Procedure.....	91
Sample preparation.....	91
Laser characteristics	91
Determination of the power output at the test conditions	92
Laser drilling	92
Optical Stereo Scope Observations	93
SEM observations.....	93
Experimental Conditions	94
CHAPTER 8 OPERATING CHARACTERISTICS OF THE CONTROL LASER (480-16 ND:YAG LASER).....	96
CHAPTER 9 EXPERIMENTAL RESULTS AND DISCUSSION	99
Results and Discussion	100

1. Cemented Tungsten Carbide - 6% Co	100
2. Cemented Tungsten Carbide - 6% Co with a 5 μ m Titanium Nitride (TiN) Coating.....	104
3. Silicon Nitride Ceramic	108
4. SiAlON Ceramic	112
5. Alumina Ceramic.....	115
6. Alumina plus TiC Ceramic.....	119
7. Silicon Carbide Whisker Reinforced Alumina-Zirconia Ceramic	122
8. TiC plus TiN Cermet	126
9. Polycrystalline Cubic Boron Nitride (c-BN)	129
CHAPTER 10 CONCLUSIONS	132
CHAPTER 11 FUTURE RECOMMENDATIONS ..	135
REFERENCES	136
APPENDIX A LASER SAFETY	150
1. Introduction	150
2. Safety Limits	151
3. Laser Classification	153
4. Class 4 Laser Safety Precautions.....	154
5. Potential Risks Even in a Properly Set Up Facility	155
6. Electrical Hazards.....	156
7. Fume Hazards	156
8. Conclusions	157
References	157
APPENDIX B Raw Data	159

LIST OF TABLES

Table	Page
Table 1 Operational comparison of the three types of industrial lasers (Whitehouse, 1992)	6
Table 2 Laser drilling characteristics for NiAl.	40
Table 3 Laser drilling characteristics for M5.....	40
Table 4 Drilling characteristics for SiC CMC.	41
Table 5 Specifications for the Nd:YAG Laser System (Model 480-16).....	86
Table 6 Operating characteristics. HY-2 Head for Digital Power Probe (100-1100 watt range)	96
Table 7 Operational characteristics using HY-1 power probe.....	97
Table 8 Operational characteristics at constant pulse rate. HY-2 Head for Digital Power Probe.....	97
Table 9 Operational characteristics at constant repetition rate using lower range probe HY-1 Head	98
Table 10 Tool Materials, Their grades and Specific Manufacturer	100
Table 11 Dimensional data for WC-Co6%.....	160
Table 12 Dimensional data for WC-Co 6% + TiN coating	161
Table 13 Dimensional data for alumina.....	162
Table 14 Dimensional data for alumina + TiC	163
Table 15 Dimensional data for SiC whisker reinforced, zirconia toughened alumina.....	164
Table 16 Dimensional data for silicon nitride	165
Table 17 Dimensional data for SiAlON	166
Table 18 Dimensional data for TiC/ TiN cermet.....	167
Table 19 Dimensional data for polycrystalline cubic boron nitride.....	168

LIST OF FIGURES

Figure	Page
Figure 1 Applications of various types of lasers. (Steen, 1991)	3
Figure 2 Range of wavelengths for current commercial laser	4
Figure 3 Operational ranges of commercial solid state lasers.(Steen, 1991)	7
Figure 4 Energy levels for Neodymium	9
Figure 5 Laser reflective cavity design for flash rod pumped lasers	10
Figure 6 Elliptical cavity reflection pattern	11
Figure 7 Slab laser operating principal.....	13
Figure 8 Slab laser design (Manes, 1990)	14
Figure 9 General construction of an Nd:YAG laser (Steen, 1992).....	17
Figure 10 Beam divergence.....	21
Figure 11 Depth of field vs. power density.....	24
Figure 12 Beam diameter vs. focal length.....	25
Figure 13 Power density vs. focal length.....	27
Figure 14 Typical laser output from Nd:YAG.....	31
Figure 15 Diagram of laser drilling.....	53
Figure 16 Spatial intensity distribution for TEM ₀₀ laser beam.....	53
Figure 17 Power supply enclosure.....	71
Figure 18 View of power supply enclosure, laser enclosure, and CNC station housing.....	72
Figure 19 Curves of nominal performance characteristics of Control Laser Corp. Nd:YAG laser.....	73
Figure 20 Laser system components.....	80
Figure 21 Cooling system.....	81
Figure 23 WC-Co 6% Cross-sections of holes drilled at 0.65, 1.50, and 4.00 ms pulse width.....	102
Figure 24 WC- Co 6% HAZ for increasing pulse width	103
Figure 26 WC- Co 6 wt % TiN coating. Cross sections of the holes drilled at 0.65 ms, 1.5 ms, and 4 ms pulse durations.....	106
Figure 27 WC- Co6% w/ TiN coating. Cross sections of the holes drilled at: a. 0.65 ms (1 J), b. 1.5 ms (32 J), c. 4 ms (66 J) pulse durations	107
Figure 28 Variation of the hole diameter and hole depth with pulse energy for three pulse durations, namely, shortest (0.65 ms),medium (1.5 ms), and longest (4.0 ms) silicon nitride	109
Figure 29 Cross sections of the holes drilled at 0.65 ms, 1.5 ms, and 4 ms pulse durations, respectively on silicon nitride material	110
Figure 30 Silicon nitride material. Close-up view.....	111
Figure 31 Variation of the hole diameter and hole depth with pulse energy for three pulse durations, namely, shortest (0.65 ms),medium (1.5 ms), and longest (4.0 ms) for SiAlON.	113
Figure 32 Cross sections of the holes drilled at 0.65 ms, 1.5 ms, and 4 ms pulse durations, respectively on SiAlON material.....	114
Figure 33 Variation of the hole diameter and hole depth with pulse energy for three pulse durations, namely, shortest (0.65 ms),medium (1.5 ms), and longest (4.0 ms) for aluminum oxide tool material.....	116
Figure 34 Fracturing of alumina sample at higher energy density.....	117
Figure 35 Cross sections of the holes drilled at 0.65 ms, 1.5 ms, and 4 ms pulse durations, respectively on alumina material	118
Figure 36 Variation of the hole diameter and hole depth with pulse energy for three pulse durations, namely, shortest (0.65 ms),medium (1.5 ms), and longest (4.0 ms) for aluminum oxide plus TiC tool material.....	120
Figure 37 Cross sections of the holes drilled at 0.65 ms, 1.5 ms, and 4 ms pulse durations, respectively on alumina plus TiC material	121
Figure 38 Variation of the hole diameter and hole depth with pulse energy for three pulse durations, namely, shortest (0.65 ms),medium (1.5 ms), and longest (4.0 ms) for SiC whisker reinforced alumina-zirconia tool material.....	123

Figure 39 Cross sections of the holes drilled at 0.65 ms, 1.5 ms, and 4 ms pulse durations, respectively on silicon carbide whisker reinforced alumina - zirconia material	124
Figure 40 Recast layer on whisker reinforced alumina- zirconia	125
Figure 41 Variation of the hole diameter and hole depth with pulse energy for three pulse durations, namely, shortest (0.65 ms), medium (1.5 ms), and longest (4.0 ms) for TiC-TiN cermet tool material	127
Figure 42 Cross sections of the holes drilled at 0.65 ms, 1.5 ms, and 4 ms pulse durations, respectively on TiC / TiN cermet material	128
Figure 43 Variation of the hole diameter and hole depth with pulse energy for three pulse durations, namely, shortest (0.65 ms), medium (1.5 ms), and longest (4.0 ms) for polycrystalline c-BN tool material	130
Figure 44 Cross sections of the holes drilled at 0.65 ms, 1.5 ms, and 4 ms pulse durations, respectively on cubic boron nitride material.....	131

CHAPTER I

INTRODUCTION

Conventional machining using a tool substantially harder than the work material, such as mechanical turning, drilling, milling, and grinding in which the unwanted material removed in the form of chips, is a commonly used manufacturing process. In spite of significant waste of material as metal chips and high energy associated with the process compared to the non-traditional material removal methods, such as electrical discharge machining (EDM), laser machining, it is still used extensively because of its inherent advantages, namely, versatility, high material removal rates, generally more economical, ease of implementation, etc. However, the conventional machining process has certain inherent limitations, such as the difficulty of drilling small holes and/or holes with a long aspect ratio (l/d), difficulty in machining very hard materials, such as ceramics, cemented carbides, hardened steels, cermets, and ceramic composites. It is in drilling and drilling-like material removal processes where non-traditional machining processes, such as electrical discharge machining, lasers drilling, etc. can excel in their performance, especially when the diameters are very small (~ 1 mm) and/or holes with long aspect ratios ($l/d \sim 20-200$).

The use of lasers in drilling is particularly attractive for these materials for no cutting tool is used and consequently there are no tools to wear. In addition, no forces are involved and hence no stresses imposed on the work holding fixtures. Also, no deflection of the tool occurs as in mechanical drills. However, laser processing of materials has certain unique characteristics and problems that need to be addressed, such as the complex laser/material interactions, thermal damage, re-deposition of ablated material,

etc., to better understand and control the process. In the next few sections, an overview of the lasers used in materials processing with emphasis on Nd:YAG laser will be presented. Various parameters pertinent to laser beam machining as well as a brief description of some of the advanced materials that are used in the manufacturing are presented

Brief history of lasers

Einstein in 1917, using a mathematical argument, postulated the possibility of stimulated emission phenomenon. However, it was only in 1957 that a viable concept for this, namely, *maser* (Microwave Amplification by Stimulated Emission by Radiation) was developed by Schawlow and Townes in their classical paper on, "Infrared and Optical Masers," published in the Physical Review, vol. 112, 1958, pg. 1940-49 [1958]. It was, though, on March 22, 1960 that Schawlow and Townes were issued a patent on this idea. On May 16, 1960, another pioneer in the field, Theodore H. Maiman, a researcher at Hughes Research Laboratories in California working on a U. S. Department of Defense (DoD) contract, demonstrated for the first time the functioning of the first ruby laser in which a coherent beam of light is emitted at the same frequency. It may be noted that *laser*, like its cousin *maser*, is an acronym for Light Amplification by Stimulated Emission of Radiation. Soon after, there were several companies that began producing lasers commercially. Since then, many different types of laser have been proposed and developed using all states of matter (even without elemental matter as in the case of free electron lasers) and using various methods of excitation for a wide range of applications (Figure 1). They include scientific, engineering, medical, diagnostic, and military applications.

General applications of lasers.							
Application	Property of beam most used						Laser normally used
	Mono - Chromatic	Low Divergence	Coherent	High Power	Single Mode	Efficient	
Powerful Light							He/Ne, Argon
Alignment							He/Ne
Measurement of Length							He/Ne, Ruby, Nd-Glass
Pollution Detection							Dye, GaAs
Velocity Measurement							He/Ne, Nd-Glass
Holography							All, Mainly Visible
Speckle Interferometry							He/Ne
Inspection							He/Ne, Ruby
Analytical Technique							Nd-YAG
Recording							GaAs, GaAsP
Communications							He/Ne, GaAs, Iodine
Heat Source							CO ₂ , Nd-YAG or Glass Excimer
Medical							CO ₂ , Ruby, Argon, Excimer
Printing							He/Ne, Argon
Isotope Separation							Dye, Argon, Copper
Atomic Fusion							CO ₂ , Nd-Glass
Barcode coding		Main property		Second property		Third property	

Figure 1 Applications of various types of lasers. (Steen, 1991)

Suffice to say that lasers have found uses in nearly all areas of technology and have a significant impact on our everyday life in this technological society. Figure 2 shows the range of wavelengths for current commercial lasers. The first date in the figure is that of discovery and the second is of commercialization. Of the various varieties of lasers, those lasers that dominate in the area of laser material processing (high energy lasers) in the industrial manufacturing sector are the CO₂ gas laser, Nd:YAG and Nd:Glass solid state lasers, and the excimer laser.

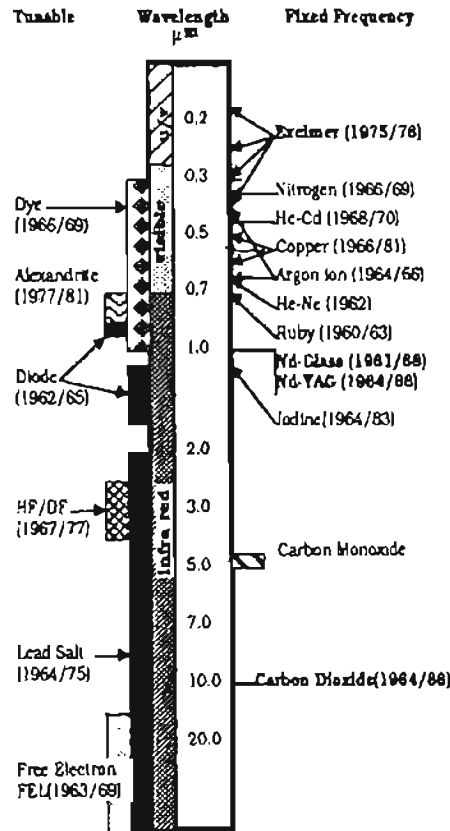


Figure 2 Range of wavelengths for current commercial laser. First date is date of discovery, the second is of commercialization (Steen, 1991)

Requirements of a Laser System for use in Laser Beam Machining

For a laser beam apparatus to be useful in machining, it must meet several requirements including:

1. Adequate power output to perform the required method of material removal (ablation, melting, vaporization, drilling, etc.).
2. Controlled beam profile
3. Reproducibility of the various laser beam characteristics.
4. Reliability of the laser beam equipment
5. Suitable safety characteristics
6. Capital and running costs of the laser beam equipment.

Of the several requirements listed above for a laser system's suitability for use in machining, the first one could be considered most fundamental since large powers are essential for material removal. For laser power densities below a threshold value (300 J/cm^2 for copper), the surfaces of most metals show a high reflectivity to beam energy and no material removal occurs. In the case of ceramics with a high temperature melting point, this threshold is even higher (e.g., for aluminum oxide it is $1000\text{-}2000 \text{ J/cm}^2$). Hence, high energy densities are a prerequisite for the machining of ceramics.

Lasers that meet the requirements above will be the most prevalent in manufacturing/machining. A review of current literature and an overview of the manufacturing sector show that three laser technologies dominate in the area of laser beam materials processing for the reasons stated above. They are the:

1. CO_2 gas laser
2. Neodymium: Yttrium Aluminum Garnet (Nd:YAG) solid state laser

3. Excimer gas laser

Table 1 gives various characteristics of the above three types of lasers [Whitehouse, 1992]. Other laser types are also used in industry but tend to fill niche applications. For the purpose of this investigation, we will focus on the use and application of the Nd:YAG laser for drilling of advanced materials. Figure 3 (Steen, 1991) shows the operating ranges (energy versus pulse repetition rate) of various solid state lasers.

Table 1 Operational comparison of the three types of industrial lasers (Whitehouse, 1992)

Operational Comparison of CO₂, YAG, and Excimer Lasers			
	<u>CO₂</u>	<u>Nd:YAG</u>	<u>Excimer</u>
Active Medium	CO ₂ , N ₂ , He Gases	Nd:YAG Crystal	Noble and Halogen Gases
Excitation	Electrical Discharge	Arc Lamp	Electrical Discharge
Wavelength (Microns)	10.6	1.06	.19/.25/.31
Average Power (kW)	1-10	0.1-1	0.1-0.2 (Pulse)
Peak Power (kW)	10	50	50,000
Rep Rate (kHz)	10	20	0.5
Efficiency (%)	5-15	1-3	1-3
Beam Size (mm)	10-30	2-10	6x20-10x30
Beam Quality (TDL)	1-3	1-3 Limited 10-100 Full	1-10 Limited 100 Full
Consumables	CO ₂ , N ₂ , He Gases	Arc Lamps	Noble, Halogen and Buffer Gases
Transmissive Optics	ZnSe	Quartz	UV Quartz
Reflective Optics	Metal	Metal or Dielectrics	Dielectrics
Fiber Delivery	None	Quartz	UV Quartz
Safety Shield	Acrylic, Glass	Filters	Filters
Capital Cost (\$/Watt)	50-200	200-400	1,000-2,000

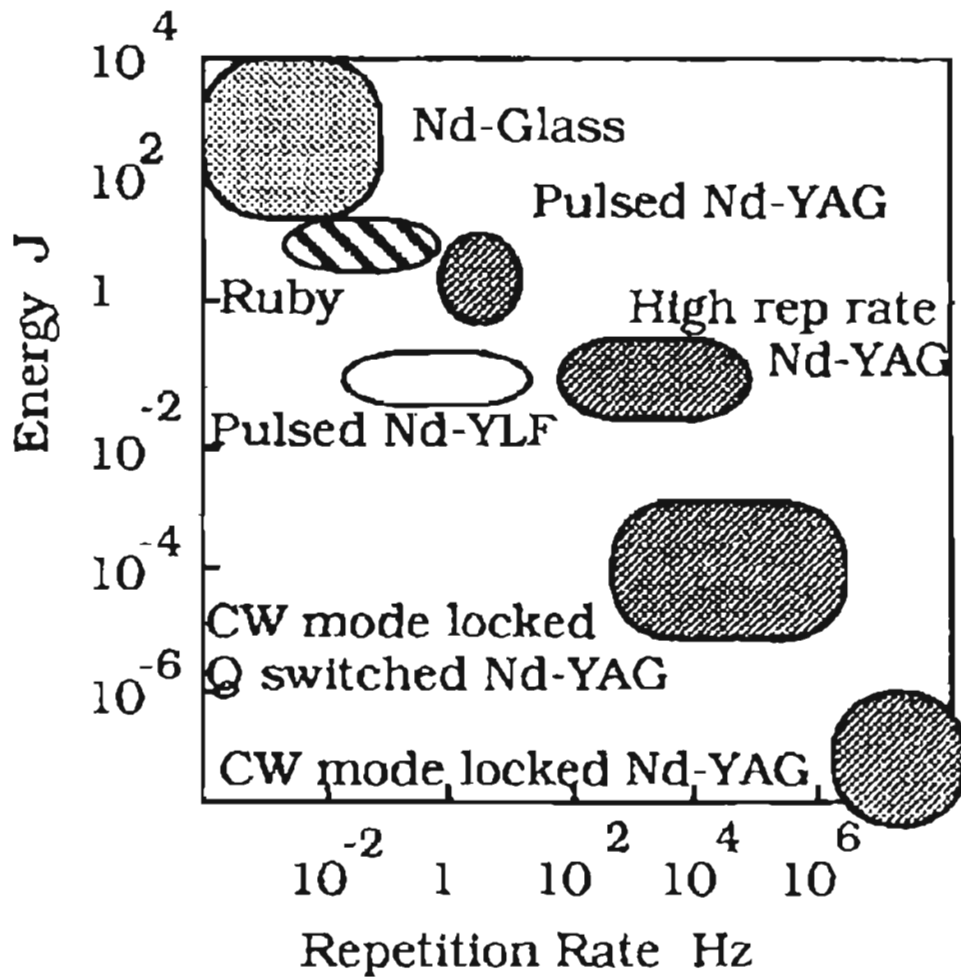


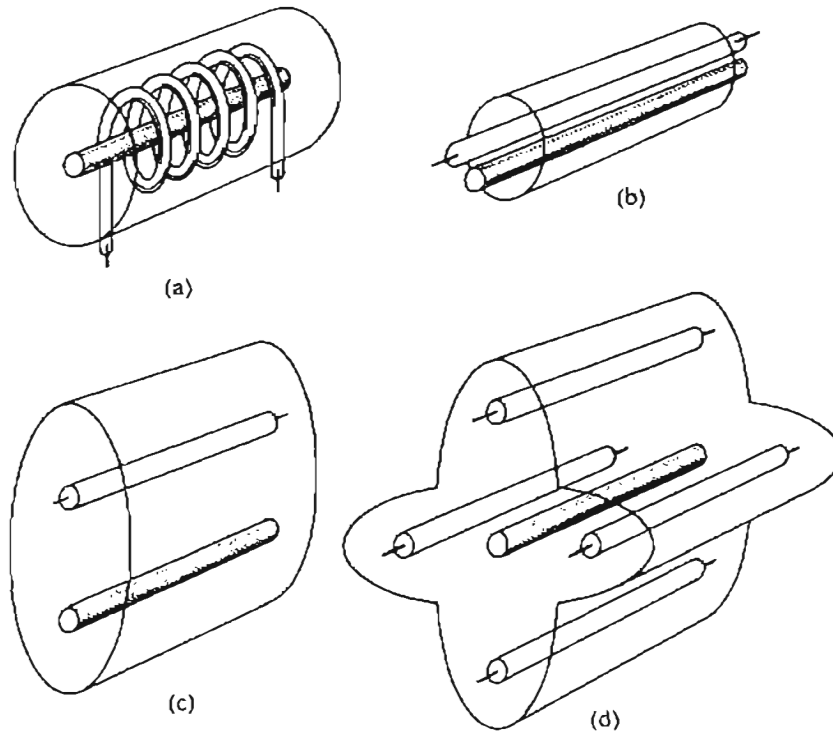
Figure 3 Operational ranges of commercial solid state lasers.(Steen, 1991)

Description of one of the major laser technologies: The Nd:YAG laser

The Nd:YAG solid state laser was invented in 1964 at Bell Laboratories. Many companies including Quantronix, Holobeam, Control Laser, and Coherent were quick to commercialize this invention. But the market grew very slowly due to poor quality of the lasers and low powers. The market picture changed in 1976 when Quanta-Ray introduced the first reliable high performance YAG laser. The design used an unstable resonator and was robust. It gave 1 J/pulse at half the price of others. Since then high powered pulse Nd:YAG lasers including slab lasers were developed with an output power of 1.5 kW. Use of optical fibers for beam delivery has also facilitated its use tremendously in industry.

The neodymium: yttrium aluminum garnet laser or Nd:YAG laser is a solid state laser where the lasing medium, Nd^{3+} , is suspended in or doped into a crystalline matrix optical resonator consisting of $\text{Y}_3\text{Al}_5\text{O}_{12}$. Since the resonator is electrically non-conducting, excitation is accomplished by optical pumping methods. They emit light predominately at 1.064 micrometers wavelength. Figure 4 is the energy diagram for Nd:YAG laser (Steen, 1991). The quantum efficiency is ~40 %. The operating efficiency is low since pumping is done with broad band illumination of which only a fraction of the radiation is able to excite the Nd atoms in the crystal. Consequently, their efficiency is typically less than that of CO_2 lasers (usually less than 5%). Newer, more efficient designs, simpler optics, and better material interaction with certain work piece materials at this wavelength help make this type of laser a very strong competitor with the CO_2 laser both in performance and economy.

rod are housed within a cavity with highly reflective internal surfaces to maximize the amount of light the lasing rod receives. Figure 5 illustrates some typical optical pumping cavities.



Some of the more common flashtube geometries used for optical pumping: (a) a helical flashtube round the laser rod; (b) close coupling between flashtube and rod; (c) flashtube and rod along the two foci of an elliptical cavity and (d) a multi-elliptical cavity.

Figure 5 Laser reflective cavity design for flash rod pumped lasers

Cavities (c) and (d) in Figure 5 are the most efficient optical coupling designs. As shown in Figure 6, a cavity shaped as an ellipse is designed such that the flash tube and the rod are placed at the separate foci of the ellipse. This will allow most of the light emitted from the flash tube to reach the lasing rod either directly or indirectly by reflections off the cavity walls.

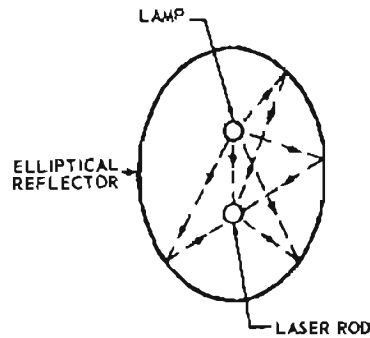


Figure 6 Elliptical cavity reflection pattern

Inefficiencies in the flash tubes in the form of heat require that some method of cooling the laser be applied especially to protect and prolong the life of the brittle ceramic Nd:YAG or Nd:Glass lasing rod. In addition, the thermal lensing effect associated with the solid state lasers can damage the lasing rod due to thermal stresses. To reduce thermal loading, cooling has to be enhanced. Otherwise, the life of the lasing rod can be very short especially at high power ratings. Low power systems, may simply use a heat sink but the more powerful lasers would require forced air or even water-cooling. Water can be used to flood the cavity. However, water can absorb a significant amount of flash lamp energy and turbulence can cause optical distortions. To overcome these problems, the cavity is cooled externally and waterjackets made of high transmissive glass are used around the flash tube and the lasing rod.

An example of Nd: YAG laser with the latter cooling method is described in the U. S. Patents 5093551 (1992) and 5081636 (1992). The patents claim an efficiency for the laser of 4 to 4.5% and an average power output from 400 to 500 watts by producing a cavity with superior reflectivity (gold coated) and a samarium coated transparent waterjacket for improved transmission of the pumping wavelengths.

Current single rod designs have power outputs of 400 to 600 watts CW or pulse. Theoretically, the upper limit on the maximum power output of a single rod Nd:YAG laser is about 900 watts. The limit arises from the non-uniform heating of the laser rod from both the flash lamp and the laser beam as it travels through the rod coupled with the thermal gradient produced by the cooling system. Since the refractive index of the Nd:YAG rod is temperature dependent, this inhomogeneous temperature distribution produces beam distortion. A practical limit is also placed on the maximum power output by the possibility of rod failure by fracture due to the thermal stresses produced. Thus, Nd:YAG rod volumes are limited to reduce beam distortion and the possibility of rod fracture. Incidentally, the possibility of fracture can be reduced if surface flaws are kept to a minimum. Grinding and polishing is used in the finishing of the laser rods. It is conceivable that non-traditional finishing techniques, such as the magnetic field assisted polishing techniques explored by Umehara and Komanduri (1996) and colleagues at Oklahoma State University can be used to produce a better, smoother surface finish.

To increase single crystal output power, without a sacrifice in reliability and beam quality, a new design would have to be employed to overcome the intrinsic limitations of the round rod design. Such a design is the slab laser invented and patented in 1972 by Chernoch and Martin (U. S. Patent No. 3,633,126). Developed in the late 1970's at General Electric (by Marshall Jones of General Electric Corporate R &D in Schenectady, NY for high energy applications (1.5 kW and higher)), it is in the 90's that it has become more prevalent on the industrial scene. What makes the slab laser unique is the shape of the lasing crystal. Shaped as an oblique rectangular prism, the base ends cut at the Brewster angle for 1064 nm light wavelength such that the laser light will be bent

towards one of the smooth, highly polished internal surfaces. At the Brewster angle 100% of the light beam will reflect toward the opposite parallel surface in a zigzag fashion. Figure 7 illustrates the concept.

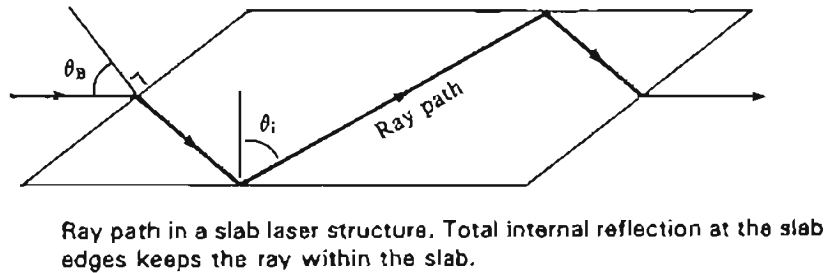


Figure 7 Slab laser operating principal

As the beam zigzags through the crystal, any diffraction effects caused by the thermal gradient within the crystal will be effectively canceled out. Thus, the crystal can be optically pumped to a greater degree to obtain more power output with significantly less beam distortion than cylindrical rods with comparable output power.

Optical pumping methods which use conventional flash tubes and arc lamps are limited in their usefulness in providing the irradiance required to pump the slab laser to its full potential. Thus, more powerful pumping sources, such as suitable arc lamps or diode laser arrays, are used. The latter are most attractive since they can produce high irradiance in the optimal wavelength required for excitation of the dopant ions, have higher energy efficiencies than flash tubes or arc lamps, and can be mounted directly on one face of the slab crystal. Thus, a housing with a highly polished internal surface is not critical. Cooling of the slab crystal is applied to two other faces of the slab and can even

be applied to four faces if the laser diode array is designed such that intrinsic cooling is used. The following illustration shows one such design by the Lawrence Livermore National Laboratory (Manes 1990).

Conceptual design for 2 kW average, 8 kW peak power diode pumped solid state laser

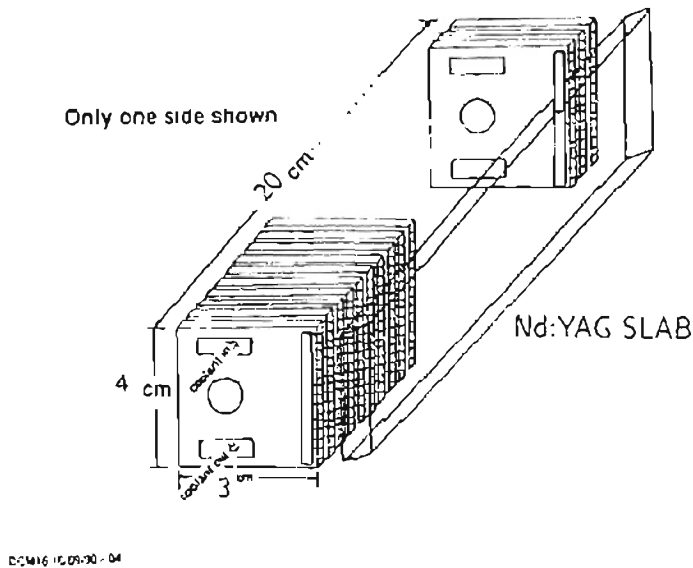


Figure 8 Slab laser design (Manes, 1990)

The beam shape that emerges from the slab is rectangular but can be made round, square, or a line with proper resonator optics, resonator configuration, and intra-cavity apertures. The U. S. Patent No. 5,125,001 by Yagi et al. [1992] suggests some resonator configurations and optics for extracting a laser beam from a slab laser. The focusing of the laser beam into a line would be useful in straight-line cutting and for welding.

Currently, typical power outputs for commercial slab lasers are around 500 watts average (CW or pulsed) for a single slab crystal but will increase as suitable, more powerful pumping sources become economical and commercially available. There are new slab lasers which allows much higher output powers that use a thin slab whose cooled side is also used as one of the mirrors, so that thermal gradients occur mainly in the direction of the beam propagation and not perpendicular to it.

It is generally considered that CO₂ lasers are capable of producing high quality beams (Du et al, 1995). The beam quality is given by the ratio of the theoretical minimum of the beam parameter (which depends on the wavelength of the laser radiation) and the actual beam parameter value (which is always greater than the theoretical minimum). The theoretical minimum of the beam parameter is given by the ratio of λ to π , where λ is the wavelength. For the CO₂ laser this gives a value for the theoretical beam parameter limit of 3.38 mm mrad even at powers in the kilowatt range. In the case of Nd:YAG lasers, due to its much shorter wavelength, the theoretical minimum of the beam parameter is only 0.338 mm mrad which is 10% of that for the CO₂ laser. With this value of the beam parameter, the laser focus radius is much smaller than in the case of CO₂ laser. Consequently, much smaller holes can be drilled by a Nd:YAG laser compared to a CO₂ laser. This advantage compared to CO₂ laser can be realized only at laser powers that are not too high. At higher powers the beam diameter increases to a value which can be more than 10 times that of CO₂ lasers with comparable output power. This is due to thermal lensing effects in the lasing crystal. When the Nd:YAG laser heats up, stresses induced in the rod change the refractive index and hence distort the laser beam as it passes through the laser rod. Besides beam distortion, the

induced thermal stresses can destroy an expensive Nd:YAG laser crystal. Efficient cooling of the crystal as well as homogeneous coupling of the pumping radiation to the active medium is rather critical for high beam quality.

The short wavelength of the Nd:YAG laser also allows the use of optical fibers to transmit the laser beam which is a significant advantage in industrial applications. However, this is only possible with lower power lasers of a few hundred watts. Another advantage of the Nd:YAG laser radiation for materials processing is its higher absorptivity on work material surface (3-5 times for metal surfaces) compared to CO₂ laser. This means a lower beam power at comparable processing parameters can be used to achieve the same results. In some cases of laser material processing, laser-induced plasmas arise which can partly absorb the laser radiation. The plasma absorption coefficient depends strongly on the wavelength of the laser radiation and it is ~100 times smaller for Nd:YAG laser than for CO₂ laser. Nd:YAG lasers are particularly advantageous for use in processes with high plasma densities.

Nd:YAG Lasers

Figure 9. (Steen, 1992) shows the general arrangement of a typical Nd:YAG system. It shows a standard elliptical cavity design with active medium being neodymium in a YAG crystal rod mounted at one of the foci of an elliptical cavity and at the other foci a krypton lamp. Also mounted in the cavity is an aperture for mode control and a Q-switch for rapid shuttering of the cavity to generate fast pulses of laser light. Even though the average power may be low, the peak power can be significant, an order of magnitude or more.

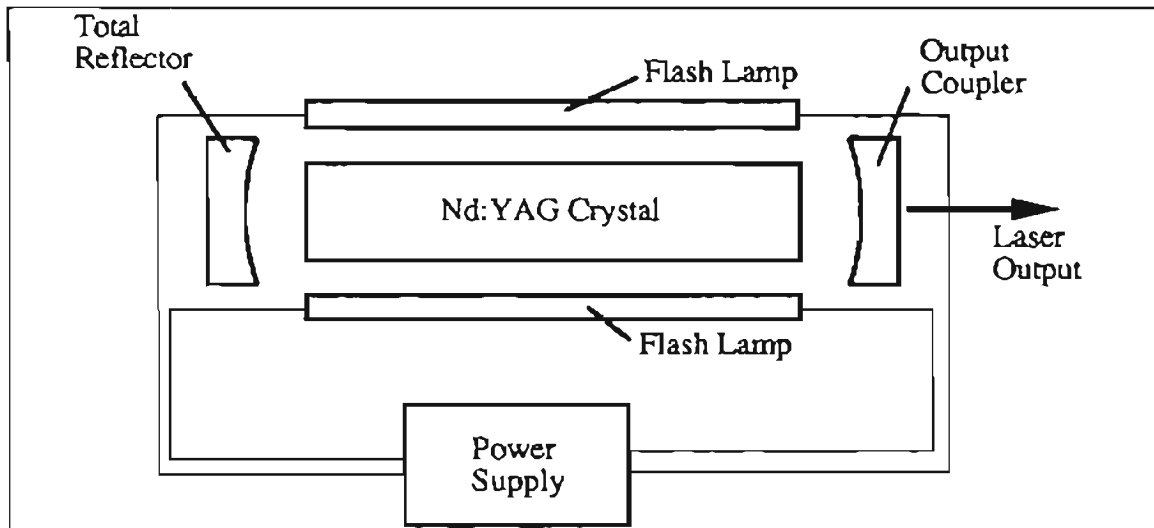


Figure 9 General construction of an Nd:YAG laser (Steen, 1992)

Nd:YAG Laser Optics

Nd:YAG lasers operate in the near infrared region and use different materials for optical elements than for a CO₂ laser. Although the absorption efficiency of light at 1.06 μm can be an order of magnitude higher than at 10.6 μm, reflective optics made of highly polished metal are used as dielectrics. Quartz is used for transmissive optical elements. Fiber optics can be used as transmissive elements and it is this feature that makes Nd:YAG lasers more attractive for industrial use. With a fiber optic line, laser assemblies can be located remotely from a work site with less than a 10 % loss in beam quality and power. Fiber optics dispenses the need for complex optical systems and the possibility of their infiltration with dust and other contaminants.

Nd:YAG Laser in Machining

As newer materials are being developed that go to the extremes of material properties, such as hardness, elevated temperature strength, etc. they become more difficult to machine and process by conventional mechanical methods. Laser beam machining can be a viable alternate for processing these materials.

Why use a Nd:YAG laser over other major manufacturing laser types and even the CO₂ laser? Some of the pros are the following: 1. Better spectral absorption by the work piece material. Certain difficult to machine materials that reflect more of the longer wavelength of the CO₂ laser can be better processed with a Nd:YAG laser, for example, beryllium copper. 2. Smaller possible spot size. Theoretically, an Nd:YAG laser can produce a smaller focal spot than the CO₂ thus, a narrower kerf width and higher power densities are possible. Although, the excimer can achieve a smaller focal spot size than either, current industrial designs of excimer lasers do not have high enough average power outputs to be cost effective or practical for macroscopic machining processes such as milling, drilling, etc.

Advanced Materials Suitable for Laser Machining

Material removal for most common materials can be handled by the typical mechanical processes of drilling, milling, and cutting. This would include many ferrous and aluminum alloys, plastics, and wood. Yet, with the constant advanced of technology, fabrication of parts may require small machined features or new materials with improved properties that make these materials difficult to process by the typical machining processes, especially as their hardness increases and plasticity decreases. Some of the

materials include hard ferrous alloys, advance aerospace alloys, polymer matrix composites, metal matrix composites, ceramic matrix composites, cermets, and very hard materials such as cubic boron nitride and diamond. Shaping of these harder materials are commonly done by an abrasive method with a material of similar or more extreme properties.

Drilling of such materials can be a formidable task with conventional methods. Plasticity of the work piece is necessary especially near the axis of rotation. The linear rotational speed decreases as the radius of the drill decreases. Drill bits with larger aspect ratios will have a greater tendency to break due to inadequate stiffness. Also, these mechanical processes tend to be time consuming and costly. Laser drilling has the capability of being able to drill holes into all non-reflective, non-transmissive materials. It can do so in short periods, with high aspect ratios with diameters into the micrometer range. It requires no contact with the work piece and thus no tool to wear out.

Since laser drilling in the near infrared range is essentially a thermal process, some disadvantages can arise due to the high heat and rapid temperature rise. Some of these disadvantages are cracking and spalling of the work piece due to thermal expansion and contraction, recast layer formation, and chemical decomposition.

Typically, the energy distribution across the laser beam is not constant but in the simplest mode exhibits a Gaussian distribution profile.

CHAPTER II

BASICS OF LASERS

Laser Parameters

Properties of the laser light

There are several aspects of the laser light that make it unique. Understanding the basic properties of laser light will help to determine which parameters are critical in the understanding of the laser drilling process. They are its monochromaticity, coherence, divergence, and intensity. Although, more detailed information is available in references on the aforementioned aspects, the following is a brief description of each.

Monochromaticity. Monochromatic means “of one color” or wavelength. Although most lasers are not absolutely monochromatic, their bandwidth are, for all intents and purposes, narrow enough to take advantage of monochromaticity in the area of machining-selective material interaction. Materials interaction with the laser light can vary at different wavelengths.

Coherence. Light acts as an electromagnetic wave when it travels through space. This wave has two components, an electric wave and a magnetic wave. They are perpendicular to one another and travel at the same speed. When the laser light is produced within the resonator, each individual wave has the same phase, frequency, amplitude, and direction as the parent waves, theoretically. This high degree of coherence can introduce polarization effects on the material interaction.

Divergence. This is a measure of the increase in beam diameter over a certain distance. Although lasers produce beams that are quite parallel, all beams tend to diverge due to diffraction effects of the aperture of the laser and are related to the ratio between the focal length and the aperture diameter. Also, higher beam modes tend to increase divergence. Values for divergence are typically given in milliradians at a point where the power density is $1/e^2$ of the maximum value. Minimal beam divergence allows better power density and a smaller focal spot size.

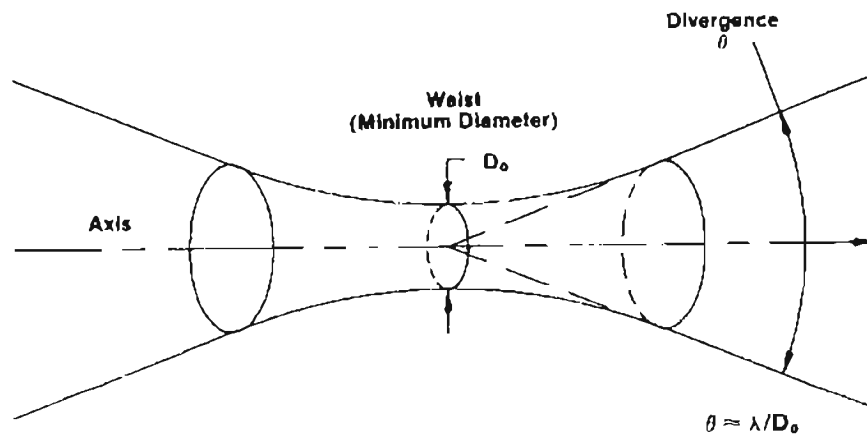


Figure 10 Beam divergence

Intensity. This is a measure of the amount of power delivered over a given area per unit solid angle. This is usually expressed as Watts per meter squared per steradian ($W m^{-2} sr^{-1}$). The ability of lasers to produce intense beams makes them quite useful in laser beam machining.

Lens Focal Length and Position

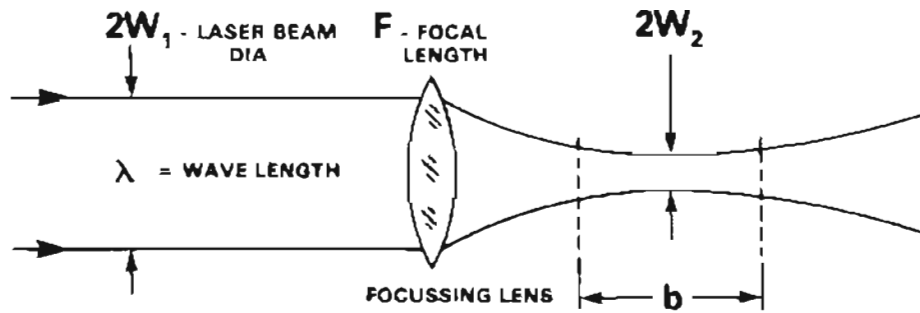
The principal advantage of a laser is that the laser beam can be highly collimated resulting in high power density ($\sim 1500 \text{ W/cm}^2$). This power density can be substantially increased using optical focusing with a plano-convex lens to yield fluxes in the order of 10^6 W/cm^2 . This results in melting and evaporation of most materials in a few microseconds. Most laser machining units have the ability to change the focal length and position of the focusing lens with respect to the surface of the workpiece. This control over the spot size has several advantages. For instance, drilling of holes of different diameters can be accomplished by varying the focal length and/or varying the focal position of the lens. The depth of focus of the given lens increases with the focal length of the lens. Thus, in order to drill very deep holes of a specific taper tolerance, it may be necessary to increase the focal length of the lens. A substantial improvement in the material removal rate, hole taper and cut quality is often possible by varying the focal position and focal length of the lens.

Beam Characteristics

The intensity distribution of the laser beam is referred to as the laser beam profile. Lasers for manufacturing applications usually exhibit a Gaussian (TEM_{00}) or a doughnut (TEM_{01}) mode (Hecht, 1992). The spatial intensity distribution of a Gaussian laser beam, $I(r)$, can be represented by a Gaussian curve of the form, $I(r) = I_0 \exp(-2r^2/w_0^2)$ where w_0 is the radius of the laser beam at the beam waist. Doughnut mode refers to lasers which have a beam profile of the form $I(r) = I_0 r^2 \exp(-2r^2/w_0^2)$. A burn pattern on Plexiglas, using a doughnut mode laser beam produces a doughnut shaped profile that has the cross sectional spatial intensity distribution similar to two Gaussian profiles side by

side. (See Figure 11) The highest laser spatial intensity occurs a distance away from the center of the beam symmetrical with the axis of propagation. Doughnut mode beams are usually generated by fast axial flow CO₂ lasers. Gaussian beams are generated by slow flow CO₂ lasers and Nd:YAG lasers. Laser beams used for manufacturing applications do not conform precisely to either of these descriptions. These terms are used to qualitatively indicate the type of the laser beam profile. Laser beam quality can be quantified by a beam quality parameter, M^2 . The value of M^2 for a Gaussian laser beam is 1 and increases as the beam profile differs from the Gaussian beam resulting in a larger spot size at the focal plane. Any increase in the spot size results in lower intensity, lower cutting speeds, greater kerf widths etc. The intensity distribution at the workpiece is critical and is sometimes possible to accomplish a given task only with a high quality beam rather than a high power, low quality beam.

Factors that determine the depth of field and the minimal focal diameter of the beam are important parameters when working conditions for a laser system are determined. Figure 11 shows that both these parameters are functions of the wavelength, the energy of the laser beam, the diameter of the unfocussed beam, and the focal length of the lens [Coherent, Inc. Engineering Staff, 1980]. The formula in the figure is valid only for a laser operating in the TEM₀₀ (Gaussian) mode. The degree of divergence of the beam will directly affect the power density at the primary focal plane. It is important to note the relation between the depth of focus for a lens with a particular focal length and the power density that exits at the minimal focussed diameter.



$$2W_2 = \frac{4\lambda F}{\pi W_1} = \text{MINIMAL FOCUSED DIA.}$$

$$b = \frac{2\lambda}{\pi} \cdot \left(\frac{F}{W_1} \right)^2 = \text{DEPTH OF FOCUS}$$

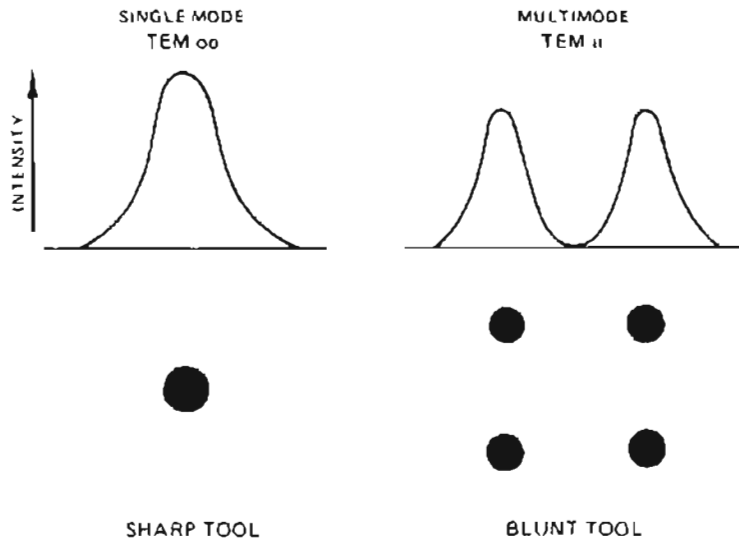


Figure 11 Depth of field vs. power density.

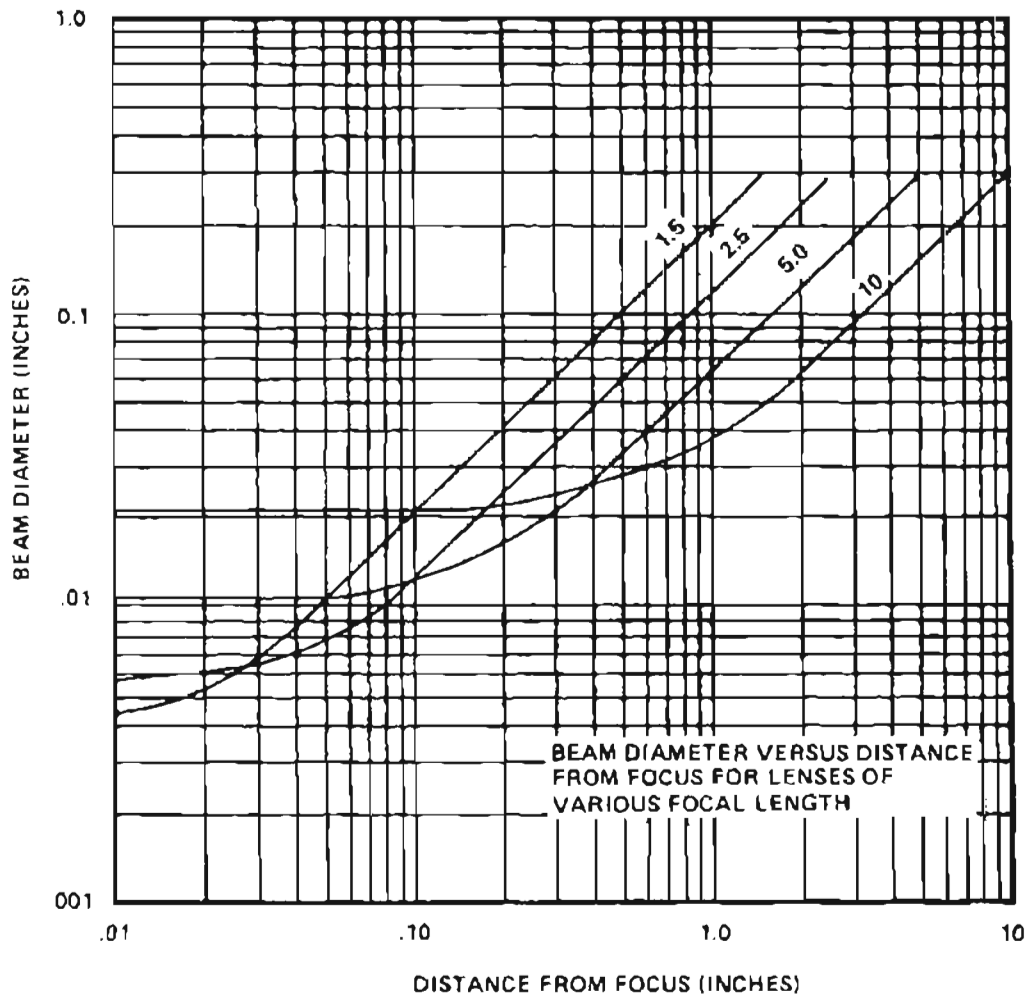


Figure 12 Beam diameter vs. focal length

Figure 12 shows the variation of the diameter of a focussed beam (spot size) with the distance from the focal plane for lenses of different focal lengths [Coherent, Inc.]. It shows that at short depths of field, smaller spot size and thus higher power intensity results. Similarly, at long depths of field, a larger spot size occurs and thus a lower power density results. Figure 13 shows the relation between the depth of focus and power density and between focal length and power density, and compares these relationships for two focussing lenses (2.5 in and 5.0 in focal lengths) in a beam [Coherent, Inc Engineering Staff, 1980]. It shows that a 5 in lens produces a greater depth of focus but results in a larger spot size at the focal plane than the shorter focal length lens. It achieves only 25 % power density at the focal plane when compared to 2.5 inch focal length lens. The position of the focal point of the beam relative to the work surface has an effect on the shape and depth of holes drilled by a laser. In general, when the focal point is located above the surface, shallow holes of large diameter and with somewhat tapered sides are drilled. When the focal point is located at the surface, holes of uniform diameter are drilled. When the focal point is located below the surface, shallower holes with conical sides are drilled. It is, however, possible to increase the working distance between a lens and the focal plane while maintaining the same spot size and power density using a telescopic lens followed by a larger lens to focus it.

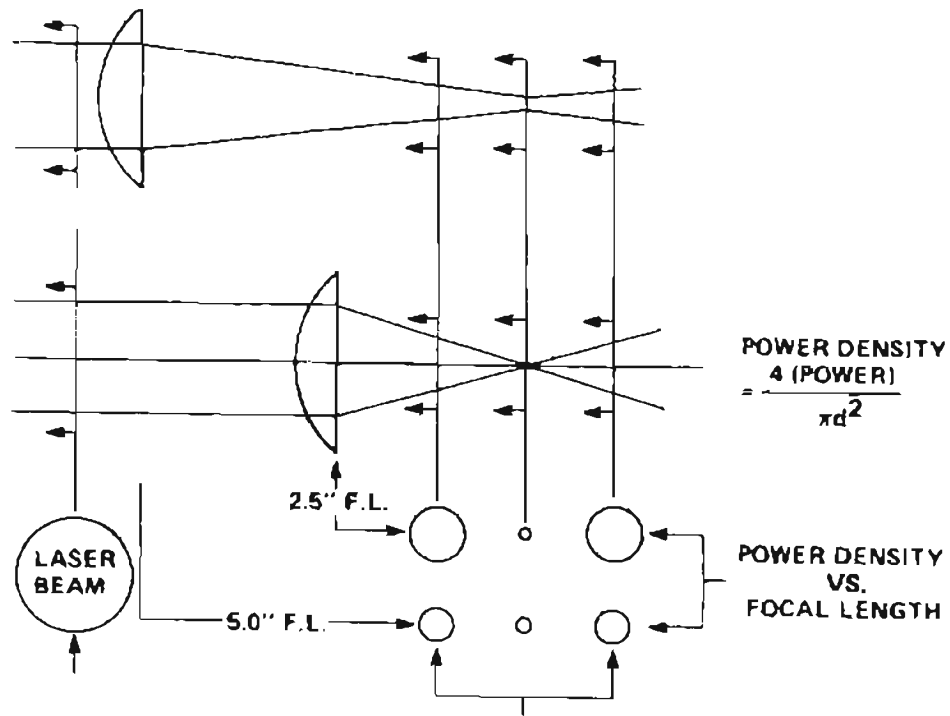


Figure 13 Power density vs. focal length.

Laser Power and Pulsing

The laser power determines the rate of heat input to the work piece. Most high power lasers have a built-in power meter to measure the power output of the laser. The losses through transmissive and reflective optics are usually small and this reading approximates the laser power available at the workpiece surface. Most lasers can be pulsed; this means that the energy emerging from the laser varies temporally according to some specific waveform. An increase in the peak power supplied to the workpiece with no substantial change in the average power can be achieved by varying the pulsing

frequency and the duty cycle (ratio of laser on time to pulse period). The pulse shapes can be triangular, square, or exponential waveform.

The power output of the laser beam determines the depth of cut during laser cutting and penetration depth during laser welding (Hecht, 1992). The pulsing of the laser beam, as compared to a continuous beam of the same average power, has an impact on cut quality. Some materials like alumina can be cut with a pulsed laser beam with significantly less thermal damage as compared to a continuous wave (CW) laser beam of the same average power. The pulsing of the laser beam has several advantages. A pulsed beam provides an increased local heating rate that results in less heat transmitted into the workpiece and more active cutting. The off duration of the laser beam allows any heat that is conducted into the work piece to dissipate uniformly within the work piece. These help to reduce the thermal stresses, and hence thermal damage, built up in the material. If some molten material is present, this may be blown away with gas assist during the off duration of the laser. If this were not removed it may be necessary to evaporate this molten material resulting in higher specific energy consumption and lower cutting speeds.

From a practical standpoint, such issues such as hole quality, hole diameter and hole depth and how to reproduce consistent results would be useful. A review of the current literature concerning these issues will be examined in the following review.

Parameters of lasers and laser beam machining

Laser drilling is essentially governed by an energy balance between the irradiating energy from the laser beam and conduction heat absorbed by the workpiece, energy loss to the environment, and energy required for phase change of the workpiece.

(Chryssolouris, 1991) There are a number of parameters to consider when modeling the laser drilling process, such as the properties of the work piece, laser, and environment (i.e. assist gas).

For the workpiece the following parameters can affect the laser drilling process:

1. Surface reflectivity of the work piece material. Surface reflectivity is influenced by:
 - a. Wavelength of laser light
 - b. Angle of incidence
 - c. Temperature of work piece
 - d. Phase state of the work piece
 - e. surface texture

2. Physical properties of work piece material
 - a. Thermal conductivity
 - b. Thermal diffusivity
 - c. Heat of melting
 - d. Heat of vaporization
 - e. Plasma absorption

The type of gas used in the laser assist can affect the process. For example, oxygen is used in cutting ferrous materials since it can exothermally react with the workpiece material, increasing the rate of material removed during laser drilling or cutting. Inert gases are used when cutting materials that would react with the atmosphere such as polymer based composites. Lower molecular weight gases will conduct heat more quickly than higher ones. Also, fluid flow as it relates to heat conduction should be considered. Thus, environment parameters that influence the laser drilling process are:

1. Use of assist gas.
2. Type of assist gas and its properties
 - a. Thermal properties/ fluid mechanics
 - b. Reactivity
 - c. Absorption of laser beam energy

The suitability of the laser for a machining operation will depend on the various parameters of the output beam. These can be broadly categorized as:

1. *Power* characteristics
 - Continuous wave or pulsed operation
 - Dynamic power range
 - Pulse agility
 - Programmability
2. *Spectral* characteristics
 - Wavelength(s) of the laser beam
 - Tunability of the wavelength(s)
3. *Geometric* characteristics
 - Propagation axis/ focal length
 - Beam mode/ intensity profile
 - Beam divergence/quality
 - Beam diameter
 - Beam polarization
4. *Stability* of the above characteristics
 - Inherent drift
 - Induced drift

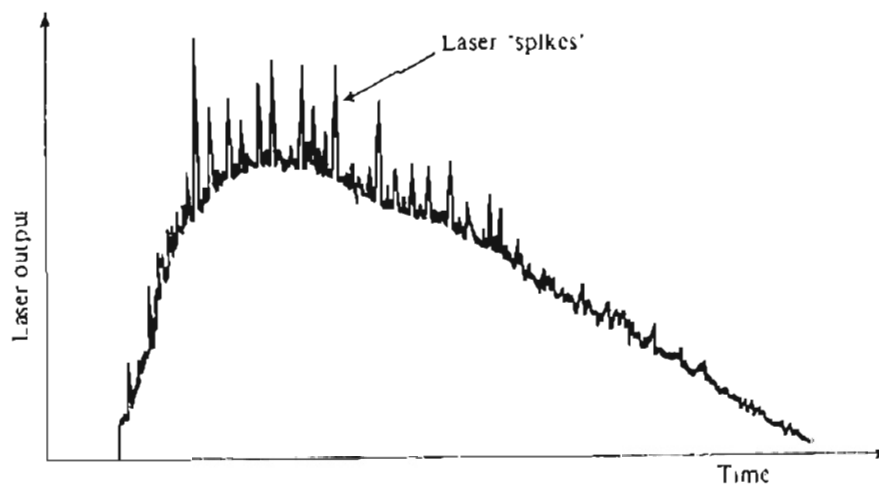
For laser drilling, pulsing tends to be the preferred method of material removal since the pulsing action allows ablated material to clear the hole and allowing more energy of the next pulse to reach the erosion front unimpeded by previously ablated material.

The dynamic power range is simply the minimum and maximum intensity that a laser beam can operate. Such a parameter is useful for process control and economic considerations.

Pulse agility refers to the ability of the laser system to produce various pulse configurations by varying the pulse shape, pulse intensity, and pulse frequency. More

detail is given later on the various types of pulse shapes used in laser beam machining. This can be accomplished by mechanical, electrical, or optical means. Electrical and optical methods predominate because of their ease of implementation with numerical control systems. Q switching is one electrical method often used to pulse a laser. The rate in which a laser is pulsed is usually measured in pulses per second (pps) or hertz (Hz).

It should be noted that the output of a duration of at least a few milliseconds from a flashtube pulsed laser with no Q-switching will produce laser spiking, possibly because of the dynamic thermal gradient within the YAG crystal during flash pumping. Such spikes occur at irregular intervals and random amplitudes. The figure below depicts the phenomenon called mode hopping.



Typical output from a flashtube pumped Nd:YAG laser, showing laser 'spiking'.

Figure 14 Typical laser output from Nd:YAG

What is interesting is that such a pulse shape can have a beneficial effect on material removal. Nevertheless, if a particular pulse shape is not suitable or more control of the pulse is desired, Q-switching can be employed.

Programmability refers to the laser systems flexibility to operate in the various modes of the above parameters. With the marriage of the laser with computer numerical control, today's lasers can operate in the CW or pulsed mode, vary the power, and change pulse characteristics as required by an application.

The wavelength characteristics of a laser are important for laser beam machining because of varying interaction of the work piece to different wavelengths. Thus, if a laser is to be optimized to performing a particular operation, the selection of the proper wavelength and hence, the proper laser system, is necessary for optimum performance.

Certain types of lasers exist that can vary the wavelength produced, for example, dye lasers. That is, they are tunable. Others vary their wavelengths by a technique of harmonic generation or frequency doubling. The drawbacks of these tunable laser systems are a reduction in efficiency and/ or a limited range of tunability such that they do not produce a significant change in laser/workpiece interaction and, as such, are not often used in laser machining.

Turning to the geometric aspects of the lasers, the propagation axis of a laser is generally a straight line and will travel along an axis coincident with the axis of the laser resonator unless it is deflected or encounters an obstacle. The beam diameter will have its center coincident with the propagation axis. The beam diameter can vary along the propagation axis because of focusing and diffraction effects. Also, the focal length of lens

used to focus the beam can affect the hole quality, with greater focal lengths producing holes with a greater aspect ratio but with an increase in the minimum focal spot size and vice versa.

Beam modes will affect the intensity distribution of a laser on a plane perpendicular to the propagation axis. An ideal beam will have TEM₀₀ mode, reduce diffraction effects to a minimum, and will produce the highest intensity about its axis. The beam mode is governed by the design of the optical resonator.

We recall that all beams tend to diverge due to diffraction effects. An ideal beam will keep divergence down to a minimum producing the smallest possible beam size. Beam size will affect the intensity of the laser beam as well as determine the kerf or hole size in a machining operation. For an ideal beam, the minimum beam diameter or waist is equal to the wavelength of the laser.

Polarization refers to the orientation of the electric field of the laser wave. It can be used when one part of a system needs to be isolated from the radiation generated from another part of the system. For example, in the production of optical disks, the same laser that is used to produce the information pit can be used to check the accuracy of the process via read beam produced by a beam splitter. To prevent interference, the read beam can be polarized to a different angle than the write beam producing the information pits. With respect to machining, it is known that energy absorption by many materials is polarization dependent. Thus, to have uniform cutting speeds in all directions, a circularly polarized laser beam is used when laser beam machining or if maximum cutting speed is desired, the orientation is optimized.

Short and long term drifts of the above parameters can occur and their effects must be noted in machining where repeatability is paramount to a quality process. Such drifts can occur because of laser design peculiarities. For example, slight changes in optical properties of the optics can occur due to slight heating. Drift can also be induced by external factors such as the environment or service conditions.

CHAPTER 3

LITERATURE REVIEW

Introduction

During the past thirty years a number of papers have appeared dealing with experimental and theoretical aspects of laser drilling, scribing, and cutting. Most of these papers have dealt primarily with CO₂ or Nd:YAG laser processing of metals and their alloys. Comprehensive reviews of different aspects of laser processing have been given in two books by Duley. The first one covers the literature up to 1974 (Duley, 1976), the second one up to 1982 (Duley, 1983) and by Von Allmen (1987), covering the literature up to 1986. Uglov and Kokora (1977) have presented a review of the large body of Soviet publications. Current reviews of the literature available on laser processing of materials which may include drilling have been given by Modest (1990), Chryssolouris (1991), Steen (1991), and Grigoryants (1994). In addition, Iyer (1997) conducted research and initial investigations on laser processing with a CO₂ laser.

Much of the literature to date on the laser drilling of advance materials with Nd:YAG laser is lacking compared to the literature on CO₂ laser processing although there are references to industrial handbooks distributed by private consortia that give recommended parameters for the processing of particular materials. Most published literature encountered deal with CO₂ laser drilling of metals, ceramics, and composites as would be expected since this has been the dominate industrial laser technology for material processing.

A review of recent scientific literature shows that the laser drilling process is still not a perfectly quantified process, primarily due to thermally induced multiphase conditions. That being the case, the trend has been to model the laser drilling process by computational numerical means. Those that involve the analytical and empirical studies concentrate on the effect of extremely short duration laser pulses on the work piece. A few deal with extending the modeling of the laser drilling processing by theoretical methods.

This discussion of the literature on laser machining will proceed as follows. In the first section experimental papers dealing with laser drilling, scribing and cutting of materials are discussed. This is followed by a review of the theoretical work on modeling of the laser machining process. Accurate measurements of material, process and laser parameters during laser processing are critical to the understanding and modeling of the process. This is often the determining factor in the success or failure of a model. Thus, in the last two sections, some of the literature available on in-situ measurements of these parameters is discussed.

Experimental Studies

Although the UV laser's photochemical effect of material removal still holds the promise of material removal with little or no thermal damage, as of yet no commercial or industrial UV laser system exists that would meet the economical and high throughput needs of drilling advanced materials. As such, lasers with high fluence such the Nd:YAG are still prominently used in industry for laser drilling and other applications that require high removal rates of material.

Laser drilling was one of the earliest applications of high power lasers. Ready (1963) investigated the effects of vaporizing material with a laser to produce a hole. He determined that the effect of a very large pulse (10^{10} W/cm²) on carbon black leads to subsurface superheating and eventually a thermal explosion. Longfellow (1971) has studied the high speed drilling in alumina substrates with a CO₂ laser. He used a massive hollow copper box with a vacuum port in the base as the fixture for holding the alumina substrate. The coaxial assist gas forces the fused alumina into the vacuum system during the laser drilling operation thus giving close tolerances holes.

Gonsalves and Duley (1971) performed experiments on CO₂ laser drilling of stainless steel sheets in air and in vacuum. They found that the time required for drilling in vacuum was three times larger than that in air and hypothesized that this was due to a substantial change in absorptance during heating in air. Duley and Gonsalves (1972) studied CO₂ laser drilling of fused quartz and found that the holes in quartz had a larger taper than the holes in stainless steel. They attributed this to the difference in the properties between metals and refractory oxides. They also presented an analytical method to extrapolate their results to other refractory oxides.

Lusquiños et al. (1997) undertook experiments to investigate the feasibility of using a Nd:YAG laser to drill slate tiles. Slate is primarily used as a roof building material and is composed mainly of quartz, clorite, and sericite. They are typically fixed to roofs by clamps or nailed to the wooden sub structure through holes manufactured by mechanical means. It was the intention of the authors to produce better quality holes in the slate with reduced manufacturing time. A 1 kW Nd:YAG pulsed laser was used on slate tiles between 3-15 mm thick and hole diameters up to 1 mm. Nitrogen gas assist was

used. The parameters of the multimode beam were varied between 50 to 800 W average, 2 to 50 J energy pulses, and 0.5 to 2.5 ms pulse width. An achromate doublet lens with an 80 mm focal length was used to focus the laser beam. Gas assist pressure varied from 2×10^5 to 8×10^5 Pa. The authors found reasonable correlation between the geometrical characteristics of the hole and various process parameters but the range of parameters that would produce complete drilling was limited in the 12mm thick slate. 1. Increasing pulse energy decreased the number of pulses required for complete drilling. (Writer's note: Apparently, an exponential decay relationship) 2. At lower average power (100 W) the inlet diameter decreases with increasing pulse width and increased gas pressure. 3. The hole profile at this power level is tapered and barrel shaped which decreases with increasing pressure. The effect is dependent primarily on the gas pressure since the process is fusion related. 4. At higher average power levels, inlet diameter has no significant dependence on the pulse width and the gas pressure. This occurs because of the 'recoil-momentum' effect caused by the vaporization process. 5. Barreling and taper of the hole profile is reduced at higher power outputs. The authors conclude that this laser process can well suit the goals stated previously.

One of the few papers that dealt with empirical studies of laser drilling of advance materials was that done by Chen et al. (1996). They investigated the effects of laser peak power, pulse duration and wavelength in the drilling of three advanced materials: NiAl, N5 and SiC CMC. It was demonstrated that cracking in NiAl was greatly reduced when high peak power, short laser pulses were used. Recast layers in all three materials were generally thinner when high peak powers, short pulse duration or long pulse bursts were employed.

In this study, three advanced materials were chosen for experimental investigation. They were 1) nickel aluminide (NiAl) alloy, 2) N5, a single crystal nickel based super alloy, and 3) a silicon carbide ceramic matrix composite. The parameters for investigation were: 1. long pulse versus short pulse drilling at 1.064 μm wavelength. 2. short pulse drilling at 1.064 μm wavelength versus 248 μm .

The long pulse, low average power conditions were: 50 W average power, 16.7 kW peak power, 0.6ms pulse duration, 5 Hz repetition rate, and multimode beam quality of 40 mrad for the M34 Nd:YAG rod laser. The conditions used for the JK704 Nd:YAG rod laser were: 140 W average, 5.8kW peak, 2.1ms pulse burst (with each burst having a 50% duty cycle, 0.6 ms period square wave like pulse), 20 Hz repetition rate, and multimode beam quality of 25 mrad. Focal lengths for both were 15.24 cm; conventional gas assist with shop air was used.

A MOPA (master oscillator power amplifier) Nd:YAG laser was used for producing short pulses. Short pulse, high peak power laser conditions were: For Q-switched pulse duration: 300ns. Pulse rate: 5 kHz and peak power 70kW. For Q-switched and mode locked pulse duration: 260ps 12ns apart. Peak power was 4mW. For both, a lens with a focal length of 40.0 cm was used and wavelength was 1.064 μm . Gas assist was compressed air at 100 psig. Drilled hole diameter was 0.13 mm.

For the short pulse drilling comparison of the wavelengths at 1.046 μm and 248 nm, a KrF excimer laser was used. A lens with 10 cm focal was used. The sample was placed at 7.94 cm away from lens. The focal spot size was 0.3 x 0.3 mm. The laser parameters for the excimer were 160mJ per pulse. 180 Hz repetition rate, and 29 W

average. The nominal pulse duration was 30 ns and the corresponding peak power was 5mW. Drilling was performed in ambient atmosphere with no assist gas.

For these experiments, holes were drilled at 30 degree angle to the surface. The result for each material is as follows. For the single crystal intermetallic nickel aluminide (NiAl) alloy, a summary of the laser drilling characteristics is shown in the table below.

Table 2 Laser drilling characteristics for NiAl.

Laser Type	M34	JK704'Burst'	MOPA switched	Q- MOPA switched/ mode locked	Excimer
Recast layer thickness	20-250 μm	20-50 μm	50 μm	50 μm	0-250 μm
Crack length	mm range, into bulk	mm range, into bulk	50 μm confined to recast layer	50 μm confined to recast layer	up to 100 μm , but very few
Drill time	1.2 sec	1.2 sec	0.25sec	0.5sec	960sec

For single crystal nickel-based super alloy N5, the results are shown in the following table. This material did not have laser-induced cracks.

Table 3 Laser drilling characteristics for M5.

Laser Type	M34	JK704'Burst'	MOPA switched	Q- MOPA switched/ mode locked	Excimer
Recast layer thickness	200 μm	10-50 μm	10-100 μm	10-100 μm	10-50 μm
Crack length	-	-	-	-	-
Drill time	1.2 sec	1.2 sec	1 sec	0.5sec	600sec

For the silicon carbide ceramic matrix composite (SiC CMC):

Table 4 Drilling characteristics for SiC CMC.

Laser Type	M34	JK704'Burst'	MOPA switched	Q- MOPA switched/ mode locked	Q- Excimer
Recast layer thickness	50 μm	50 μm	25 μm	25 μm	none observable
Crack length	-	-	-	-	-
Drill time	2-3 sec	2-3 sec	8 sec	8 sec	113 sec

Some conclusions drawn for the above materials are: 1. For NiAl cracking is reduced when high peak power, short laser formats are used. 2. Recast layer is reduced in all materials by using shorter pulses or shorter wavelength.

Another paper by Ghosh, et al. (1996) deals with parametric studies on laser cutting and drilling of zircaloy-2 with a Nd:YAG laser. Tests were carried out on 1.1 mm and 0.74mm thick sheets of zircaloy-2. A 300 W average power pulsed Nd:YAG laser was used. Argon was used as the assist gas. TEM₀₀ mode was used with a spot sized of 3.7 μm . The power density was $6 \times 10^5 \text{ W cm}^{-2}$.

The parameters of pulse energy, pulse duration, distance of nozzle to work piece, cutting speed and gas pressure were varied to observed the effect on cut quality. The criteria for a quality cut were kerf width, minimum burr around kerf, good surface finish and minimal taper across the laser cut. Also, cutting efficiency was evaluated, as well as, the microstructure and micro hardness of the heat affected zone. Observational results show that striations due to intermittent flow of molten material is typical but the cutting accuracy was still $\pm 0.025 \text{ mm}$.

Durand et al. (1996) used a short pulsed Nd:YAG laser for machining silicon nitride. The cuts were made crack free and exhibited promising characteristics for precision laser machining of such materials. They analyzed the cut kerf geometry and modeled it as a function of energy density. Their model proved fairly accurate for lower level energy densities, but the amount of material removed was found to increase with an increase in energy density up to a maximum point followed by a decrease with finite increase in energy density.

Bar-Isaac et al. (1974) studied pulsed ruby laser drilling of copper, aluminum, and lead for different focal positions. They measured the hole depth at different times and found moderate agreement with their model, assuming that the heat conduction effects were negligible. Paek and Zaleckas (1975) investigated scribing of alumina. They compared the performance of the CO₂ and Nd:YAG lasers noting that the YAG laser gave a smoother edge but left unwanted debris on the surface. This was attributed to the absorption coefficient being lower at shorter wavelengths resulting in sub-surface evaporation and explosive removal of particles, rather than surface evaporation.

Lukacs et al. (1995) have made preliminary studies in the copper-vapor laser cutting of silicon wafers and PZT.

Von Allmen (1976) drilled copper samples with Nd:YAG pulsed laser. He studied the phenomenon of liquid explosion and identified four regimes: (i) at intensities below 10^5 W/cm^2 the drilling mechanism is evaporation; (ii) in the range $10^5 - 5 \times 10^6 \text{ W/cm}^2$ there is a region of instability, causing oscillatory behavior; (iii) above $5 \times 10^6 \text{ W/cm}^2$ the power is high enough for liquid expulsion and the drilling is stable; and (iv)

above 10^9 W/cm^2 the laser beam is partially blocked due to absorption of the laser beam by the super saturated vapor and plasma above the material.

Wallace et al. (1983,1986) demonstrated the feasibility of several shaping operations based on overlapping grooves, including turning, threading and milling hot pressed silicon nitride. They also studied the effects of laser beam polarization on the shape of the groove and its dependence on the scanning direction of the laser beam. Affolter and Schmid (1987) studied the laser machining of various ceramics such as aluminum oxide, silicon carbide, silicon nitride etc. with a Nd:YAG laser. They found best results were obtained with high powers and short pulse times. They also found extensive micro cracking and expected a serious reduction of mechanical strength due to laser machining.

Sheng and Liu (1995) have discussed a laser based technique for finishing axisymmetric parts which allows efficient finishing of polymers and ceramics without tool wear, tool breakage or cutting forces. The process consists of a laser beam impinging tangentially on to the surface of a cylindrical workpiece. Asperities on the workpiece can be removed through vaporization (for plastic and composite materials) or melting (for ceramics and metals). Thus, a flexible machine tool can be developed to grind parts of differing geometries and materials by changing process parameters instead of setups or machines, as well as integrate primary machining and secondary finishing in one machine tool. Using oblique beam impingement angles can enhance the precision of the laser finishing. The paper presents the elements of the laser machine tool and preliminary results on the parametric dependencies for laser finishing of polymer workpieces. The

operating parameters which affect the surface finish are the rotational speed of the workpiece, feed, beam power and oblique beam angle.

Yamamoto and Yamamoto (1987) studied laser cutting of silicon nitride with a CO₂ laser. They found that flexural strength of the laser cut material was only 35 % of the flexural strength of the uncut material. They attributed this to the microcracking during the laser cutting process. Saifi and Borutta (1975) have discussed the laser scribing parameters for aluminum oxide, which optimize the flexural strength for annealed and non-annealed substrates while allowing easy separation of the ceramic along the scribed line. Laser parameters such as pulse length, peak pulse power and spacing between successively drilled blind holes have been investigated. The force is measured using a piezoelectric transducer. The flexural strength is measured using a 4-point loading fixture. The authors found that increasing the pulse length > 0.8 ms did not decrease the separation force markedly. However, thermally induced cracking was observed near the scribed region. In certain applications, annealing of the ceramic substrate would be necessary after scribing to relieve the thermal stresses. This causes grain growth and re-sintering of material in the blind holes causing an increase in the separation force. Study of the scribed region with high magnification SEM showed columnar grains. For larger pulse lengths, the columnar grains are deeper and scribing induced cracks are visible on surface and in cross section. The authors have concluded that short pulse lengths with high peak power gives better results in terms of lower separation force and better flexural strength retention during the scribing process.

Wallace et al. (1986) studied the characteristics of the groove formed in hot-pressed Si₃N₄ with a CO₂ laser beam at normal incidence angle when the workpiece is

moved with respect to the laser beam. They observed that the groove curves out of the plane defined by the velocity direction of the workpiece. The curved cross sections change from one side of the plane to the other if the velocity direction is reversed. This effect is more prominent at the lowest velocities and highest incident powers. The cross section was shown to vary systematically with the angle between the velocity direction and the direction of the electric vector of the incident beam, which was found to be partially polarized. They have proposed a mechanism for the curved cross section effect based on the existence of a significant difference in reflectance between the transverse electric (TE) and transverse magnetic (TM) reflections from the groove walls in Si_3N_4 for large angles of incidence. Calculations of the values of reflectance for the TM and TE reflections as a function of the angle of incidence show the existence of a large difference for the CO_2 beam wavelength of $10.6 \mu\text{m}$.

Eberl et al. (1992) machined three-dimensional pockets into materials, such as silicon nitride using multiple pass scribing and elaborate feedback control loops. Trubelja et al. (1992) studied laser scribing and cutting of carbon fibers in silicon carbide matrix composite with special emphasis on strength reduction and material removal mechanism. They found that extensive redeposit on the groove surface was β -SiC and carbon. They also found that the laser-cut samples retained 80 % of the strength of diamond cut samples. Full strength was recovered after removing $180 \mu\text{m}$ from the surface of the laser-cut material.

Trubelja et al (1994) have studied the CO_2 laser scribing and cutting on a carbon fiber-silicon carbide -matrix (C/SiC) composite containing 45% vol. of carbon fibers.

Scribing and cutting were performed in continuous wave (CW) mode using laser powers between 750 and 1500 watts, specimen translation speeds between 0.5 to 4 cm/sec and laser spot size of 300 mm in diameter. Analyzing the groove depth and width as a function of laser power and specimen translation velocity, the authors have observed that the fibers and matrix end abruptly and there is an extensive refilling of the groove. This is attributed to the ablative decomposition of this material, with the evaporated material re-condensing downstream of the laser beam. SEM examination of the groove cross section also showed extensive re-deposition of carbon and silicon carbide. X-ray and Raman spectroscopy analysis of the laser cut surfaces showed the presence of β -SiC and graphitic carbon formed by the condensate. It was also observed that there was a decrease in the bend strength of the laser cut surface by 20% compared to the corresponding strength of diamond cut material. This was attributed to the existence of heat affected zone (HAZ). However, removal of this zone by grinding facilitates in recovering the strength of the material.

Chen et al. (1997) investigated the effects of laser drilling of intermetallics, superalloys, and composites using the second harmonic wavelength of 532 nm of a high peak power Nd:YAG laser. These results were compared to the results of those at the fundamental wavelength of 1060 nm and it was found that undesirable thermal effects, such as recast layers and heat affected zones, were reduced.

Zhang et al. (1996) have studied the effects of laser machining on ceramics in terms of surface morphology, flexural strength and its variances under various machining conditions. Weibull modulus 'm' is introduced to measure the degree of variation in strength. The authors conducted their test on SiAlON 501, which is a silicon nitride

composite material. The beam parameters varied in the experiment were the pulse frequency, pulse energy (E), and the feed rate. Machining was performed under a coaxial jet of compressed air. The experimental results indicate that micro-cracks and thermally affected layer increase with increasing pulse energy E and feed rate of the ceramic workpiece but decrease very little when the pulse frequency was varied from 18 to 30 Hz. Formation of cracks result from the high power intensity of the laser beam, with very steep temperature gradients being created in the material, that causes high localized thermal stress wave. Further stress arises from recoil pressure due to evaporating surface atoms. Finally, re-solidification further imposes stress, which at the end exceeds the fracturing limit of extremely brittle ceramics. Thermal stress σ is estimated by the equation:

$$\sigma = E\alpha\Delta T$$

where: E=Young's modulus, α = coefficient of thermal expansion, and ΔT =Temperature rise.

In laser machining of ceramics, the maximum theoretically estimated value of σ is about 5-25 GNm^{-2} , which far exceeds the bend strength of ceramics. Hence the microcracks are not avoidable. The authors have also found that the mean flexural strength is about 40% of the original value of the material which, they reason is due to the thick thermally affected layer and the cracks in it caused by thermal shock.

Lunau et al. (1969) studied the effects of assist gas jet while cutting with a CO_2 laser. This was motivated by the need to increase cutting efficiency since metals have a high reflectance at 10.6 μm . They found that the use of assist gas increases penetration

by up to 20%. It also made the cut width less tapered. They attributed these effects to the transfer of heat from the vaporized material to the uncut material at the bottom. Duley and Gonsalves (1974) studied oxygen-assisted cutting of stainless steel and found that oxygen assist increased the minimum cutting speed by factors ranging from 1.5 to 2.5 for different thickness'. However, there is an optimum level of gas flow beyond which the minimum cutting speed decreases. They also found that this optimal flow rate was independent of the laser power. They presented some sample calculations to show that the cooling effect of the assist gas is insignificant and that the exothermic oxidation of iron is insufficient to provide such a large increase in the minimum cutting speed. They speculated that the increase might be due to the ability to remove material at temperatures below the melting point, which is somehow caused by the addition of oxygen.

In laser cutting, an erosion front (liquid gas region) forms at the momentary end of the cut. The material removal rate is dictated by laser heating, exothermic reactions and shear force between the gas flow and the molten layer. Standard coaxial gas -assisted laser cutting for thicker steels does not provide satisfactory performance since the oxide dross clings to the bottom edge of the cut and forms a hard burr. This phenomenon is more prominently observed in the laser machining of stainless steel due to the low fluidity of the melt and the high melting point of chromium oxide, which restrains oxygen diffusion into the molten cutting front. One solution to this problem is to use high pressure gas in the coaxial nozzle. However, this leads to fracture of the focussing lens and the formation of a Mach shock disc (MSD), which causes large variations in the effective gas pressure acting on the workpiece. The principle of the off-axial gas jet is to

provide straight non-turbulent flow to the cutting erosion front, causing further oxidation reactions and transferring momentum to the molten slag and dross. Ilavarasan and Molian (1995) have studied the laser cutting of thick-sectioned steels using gas flow impingement on the erosion front. The investigators have developed an off-axial gas jet that extends the laser's effectiveness by improving the rate at which the parts can be machined, producing high quality surfaces, increasing the cutting thickness, and increasing the range of materials that can be machined. Molian (1993) has developed a dual-beam technique involving two CO₂ gas lasers with a power capacity of 1.5 kW each to cut steel and super alloy. It was found that dual beams were capable of enhancing the cutting thickness and speed without deteriorating the quality of cut.

Thomassen and Olsen (1983) investigated the effects of nozzle pressure and cutting speed on the quality of cut in steels. They found that significant cutting characteristic differences are observed between mild steel and stainless steel, although they are similar materials, indicating that even minor material compositional differences can impact cutting characteristics. Powell et al. (1985) showed that the striations that occur during gas-assisted laser cutting are due to a periodic formation of melt phase. They show that pulsing the laser at twice the frequency of striations could minimize the roughness due to these striations. Schuocker (1986) presented a model for calculating dynamic effects (such as striations) during reactive-gas-assisted laser cutting. He also presented a method to calculate the energy gain due to reaction occurring at the interaction zone using a simple mass and energy balance.

Fieret et al. (1987) presented an overview of supersonic gas-assist effects in laser cutting. They found that the maximum cutting speed is positively correlated to cutting

pressures. Further, the occurrence of a Mach shock disc with the possible formation of a vortex ring can be associated with poor cutting performance.

Zhang and Modest (1998) investigated the effect of temperature on the absorptance of ceramics for Nd:YAG and CO₂ laser processing applications. Experimental results for graphite, alumina, hot pressed silicon nitride, sintered α -silicon carbide, SiC/SiC ceramic matrix composite, and carbon fiber SiC matrix composite. Silicon nitride had an absorptance of 0.84 to 0.86 between 1500 K and 2200 K at 1.06 μm and increased from 0.18 to 0.60 at 10.6 μm . For silicon carbide, for temperatures between 1500 K to 2500 K, the absorptance varied from 0.87 down to 0.72 at 1.06 μm and increase from 0.57 to 0.80 at 10.6 μm . The absorptance for graphite, for temperatures between 1500 K and 3500 K, varied from 0.94 to 0.96 at 1.06 μm and increased from 0.71 to 0.84 at 10.6 μm . The absorptance for alumina between 1500 K and 3000 K increased from 0.12 to 0.95 at 1.06 μm . No data was provided for alumina at 10.6 μm because of possible damage to the testing apparatus because of the low absorptance. For temperatures between 1500 K and 3000 K, the absorptance varied from 0.86 to 0.92 at 1.06 μm and varied from 0.88 to 0.94 at 10.6 μm for the carbon fiber silicon carbide composite. For temperatures between 1500 K and 3000 K the absorptance of SiC/ SiC composite varied from 0.92 to 0.93 at 1.06 μm and varied from 0.68 to 0.90 at 10.6 μm . This data is useful in predictive modeling of the laser processing of these materials. The great variance in absorptance of alumina with respect to temperature gives an indication that multiple internal reflections of the laser beam are more likely for this material.

Zhang and Modest (1998), in a subsequent publication, continued with empirical investigations to determine the amount of energy required to remove a unit mass of material. Materials tested were graphite, hot-pressed silicon nitride, and sintered alpha-silicon carbide using laser irradiation from Nd:YAG and CO₂ lasers.

Several researchers have investigated laser machining of glass and glass-ceramic matrix composite. Finucane and Black (1996) have examined the various laser cutting parameters required to generate a cut surface in glass which will require minimal post treatment to be carried out. The results obtained by them through their numerous experiments on various stained glasses were used to generate a database giving the various parameter settings. Tuersley et al. (1996) carried out tests to emphasize the influence of SiC fiber glass-ceramic matrix phase's ability to couple with the 1.06 μm emission of the Nd:YAG laser. Tuersley et al. (1998) continued research into the machining of SiC fiber/ borosilicate glass composites with a paper focused on the optimization of the laser beam parameters and the second focused on the effect of process variables. Allcock et al. (1995) have investigated the CO₂ laser marking of soda-lime and borosilicate glasses as a function of laser fluence and pulse duration. They have analyzed various fracture mechanisms. Residual surface stress following rapid laser heating has been identified as the most likely cause of microcracking. Gas phase products evolved during the interaction of the laser with glass have also been evaluated using spectroscopy of the luminous plume and fast photography techniques.

Todd and Copely (1997) describe in detail a prototype laser processing system for the shaping of advanced ceramics. Based on the data of many other researchers, as well as patent information, the authors describe how three dimensional shaping of silicon nitride.

an advanced ceramic, could possibly be performed with a CO₂ laser by controlling incident power, beam polarization, position of the focal plane, orientation of the beam relative to the surface, beam speed, and feed. Issues such as the reduction in strength are discussed, as well as, postoperative treatments to recover the reduction in strength.

Yilbas (1997) presents a study on the effect of the laser parameters and material properties on the laser drilled hole quality. Using a factorial design statistical approach the hole geometry is evaluated by assigning a relative value for each geometric feature based on the importance of that feature. The materials used in this study were stainless steel, nickel, and titanium.

Laser drilling involves the use of a stationary laser beam that utilizes its high energy density to melt or vaporize the material from the workpiece. The method of material removal is called percussion or on center drilling [Chryssolouris, 1991]. Figure 15 shows a schematic of the laser drilling process. Laser drilling is based on the energy balance between the irradiating energy from the laser beam (energy absorbed to melt/vaporize the work material), the conduction of the heat into the work piece, and the energy loss to the environment. The incident beam for drilling has a Gaussian spatial intensity distribution (Figure 16) produced by operating the laser in the TEM₀₀ mode. This thesis will focus on the one dimensional laser processing or laser drilling of advanced materials. Although geometrically simpler than 2-D and 3-D laser processes, i.e. cutting and shaping, in some respects, laser drilling is a more complex process than 2-D cutting because of the dynamic geometry of the laser-drilled hole.

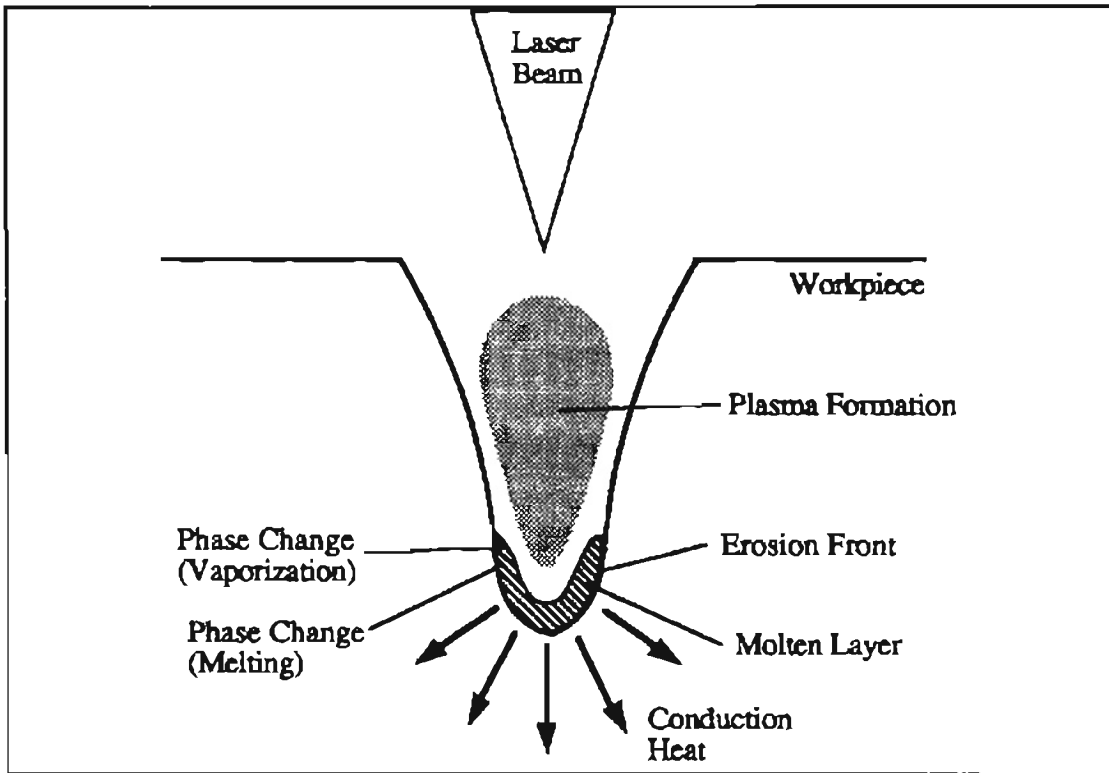


Figure 15 Diagram of laser drilling.

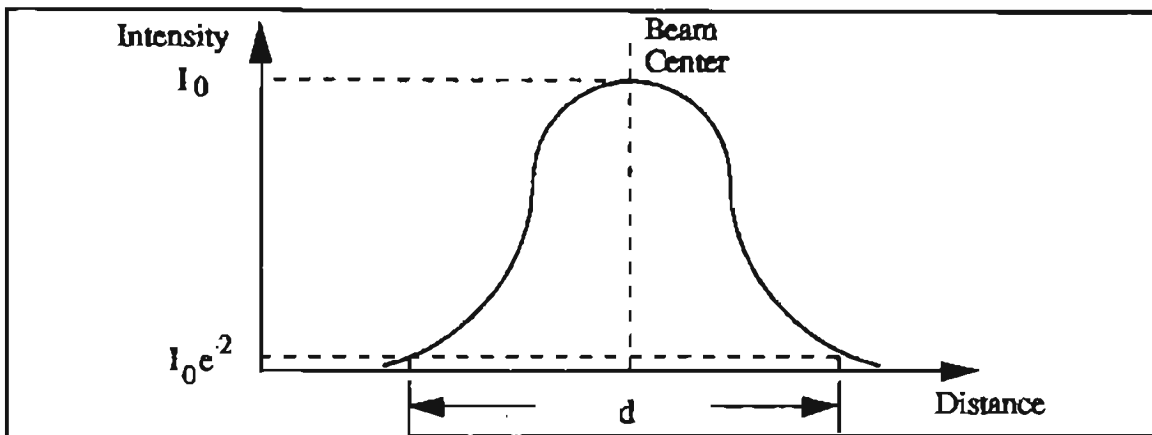


Figure 16 Spatial intensity distribution for TEM_{00} laser beam.

Theoretical Work on Laser Drilling and Cutting

Modeling as heat source on surface

A more general theory of the laser drilling process would be useful in the understanding and control of laser processing of advanced materials. The difficulty in doing so arises from the complexity of the laser drilling process. Depending on the material properties, phase changes can occur from solid to liquid to vapor and possibly plasma. All phases of material can be ejected from the drill site due to the explosive nature of the process though typically molten and vaporized material predominates. Theoretical efforts on modeling laser machining have centered on the solution to the classical heat conduction equation for a stationary or moving semi-infinite solid. Different cases have been studied with and without phase change for a variety of irradiation conditions. Since the pulse durations considered in this study are long ($\sim 20 \times 10^{-5}$ s) compared to the overall energy relaxation time of the molecular vibrations (10^{-13} s to 10^{-6} s), heat may be considered to be propagated according to Fourier's law.

A number of researchers have modeled the laser drilling process, starting from the simple case of heating of a surface with no phase change. Others have modeled a solid to liquid phase change with the melt removed as it occurs. Modest (1993) uses a general energy parameter to model material removed by ablation, micro-explosions, expulsion, etc. Jones et al. (1983) models the drilling process using a thermal balanced concept, considering that material is removed by both liquid expulsion and vaporization.

The simplest situation from a modeling standpoint is that of laser drilling with a conduction model being used to identify a melt or an ablative isotherm. Ready (1965) was one of the earliest to present an analysis specifically for calculating hole depths for

pulsed laser drilling of metals. He distinguished between moderate and high power (Q switched) pulses phenomenologically, and presented a simple one-dimensional transient model to predict hole depth. Paek and Gagliano (1972) developed an axisymmetric conduction-heating model for laser drilling of alumina. They used the calculated temperatures to calculate thermal stresses for this brittle ceramic material.

Yue et al. (1996) have developed a model to predict the profile of laser drilled hole based on the concept of threshold intensity and have extended the model to apply to deep penetration laser welding. The common ground for laser drilling and welding as well as their divergences are discussed in this paper. Brugger (1972), Maydan (1971), and Lax (1971) have solved the non-moving slab problem assuming that the intensity of the incident beam decays exponentially with distance into the material, i.e., volumetric absorption.

The modeling problem is more difficult when phase transition takes place. Dabby and Paek (1972) presented a one-dimensional transient conduction model while including the penetration of radiation into the medium and vaporization. They found that it is possible for material removal to occur by the mechanism of sub-surface explosions.

While still using a one-dimensional model to describe laser drilling, von Allmen's study (1976), also considered the expulsion of material. He assumed that part of the liquid vaporizes according to the rate equation given by Batanov et al. (1973) and that if the pressure build-up due to the evaporation is strong enough, the liquid is forced out along the walls by laminar flow. Borsch-Supan et al. (1984) considered internal evaporation by including the fact that a change of state does not occur at a fixed temperature but rather according to a rate equation of the Arrhenius type. They assumed

that any evaporated material could freely escape from the solid (making explosive removal of solid impossible).

Risch and Laub (1990) developed a model for one-dimensional ablation that includes translational non-equilibrium gas flow at the surface, thermochemistry and in-depth heat conduction. They found good agreement for carbon phenolic at radiances from 0.3 to 5 kW/cm². Wei and Ho (1990) studied quasi-steady drilling of metals and presented a model that identifies interfaces while including the effect of surface tension forces and vapor pressure. They found limited agreement with experimental results for copper by assuming complete absorption of laser energy.

The modeling problem becomes even more complicated (three rather than two-dimensional) if the laser is moved across the target (welding, cutting and scribing). Gonsalves and Duley (1972) used a moving point heat source solution from Carslaw and Jaeger (1959) to make comparisons with experimental data for CO₂ laser cutting of stainless steel. A general heat conduction solution was given by Modest and Abakians (1986), who studied a moving, semi-infinite body irradiated by a Gaussian laser source either uniformly in time or in pulsed mode. The process of scribing with a moving laser was modeled by Modest and Abakians (1986) for irradiation by a CW laser with Gaussian energy distribution onto an opaque semi-infinite solid. They included the effect of angle of incidence of the laser beam with respect to the walls of the groove. They assumed one-step evaporation of the material (without beam interference), parallel laser beams, negligible reflection effects, and small heat losses. The conduction heat losses were calculated using simple integral method. The assumption of a parallel laser beam was later relaxed by Biyikli and Modest (1988) who investigated the effects of beam

focusing and focal plane position. In a follow up paper by Abakians and Modest (1988), semi-transparent bodies were considered; they showed that materials would have to display substantially different behavior as compared to surface absorption of laser energy.

Roy and Modest (1990) developed a model where one of the weakest assumptions made by Modest et al. (1990, 1991, 1992) was relaxed. Rather than treating conduction losses in a quasi-one-dimensional fashion, the full three-dimensional conduction was solved using the boundary element method. They reported that a more accurate treatment of heat conduction losses has a considerable effect on the depth of the groove, for small scanning speeds. They also found that the groove width is always predicted well by the quasi-one-dimensional model of Modest and Abakians (1986).

Bang and Modest (1991, 1992) included multiple reflection and polarization effects in deep grooves for materials of low absorptance. They conclusively showed that beam trapping (specular or diffuse) substantially reduces the taper of the groove and increases the material removal rate, particularly at low scanning speeds. They obtained good agreement with experimental data for silicon nitride considering the uncertainties in the knowledge of material and laser parameters.

Modest and Ramanathan (1994) have developed a three-dimensional model to predict the temperature distribution inside the solid, and the shape of one or several overlapping grooves formed by partial evaporation of a thick, rectangular body, when the body is irradiated by a moving laser source. The governing equations are solved using a finite-difference method on a boundary fitted coordinate system. Results are presented for ablative groove development, including the effects of laser entry and exit, single and overlapped groove shapes and temperature distributions in the solid at different traverse

speeds, pulsing conditions and power levels. The authors obtained good qualitative agreement between the theoretical and experimental results.

Yilbas (1997) examined the heat transfer mechanism, including conduction, phase change and convection processes taking place during Nd:YAG laser irradiation of steel workpieces. To validate the theoretical predictions, optical methods and streak photography techniques were employed and they found that surface temperatures and evaporating front velocities obtained theoretically are in good agreement with the experimental results. Mazumder and Steen (1980) had also developed a three-dimensional heat transfer model for laser material processing with a moving Gaussian heat source. Sami and Yilbas (1996) have numerically solved the heat transfer mechanism relevant to pulsed laser heating using the kinetic theory approach for different types of laser pulses.

A number of researchers have investigated laser heating of metals with temperature-dependent material properties (absorptivity, thermal conductivity, and volume heat capacity). Dobrovolskii and Uglov (1974) analyzed the effect of heating a semi-infinite slab with a Gaussian laser beam where the surface absorptivity varied linearly with temperature. They solved for the two-dimensional temperature distribution and compared the result of their theory to a one-dimensional model neglecting radial effects. Nissim et al. (1980) treated the moving laser beam with elliptical beam profile, assuming conductivity to be temperature dependent. Rykalin et al. (1982) numerically solved the temperature distribution in a laser-heated slab with absorptivity, thermal conductivity and volumetric heat capacity all varying with temperature. They showed that the combined effect of non-linearities gives substantially new results in a number of

cases. Yilbas and Al-Garni (1996) proposed a heat transfer model that provides useful information on the laser induced interaction mechanism. Steady state and time dependent heating models are introduced and temperature profiles inside the materials were predicted.

The surfaces of most metals and some ceramics subjected to laser irradiation, which attain high temperatures, are oxidized. This in turn leads to very different absorptance values, particularly for metals. For example, pure aluminum has a reflectance of 98% at the CO₂ laser wavelength of 10.6 μm. However, oxidized aluminum, i.e., alumina (Al₂O₃), has a reflectance of only 2% at this wavelength. Thus, the effects of chemical reactions at the surface are important and have been studied by a number of authors. Uglov et al. (1983) calculated the effects of oxidation on metallic targets and concluded that the non-linearity due to oxidation must be included in modeling. Kirichenko and Luk'yanchuk (1983) analyzed theoretically the kinetics of oxidation reactions for metal specimens in air during laser heating. They found that those points on the surface that are at a higher temperature oxidize faster and consequently absorb more energy resulting in thermal runaway. This results in much stronger temperature gradients in the material, than if the effects of oxidation are neglected. Roy et al. (1991) studied the effects of variable thermal properties on laser scribing using a three-dimensional conduction model. They found that the effect of variable properties could affect groove depths and material removal rates by 20%. They measured the normal spectral reflectivity for silicon carbide and silicon nitride. They measured the variation of reflectance between 9 and 11 μm, at temperatures up to 1273 K.

Engin and Kirby (1996) have recently developed a laser machining model for ceramics and glass ceramics from the analytical treatment of a one-dimensional vaporization problem with a distributed heat source. The developed solutions are used to predict the behavior of high intensity Nd:YAG laser pulses on a typical ceramic or glass ceramic material. Predictions include the critical intensity required for vaporization of material, material removal rate, thickness of the affected residual surface layer after a single laser pulse of given shape and intensity.

Borkin et al. (1985) studied the effects of self-focusing of radiation in the case of laser drilling of metals for different polarizations. They showed that beam-guiding effects are very different in opaque metals as opposed to transparent insulators. They also found that in the case of metals most of the reflections are relatively tangential to the surface (whispering gallery modes) while in insulators the reflections are relatively normal to the surface (bouncing ball modes). They found that beam-trapping effects in some materials could lead to a drop-shaped cavity.

Yakovlev (1996) has proposed a model for the structure of glass that makes it possible to analyze changes in its properties under various heating regimes. He has shown that the change in the properties of glass as temperature varies is associated with the temperature dependence of the concentration of oxygen-atom vacancies. He has also proposed an analysis of the sharp change in the properties of glass upon heating using a modified model involving structural phase transitions. Atanasov and Gendjov (1987) have proposed a theoretical model for laser cutting of glass tubing. The thinning down of the wall of the glass tube has been taken into account in the model. The dependence of the duration of cutting upon absorbed laser power has been derived and compared with

experimental data. This model gives a good physical comprehension of the laser cutting of glass tubing through melting.

Modeling from Fundamentals:

It is apparent from an overview of the research literature that the laser drilling process is indeed complex. In essence we have a highly concentrated beam of photons interacting with matter. The primary reaction to this interaction is the conversion of the photon's energy into thermal energy within the workpiece as the photon is absorbed by the electrons. This is true for wavelengths in the infrared and visible region but becomes a photochemical reaction as the photon energy reaches the level required to uncouple chemical bonds. Since the wavelength produced by the Nd:YAG laser produces a thermal process, most of the research concentrates on modeling the laser drilling process as a surface heating phenomena. Research that models the laser drilling process from a more fundamental basis of photon interaction with matter is not as prevalent in the narrow category of laser drilling but would, in this researcher's estimation, provide useful information in modeling the laser drilling process.

Interestingly, numerical methods and high speed computing could be useful in modeling the laser drilling process. At the Oklahoma State University Advanced Manufacturing Process and Materials Research Laboratory, research in molecular dynamics (MD) modeling, used to model the mechanical removal of materials, could also be used to model the laser drilling process, given some fundamental information on the physics of the photon/workpiece interaction.

In situ Measurements during Laser Processing

The measurement of material, process and laser parameters during laser processing is critical to enhance the understanding of the process. This information can be utilized to obtain better results from the process by using control and feedback loops. The measurements are also useful in providing new data on phenomena, which may be used to model the problem more accurately. However, most of the general literature is limited to presenting laser and process parameters that yield the best quality of cut. This information is often incomplete and is not of much use to others seeking to understand how measurements are taken. How some of the measurements made during laser processing will now be reviewed, followed by a detailed review of the literature on measurement of temperature and reflectance during laser processing.

Arnot and Albright (1983) photographed the plasma plume during CO₂ laser spot welding of steel. They found that plasma plumes were always larger in argon than in helium. They also found that the plasma of argon detached from the surface at high power densities preventing any further heat input to the target surface. Arata et al. (1984) photographed the plasma during CO₂ laser welding of steel using high speed photography and transmission X-ray methods. They found that reducing the ambient pressure to a few torr completely suppressed the plasma plume and yielded substantially higher penetration.

Ramanathan and Modest (1995) have used high speed photographic techniques to study plumes generated during drilling of ceramic and ceramic composites with a CO₂ laser. The principal objective of this study was to identify the mechanism of material removal (spattering, particulate and fiber debris, liquid droplets) and plume phenomena.

High speed photographic visualization (1000 frames per second) was undertaken for two monolithic ceramics, sintered α -SiC and hot pressed silicon nitride plus two continuous fiber-ceramic matrix composites (C-SiC) and silicon carbide fibers in a silicon carbide matrix. This study has provided several valuable insights into the material removal mechanisms and plume phenomena. It was observed that the plumes for ceramic-based materials were not as luminous or dynamic as that observed for steel. The plumes were initially tall and columnar and rapidly diminish to an approximately Gaussian shape, after which the shape remain relatively unchanged. This observation has led the authors to believe that during the initial phase the material removal mechanism is vaporization for all the materials under study. Subsequently, the material removal mechanism is purely ablative for monolithic α -SiC and graphite, while the removal process is aided by periodic ejection of liquid silicon for silicon nitride and by fiber/particle ejection in the case of continuous-fiber/ceramic-matrix composites viz. C-SiC and SiC-SiC. This macroscopic ejection of material in the composite materials is attributed to stress build-up and fracture in the voids of these materials, eventually resulting in the expulsion of matrix and fiber.

Grum and Zuljan (1996) have analyzed the heat effects in laser cutting of steels. They analyzed the emission of infrared rays from the cutting front with a photodiode, statistically analyzed the temperature signals and optimized the laser cutting process based on a critical cutting speed. The measured infrared radiation was converted into a temperature reading that was related to the formation of macro- and microstructures and to the change in the microhardness in the surface layer of the cut. On the basis of the

experimental results the authors proved that heat effects in the cutting front decisively influenced the quality of cut.

One of the problems in dealing with ceramics (as compared to pure metals) is that ceramics, upon heating, may decompose into a variety of compounds over a wide range of temperatures. Thus, in order to determine the decomposition reaction and the decomposition temperature, elaborate thermodynamic equilibrium calculations or accurate measurements of the reaction coefficients need to be undertaken. Kinetics and mechanisms for thermal decomposition of silicon nitride were calculated by Batha and Whitney (1973). They reported that their calculations agreed with other mass spectroscopic studies. Their calculations showed that silicon nitride decomposes into liquid silicon and nitrogen and provided equations for the rate constant of the reaction. Drowart et al. (1958) studied the thermal decomposition of silicon carbide using mass spectrometry and found that the predominant vapor species are Si, SiC₂ and Si₂C. Scace and Slack (1960) found that SiC dissociates into carbon and a silicon rich liquid around 3100 K. Baird and Taylor (1958) reported that silicon carbide decomposes at temperatures between 2600-2750 K into carbon and a silicon rich vapor under high pressures. DeBastiani et al. (1990) performed some CO₂ laser scribing experiments and found no evidence of any liquid phase in the groove. They also found that during laser scribing, different dissociation products are obtained for single crystal silicon carbide and sintered silicon carbide, probably due to sintering additives. Singhal (1976) presented a thermodynamic analysis for silicon nitride and silicon carbide at high temperatures in an oxidizing atmosphere. He reported that the partial pressure of Si vapor at 2000 K is substantial and may limit its high temperature application. He also determined that the

decomposition of silicon carbide is strongly dependent on the carbon potential and any carbon deposits on the surface will lower its volatilization.

Schenk et al. (1990) used emission spectroscopy and mass spectrometry to resolve spatial and temporal characteristics of laser induced plumes. Kunz et al. (1990) also performed spatially and temporally resolved emission and transmission measurements over a plume created over a carbon target irradiated with a CO₂ laser. The probe laser was a tunable dye laser operating in the range 300 to 700 nm. The motivation behind this experiment was to determine the dissociation products of carbon under different ambient pressures.

The focused spot size of the laser beam needs to be known for comparing any model with experimental results. Lim and Steen (1982) developed an instrument that uses a rotating, reflective needle to measure the beam profile at the focal plane. This device has a spatial resolution of 20 μm and a temporal resolution of 0.1 ns. It can handle fluxes ranging from 50 W/cm² to 10⁷ W/cm². The problem with this device is that the reflections of the laser beam from the needle return into the laser cavity, thereby affecting the mode of the laser beam. Herziger et al. (1987) presented another device to measure the two-dimensional laser beam intensity for a high power CO₂ laser. This device has a 10 μm resolution and operates through a rotating needle and pinhole arrangement. Hachfeld (1992) has given a review of the problems associated with beam quality measurements and definitions. Even if the beam profile can be measured accurately before and after the process, it has been shown by Gregersen and Olsen (1990) that, for a strongly reflective material during welding, the back reflections into the laser

significantly change the state of polarization of the laser beam and the output laser power. This makes it necessary to measure the beam profile during the process.

When a material is heated with a laser, the surface may oxidize, decompose, violently boil, melt and vaporize. All of these may change the absorptance of the material from that of the original specimen. The incident energy that is not absorbed by the material is reflected. This energy may be reflected equally in all directions (diffuse) or otherwise. Knowledge of the value of the absorptance at the laser wavelength and at the material removal temperature is essential for the success of modeling efforts. The literature available on the measurement of absorptances is hence reviewed in the following section.

Absorptance Measurements

Chun and Rose (1970) were amongst the earliest to initiate reflectance measurements during the laser drilling process. They measured the energy reflected from a metal target, irradiated with a Nd:YAG laser, using an integrating sphere. They found that the absorptance increased rapidly for metals such as copper and molybdenum, once evaporation was initiated. They also postulated that in the first 50 to 100 μs the material was removed through vaporization. After this period, the combination of buildup of vapor pressure, heat diffusion and formation of melt results in the vapor pressure ejecting the molten material through the sides of the laser-drilled cavity. Kocher et al. (1972) made measurements of laser transmission through sapphire using a Nd:YAG laser. They found that the absorption coefficient of sapphire increased by five orders of magnitude (10^{-2} to 10^3 cm^{-1}) within 10^{-7} seconds. Sturmer and Von Allmen (1978) measured the

time-resolved, specularly reflected CO₂ laser power from metallic targets in different ambient conditions. They found that target damage was strongly influenced by a laser supported detonation wave in the ambient gas.

Von Allmen et al. (1978) made measurements on Nd-YAG lasers irradiating metal targets (10^7 to 10^9 W/cm²) using an elliptical reflector. They found that the unusually high absorptances were due to plasma above the material, which absorbed the incident laser energy and transferred it by heat conduction to the target. Schellhorn et al. (1986) measured the reflectance of metallic targets, subjected to CO₂ laser irradiation, and found that the reflectance decreases, as the intensity decreases, due to plasma formation. Watanabe et al (1992) measured the reflectance of aluminum alloys during spot welding with a Nd:YAG laser beam. The reflectance was measured using an integrating sphere to determine which were the easiest alloys to weld.

CHAPTER 4

PROBLEM STATEMENT

Much of the research on laser machining and particularly laser drilling has been with CO₂ laser and on metals. A lesser amount of work was conducted on ceramics using a CO₂ laser. This is because of the high melting temperatures of these materials and insufficient energy available with most Nd:YAG lasers till recently. Because of the complex nature of the laser drilling process, there remain areas of research to understand the process and to determine the optimal parameters for drilling a material, especially the hard and difficult-to-machine materials. Much of the complexity arises from the multiple phases present in the material induced by the photo-thermal laser interaction as well as the dynamic geometry of the laser/workpiece interface.

The first objective of this investigation was the acquisition of a suitable Nd:YAG laser for laser processing advanced materials and installation in the Laser Materials Processing Laboratory at the Mechanical Aerospace Engineering Research Laboratory. It may be noted that this laboratory is being established for the first time at Oklahoma State University.

The second objective is to align the laser and operate it under safe, appropriate conditions.

The third objective is it to provide proper safety procedures for the safe operation and use of the Nd:YAG laser in particular and all the other lasers (CO₂ and excimer lasers) in the laboratory, as well as, to train new research students working in this area.

The fourth objective is to provide means for computer numerical control (CNC) of the X, Y, and Z-axis motions of the workpiece and to link it with the laser controller.

The fifth objective is to conduct laser drilling experiments on a range of difficult-to-drill materials, such as cemented carbides, polycrystalline cubic boron nitride, cermets, various types of ceramics (alumina based and silicon nitride based), and ceramic composites (SiC whisker reinforced alumina plus zirconia). The objective is to determine the response of these advanced materials with the Nd:YAG laser beam under several parameters, such as pulse width and pulse energy density. The cross sections of the laser drilled holes are to be analyzed using optical and scanning electron microscope to determine the hole diameter and hole depth for single pulse operation. The surfaces of the holes are to be inspected for surface integrity including the recast layers, thermal cracks, uniformity of hole size, etc.

The sixth objective is to obtain experimental data of the cross sections of the material removed from various tool materials by the laser beam to correlate with the analytical thermal modeling currently underway at O.S.U. by Hou and Komanduri.

CHAPTER 5

DESCRIPTION OF THE ND: YAG LASER SYSTEM AND OPERATING PROCEDURE

The laser system used in this investigation is a high power (90 J Max. energy, 4 msec pulse width, at 1064 nm wavelength, Max. power 400 watts nominal), Class IV Nd:YAG pulse laser manufactured by the Control Laser Corporation (Model 480-16). Figures 17 and 18 are photographs of the Nd:YAG pulse laser system. It can be used for a range of manufacturing operations, such as cutting, welding, drilling. The laser system utilizes neodymium (Nd) as the active lasing element in a crystalline host of yttrium-aluminum-garnet (YAG). Table 5 gives the specifications of the laser used and Figure 19 gives the characteristics of the laser. Lasing takes place at near infrared wavelength of 1064 nm. The basic components required for lasing are the laser oscillator and amplifier heads, a rear high-reflective mirror, and a front partially transmissive mirror. A Nd:YAG rod and a krypton arc lamp are mounted inside the laser heads in a dual elliptical, high reflective, gold-plated cavity. When the lamps are energized by the high-current, high voltage pulses, they emit broad band spectral energy (white light) which is focused on the Nd:YAG rod by the elliptical cavity. This energy stimulates the Nd atoms in the rod causing them to release photons at a wavelength of 1,064 nm. The photons travel between the front and rear mirrors through the oscillator rod, creating additional photons. These photons form the coherent beam of radiation which after reaching a sufficient energy level (or lasing threshold) passes through the partially transmissive front mirror. The emitted radiation from the front or output mirror is then doubled by the amplifier head and reaches the workpiece.

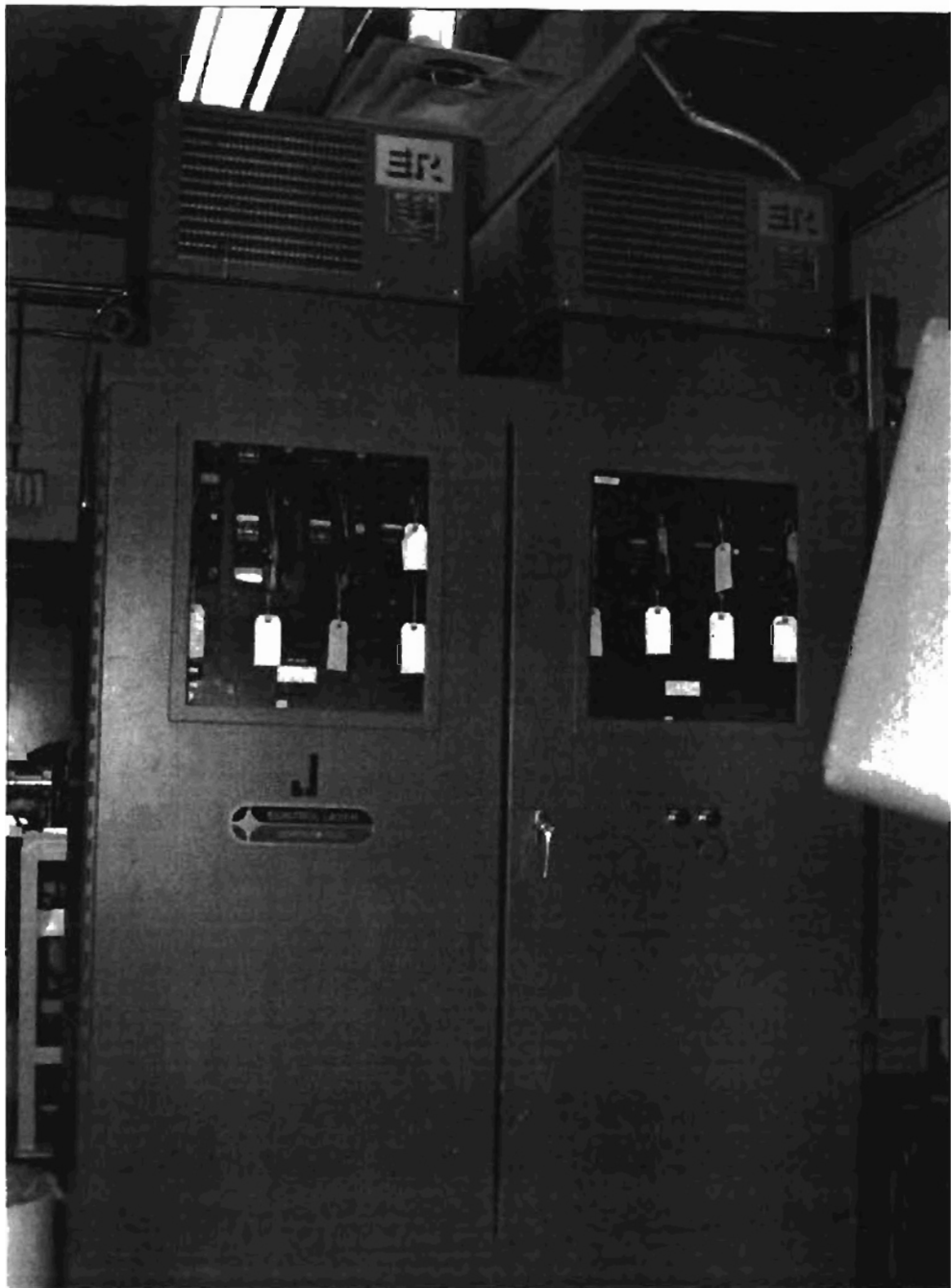


Figure 17 Power supply enclosure



Figure 18 View of power supply enclosure, laser enclosure, and CNC station housing.

SERIES 400 Pulsed Nd:YAG LASERS

HIGH-ENERGY
CONFIGURATION
(MODELS 440-8 and 480-16)

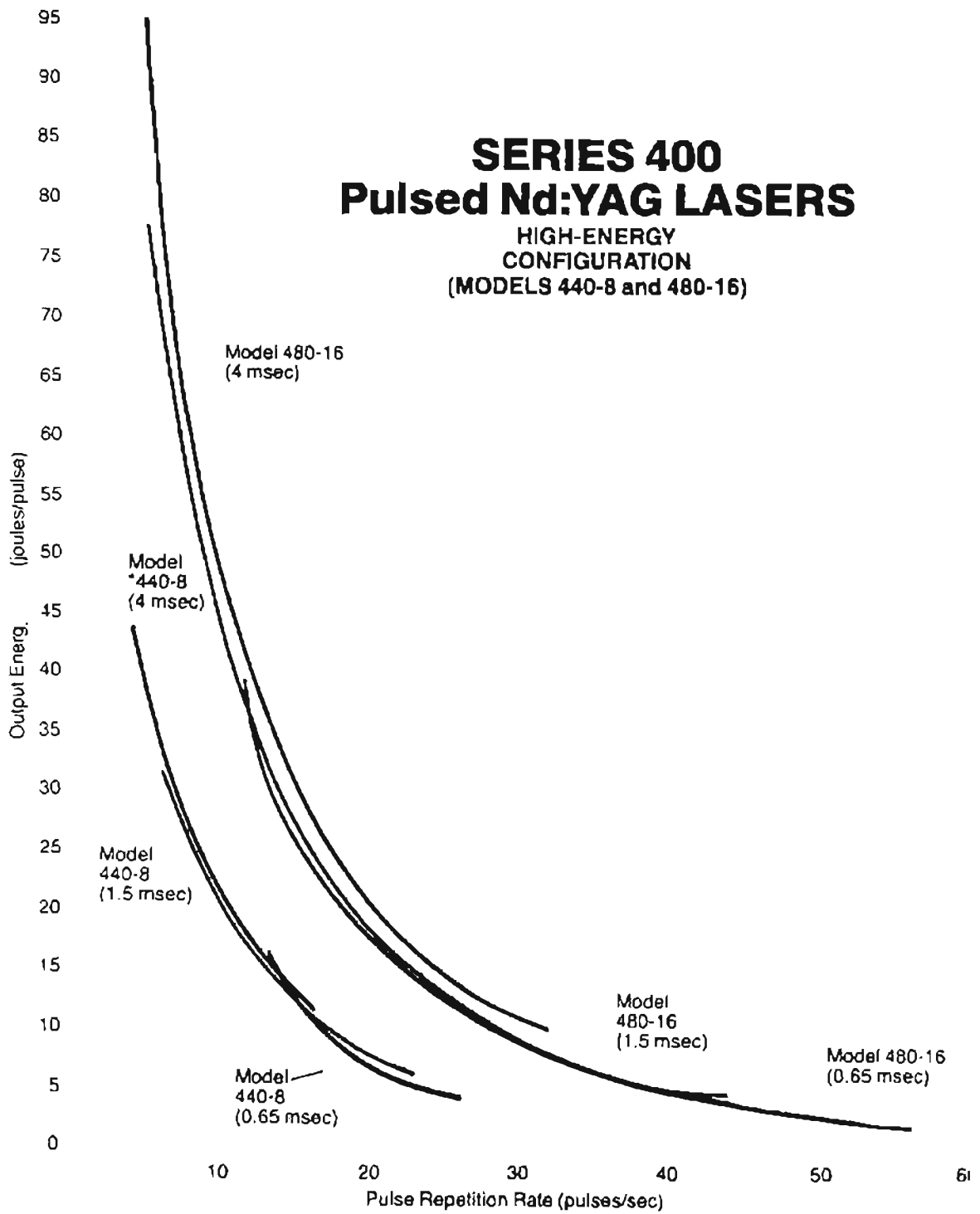


Figure 19 Curves of nominal performance characteristics of Control Laser Corp. Nd:YAG laser.

Figure 20 shows schematically the four major elements of the laser system. They are (1) the optical rail assembly, (2) the laser controller, (3) power supply assembly, and (4) the cooling system assembly. In the following these components are described briefly. This is followed by the description of the operating procedure, namely, system preparation, system operating instructions, and shutdown instructions (both long term shutdown and emergency shutdown).

I. Elements of the Laser System

1. Optical Rail Assembly :

The enclosure for this assembly is 8 ft. long x 9 in. wide x 12 in. high. The components of the optical rail assembly are mounted to an aluminum rail in this enclosure. All hinged covers on optical enclosures are interlocked for safety reasons. Thus, removal or opening of these covers will immediately close the rail mounted shutters which block the laser beam path.

(a) Optical Heads: The components of the optical head include a Nd:YAG rod, two parallel mounted krypton arc lamps, two quartz glass filter plates and a dual elliptical pumping cavity. The elliptical surfaces of the pumping cavity is made of brass ultra-precision machined and is electroplated with nickel-gold. All internal components of the head assembly are cooled by de-ionized water circulation system.

(b) Mirror Mount Assembly: The front and rear mirrors are mounted in kinematic suspension mounts that provide direct adjustment of the mirror angle with independent X-Y angular positioning.

(c) Safety Shutters: The laser system is equipped with rail mounted, three solenoid actuated shutters. These shutters are controlled with the laser controller that can be programmed to open and close when proper command codes are entered or operated manually. Optical enclosure covers are equipped with interlock circuits that will close the shutters and shut down the system power when the covers or panels are opened.

(d) He-Ne Alignment Laser: A 5 mW Helium-Neon laser system (Model HAL-122) is used for proper alignment of all optical components and beam control through delivery optics. It is mounted on the rear of the optical rail behind the rear, or maximum reflective (MAX-R) mirror mount assembly. The He-Ne laser mounting assembly is adjustable through the use of a 6-point, angular positioning system in a kinematic suspension. A He-Ne prism mount assembly is used for optically coupling the He-Ne laser output with the Nd:YAG optical elements, and beam delivery optics. The prism is housed in a kinematic suspension mount that provides direct adjustment of the prism angle, with X-Y-Z angular positioning. The prism mount is located directly behind the rear mirror mount assembly on the end of the optical rail.

(e) 45° Dichroic Mirror Assembly: A 3-point dichroic mirror assembly is mounted at the output end of the optical rail to deflect the laser beam downward 90° to reach the workpiece below the rail. The mirror is anti-reflective (AR) coated for 1.064 μm and can sustain peak power densities of up to 250 MW/cm².

(f) Beam Delivery Optics/Gas Nozzles: Appropriate beam delivery optics along with a gas assist nozzle are used in this system.

(g) Beam Bending Assembly: The function of the beam bending assembly is to provide directional control and delivery of the collimated beam. The components of this assembly are mounted on an optical rail carriage including two 90°, 3 inch dichroic mirror mount assemblies and a photo diode. Two mirror mount assemblies are positioned at 45° to the output of the upcollimator and are mounted parallel to each other affecting two 90° bends of the beam path. The photo-diode assembly is positioned behind the primary dichroic mirror to allow exposure of the photo-diode to the small percentage of radiation that passes through the mirror surface. The primary mirror mount is stationary and the secondary mirror mount (Oriol Model 123) is rotationally adjustable with X-Y-Z angular positioning.

2. Laser Controller:

The input section of the laser system, it is a minicomputer designed to control all operating parameters of the laser system and has the capacity of controlling positioning systems with up to five axes of motion. The control is housed in a pendant console externally mounted on the power supply enclosure. In addition, this system has a portable remote control console for convenience. The components of the controller consist of a CPU, memory, a CRT display unit, a mini-cassette tape deck, and a keyboard. The CPU operates in conjunction with 2 RAMs and 10 EPROMs. Input to the CPU is by either magnetic tape or the keyboard. In response to the program commands and the input parameters entered at the keyboard, the CPU provides appropriate signals to the servo, and laser control logic circuits, which in turn actuate positional drive motors and operate the laser. Information is inputted to the CPU by either a magnetic tape or the keyboard. It

may be noted that use of controls, adjustments, or performance of procedures other than those specified herein may result in hazardous radiation exposure.

3. Power Supply:

The main components of the power supply are the controller, the power distribution, power supply circuits, and the pulse forming networks. Internal temperature of the power supply cabinet is controlled by a dual high capacity air conditioning system mounted externally on top of the power supply cabinet.

(a) Power Distribution Enclosure: It houses the main power input switching, fuses/circuit breakers, distribution and relay circuits, and control/logic circuits for the controller.

(b) Pulse Forming Network (PFN): It is comprised of eight power modules connected in parallel, SCR charging circuits with related inductors and capacitors, and a flash lamp simmer supply circuit. Two complete pulse forming networks are used in this system. The PFN is charged through two opposed silicon-controlled rectifiers which alternately fire at 9 kHz producing an 18 kHz sawtooth wave that is introduced into the single-end primary of a step-up transformer. This transformer converts the input voltage to required levels and the output of the transformer secondary is converted to DC by four bridge rectifiers in the power modules. When the PFN capacitors are charged to the required voltage and set through the laser controller, the charge is discharged through the flash lamps. The flash lamps are energized through the simmer supply circuits which introduce high voltage/high current flow through the lamps, and in turn ionize the krypton gas medium thus effecting optical pumping of the Nd:YAG rod.

(c) Power Modules: The function of these modules is to charge the PFN capacitors at constant current to a predetermined voltage and to regulate this voltage to within 1%. These modules rectify 220 V, 3-phase AC from the input power circuit to the required DC charging voltage. The high energy module has a 1700 V charging capacity.

4. Cooling System Assembly

The cooling unit (480-16 DE-I) is independently housed in a cabinet measuring 4 ft wide x 32 in. high x 26 in. deep (see Figure 21). The system is of the liquid-to-liquid heat exchanging type and involves two separate water circulation circuits. Secondary cooling is effected by the circulation of the city or tap water which flows through coils in the deionized water reservoirs at a given flow rate, thus stabilizing the deionized water at the required temperature range. The primary coolant (deionized water) is pumped from a reservoir through three parallel channels in the laser heads, and routed around the rod and both flashlamps. After leaving the cavity, the heated deionized water is returned to the reservoir, which is connected in parallel with a deionization filter. This filter is fed a 3/4 GPM supply of the returned water, and once filtered, returns the water to the reservoir for cooling, and recirculation to the head.

A resistance sensing device in the return line between the deionization filter and the reservoir monitors contamination of the water. Once a given level of contamination is reached, an indicator on top of the cooling system enclosure, which is normally illuminated, will go out giving indication that the deionization filter cartridge should be replaced.

A thermostat located in the DE-I water return line automatically opens and closes a valve that allows city water to flow through coils inside the DE-I reservoir. When the temperature of the deionized water has dropped to a given level, which is controlled by the thermostat, the control valve for the city water closes, thus completing the cooling process.

The water in the DE-I reservoirs is maintained at a temperature of 25°C or less. If the deionized water temperature should exceed the preset maximum of 40°C, a safety interlock circuit is activated by a temperature sensor located in the inlet lines to the heads. The laser is disabled, and the message "OVER TEMPERATURE" is displayed on the CRT of the laser controller (LaserBrain). The laser will not operate until the proper deionized water temperature range has been reached. This safety feature is incorporated to protect the Nd:YAG rod and flashlamps from severe damage due to overheating.

The capacity of the deionized water system is monitored through the use of dual level float switches located in each of the deionized water reservoirs. These switches are connected in series with the laser system interlock circuits and the I/O logic circuits of the Laser Controller. If the water level in either reservoir drops to the primary level of the switch, a signal is sent to the Controller, and the message "LOW WATER" is displayed on the CRT in the standby mode. When the level drops to the secondary or lower level of the float switch, the interlock circuit is opened, laser system power is disabled, and the aforementioned fault message is displayed. The system will not function until the reservoirs are filled to the proper minimum level, as indicated on each of the visual water level tubes.

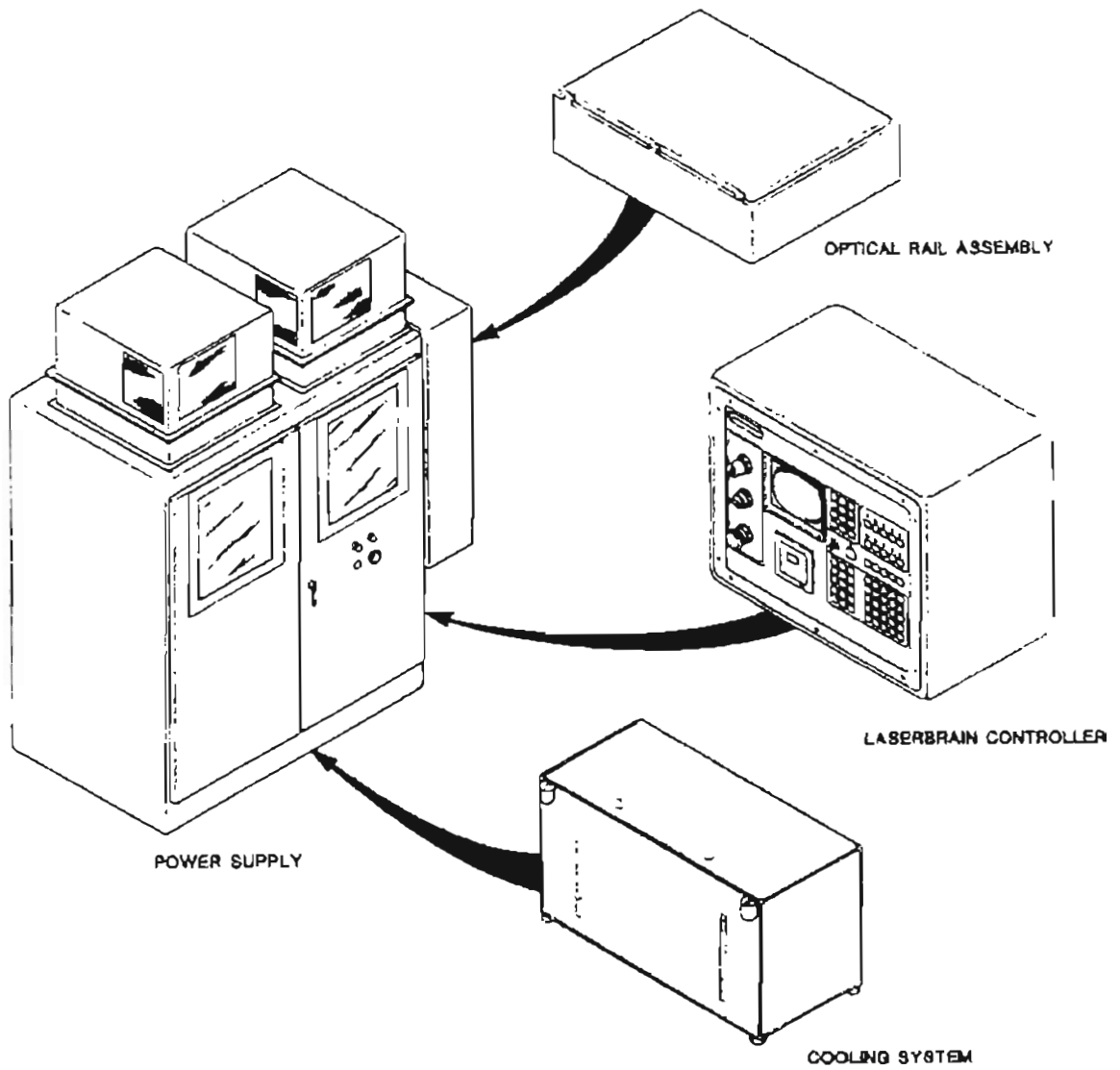


Figure 20 Laser system components.

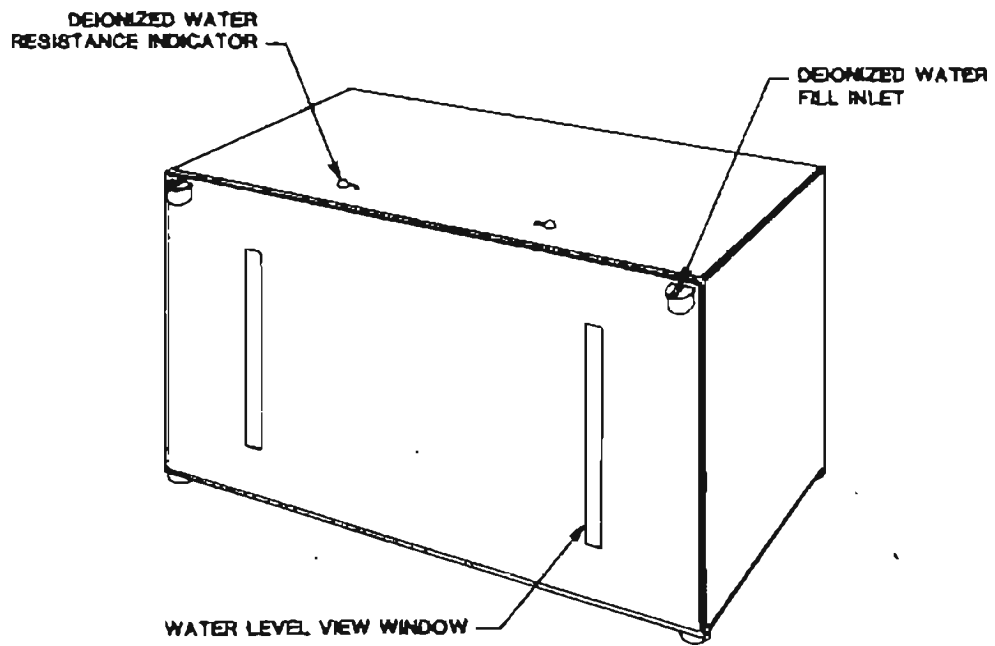
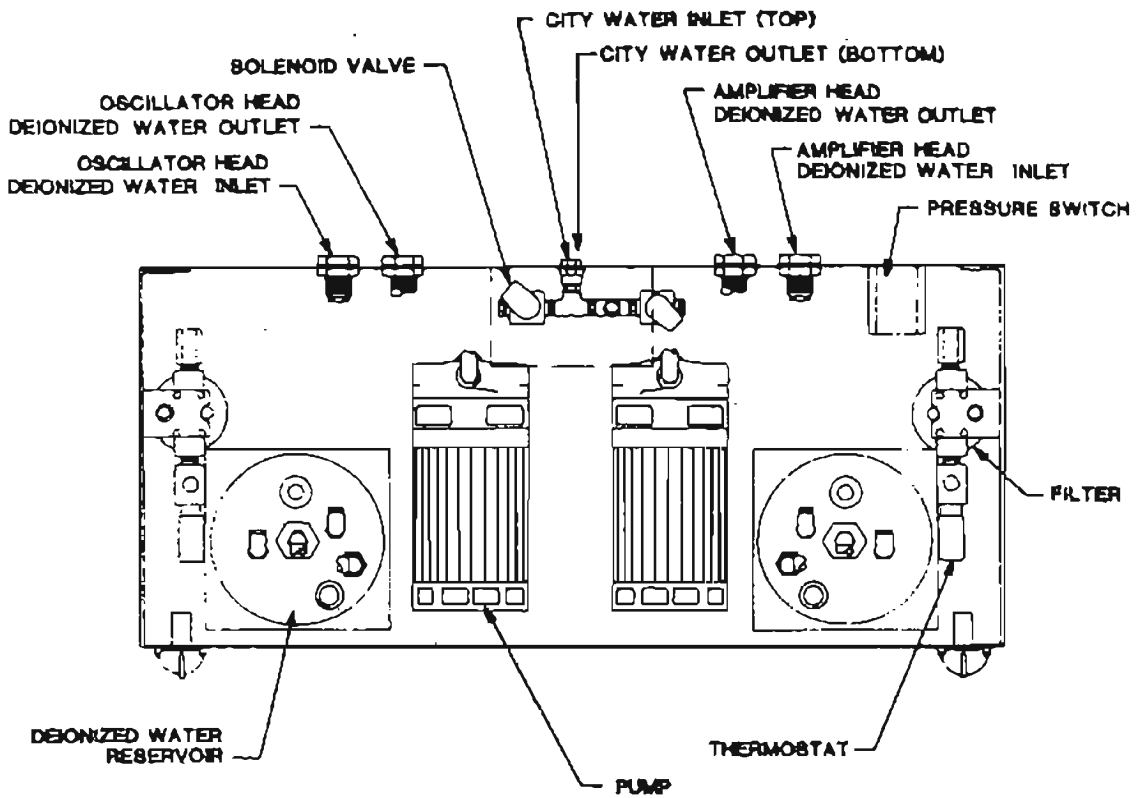


Figure 21 Cooling system

II. System Preparation

- a. Verify that water and electrical connections described in the previous section have been properly made.
- b. Secure all panels, covers, and doors in their proper operating configuration.
- c. Insure that only essential personnel are in the laser area and that they are suitably protected from exposure to laser radiation. Laser goggles which block 1,064 nm laser radiation must be worn when operating a Class III or IV Nd:YAG laser. Instant and permanent damage can occur when the naked eye is exposed to laser radiation. Insure that personnel are not exposed, either physically or visually, to direct or scattered laser radiation.
- d. Check the operation of the safety shutters before high voltage is enabled to start the lasing process.
- e. Do not fire the laser unless a part or some type of power absorbing material is in position to absorb the laser beam. For testing purposes, firebrick or similar material is recommended.

III. System Operating Instructions

- a. Turn on Procedure

- (1) Pull out the EMERGENCY STOP push/pull switch.

- (2) Turn the MAIN POWER key switch to START and release. This activates the laser controller (LaserBrain). If the EMERGENCY STOP switch is illuminated at this point, an interlock condition exists. Press the STANDBY pad and a readout of the particular condition will be displayed. Correct the condition and reset the CONTROL POWER switch.

- (3) When an interlock message is displayed, check for an open door, panel, or cover. Also check the deionized water level, the flow of tap water to the cooling system, and make sure the EMERGENCY STOP switch on the power supply enclosure is pulled out. Reset the CONTROL POWER switch by turning to CONTROL ON and back to OFF/RESET and then back to CONTROL ON.

- (4) Turn the CONTROL POWER switch to CONTROL ON. (Pumps, fans, AC units, etc. are activated). If water pumps and fans do not come on, check AC input power connections and proper phasing of the input lines. Also check fuses on TB-1.

- (5) Move the CONTROL POWER switch to LASER ON and observe CRT display. This activates the high voltage to both PFN. If the "NO SIMMER" display does not clear, it is often an indication of a failed krypton arc lamp.

b. Operating Procedure

After initial turn-on, the system is ready for normal operation. Laser operating parameters can be programmed at this time.

IV. Shut Down Instructions

a. Long Term Shutdown

- (1) Turn the CONTROL POWER switch to CONTROL ON. This disables the high voltage to PFN's.
- (2) Turn the CONTROL POWER switch to OFF/RESET. This disables the system service circuits.
- (3) Turn the MAIN POWER key switch to OFF. This disables the laser controller (LaserBrain). The program in the laser controller (LaserBrain) will be erased when the system is shut down. It should, therefore be saved on tape prior to shutdown.

b. Emergency Shutdown

- (1) Press the EMERGENCY STOP push/pull switch.

- (2) Turn the CONTROL POWER switch to OFF/RESET.

Table 5 Specifications for the Nd:YAG Laser System (Model 480-16)

Parameter	Specification
Maximum Energy* (high-energy)	34 joules/pulse (0.65-msec pulse width) 90 joules/pulse (4.00-msec pulse width)
Maximum Repetition Rate* (high-energy)	56 pulses/second (0.65-msec pulse width) 32 pulses/second (4.00-msec pulse width)
Beam Diameter	10.0 mm
Beam Divergence	10.0 mrad
Krypton Arc Flashlamp	2 per laser head
Average Flashlamp Life	10 ⁶ pulses (at rated maximum energy)
Electrical Requirements	230-VAC ±5%, 3-phase, 45 kVA, 160A in-rush currents
Water Requirements (City Water)	15 GPM 70°F Max. 35 psi

*Nominal performance figures. These can vary due to voltage and frequency of the electrical source.

CHAPTER 6

ALIGNMENT OF THE ND:YAG LASER OPTICAL SYSTEM

To obtain maximum output power from the laser system, it is necessary to adjust the alignment of the optical rail assembly components either with an autocollimator or with a He-Ne laser. Due to misalignment of the optical rail assembly components caused by handling and shipment of the laser system, a total realignment of the entire optical system became necessary. In this investigation, the laser optical system was aligned with a He-Ne laser. The alignment kit (Part No.KIT400ALN) containing the necessary apertures were supplied as a standard accessory. The following steps were taken for the optical alignment of the laser optical system [Control Laser Corp. Manual, 1983].

1. All components from the optical rail, except the He-Ne alignment laser and the front and rear mirrors, were removed.
2. The front mirror was repositioned as close to the front end of the rail as possible.
3. An aperture was placed in both mirrors and the He-Ne laser was aligned such that the beam passes through the center of both mirrors.
4. The front mirror was repositioned to its normal position and verified so that the He-Ne beam is still centered on both mirrors. If not, the mirrors are not of the same height, or on the same lateral axis. The beam is centered before continuing further.

5. The oscillator (rear) head is placed on the rail. It was insured that the reflective surfaces of the mirrors are spaced 34 in. apart and facing the rod ends.
6. The apertures were placed in the ends of the rod holder, and the laser head was adjusted so that the He-Ne beam is centered on the rod ends.
7. The amplifier (front) head was placed on the rail and Step 6 was repeated. Care was taken to see that all the components were locked down after adjustment.
8. A white card was placed in front of the dichroic mirror and a mark was made at the spot where the He-Ne beam hit.
9. The upcollimator was placed on the rail, and adjusted so that the He-Ne beam is centered in the front and rear lens. It was insured that the beam strikes the same spot on the card. The beam must enter and exit the upcollimator in the center of the lenses.
10. The He-Ne laser was turned off.
11. Use the autocollimator to align the mirrors to the oscillator head. If the rod ends are not parallel, turn the He-Ne back on and adjust the tilt on the front mirror so that the reflection bounces back into the He-Ne.
12. Turn off the He-Ne.
13. Place the autocollimator in front of the front mirror and locate the mirror spot.
14. Adjust the tilt on the rear mirror so that its spot coincides with the front mirror spot.
15. Remove the autocollimator from the rail.

16. The safety shutters were placed in position on the rail.
17. After the laser safety goggles (designed to block the 1,064 nm radiation) were worn the laser was turned on and the power output of the oscillator head was measured.
18. Adjust the rear end mirror to optimize power output.
19. The laser was operated at a very low power setting, and an IR (infrared) viewer is used to insure that the beam passes through the amplifier head and the upcollimator with no clipping.
20. It was verified that the beam strikes the same spot on the white card as the He-Ne beam.
21. The laser was turned off, and the white card was removed.
22. The top aperture plate from the alignment kit was placed in the opening in the laser rail between the dichroic mirror and the focusing optics assembly.
23. The objective lens from the focusing optics assembly was removed.
24. The aperture tube and bottom aperture, from the alignment kit, was screwed into the focusing assembly in place of the objective lens.
25. A white card underneath the focusing assembly was placed.
26. The He-Ne laser was turned on and the dichroic mirror was adjusted to center the beam through both apertures.
27. The spot on the card where the He-Ne beam hits was marked.

28. The He-Ne laser was turned off.
29. The laser was turned on, and it was verified that the beam is centered on the same spot on the white card.
30. The laser system was turned off. The CONTROL POWER switch was set to OFF/RESET and the MAIN POWER key switch was turned to OFF position.

The apertures and aperture tube were removed from the system and the objective lens assembly was replaced. This completed the alignment procedure for the standard straight rail and basic delivery optics system.

CHAPTER 7

METHODOLOGY

Test Procedure

The following are the standard test procedures for laser drilling experiment. It involves the following points:

Sample preparation

It is known that in the laser processing of materials a thin surface coating on the work piece can be added to enhance laser absorption on the surface of materials with a low absorption coefficient (such as metals cut by CO₂). Carbon based polymers and other non-metals can absorb a significant amount at the Nd:YAG laser wavelength. Since we are trying to also determine a basic physical characteristic of the work piece material, that is, absorption of laser light at 1043 nm, a clean surface is necessary to eliminate the possible effects of surface contamination, fingerprints, etc. The following will remove most common surface contaminants.

1. Clean sample in detergent solution and ultrasonic cleaner.
2. Rinse in distilled water and ultrasonic cleaner.
3. Clean and rinse in methanol in ultrasonic cleaner.
4. Air-dry and handle with clean gloves to prevent oils and dirt from contaminating the surface.

Laser characteristics

It was noted before that one of the considerations of a laser-drilling device was the stability of the laser beam characteristics. For the Control Laser Nd:YAG laser

certain effects can affect the quality and stability of the laser output such as normal degradation of the laser flash lamps, environmental conditions, environmental temperature cycling, and malfunctions, etc. Also, it is a requirement to know the amount of energy reaching the workpiece surface and the laser beam profile to provide accurate, consistent data for the laser drilling model. The following procedure is used to monitor the stability and measure the laser beam power and energy characteristics for each set of experiments. To monitor the beam profile:

Monitor laser beam profile with black photographic paper or thermal paper. The paper should be placed 12 inches below the focal point. Voltage of the laser set to 1000 V and the number of pulses before opening the shutter should be 25. The pulse rate is set to the maximum pulse rate common to all pulse widths, in this case 3 pulses per second. A single pulse is directed on the paper. The impression left on paper should be circular and uniform. If not then alignment of optical path may need adjustment.

Determination of the power output at the test conditions

Using the Optical Engineering Digital Power Probe, measure overall laser beam power at each test condition. Calculate energy per pulse by dividing the watts measured by the pulses per second. The average power is measured according to the Optical Engineering Digital Power Probe manual provided.

Laser drilling

With the energy per pulse at each test condition determined, the effect of a known amount of energy at the particular test conditions can be observed on the workpiece

material tested. The follow steps is the procedure used for the laser drilling of each workpiece sample.

1. Place two symmetrical samples on laser XYZ table.
2. Place focal point of the laser beam on surface of workpiece at the centerline of where the two samples meet.
3. Turn on assist gas. In this study, helium is used because of its chemical inertness and low molecular weight. (This may improve material removal and heat transfer rate because of the higher kinetic velocity of the helium atom at a particular temperature.)
4. Pulse single shot at various power levels and pulse widths (700, 1050, 1350, 1700 volts and 0.50, 1.65, 4.00 ms).
5. Rotate samples after each laser pulse: Left clockwise, right counterclockwise for each set of experiments.

Optical Stereo Scope Observations

Using an optical stereoscope, the profiles of the laser-drilled holes were observed. Using the x-y sample table with micrometer positioning, the hole depth and the hole entrance diameter were measured.

SEM observations

Using a scanning electron microscope, the workpiece materials were observed for details such as cracking, HAZ, material re-deposition, etc. The following are the procedure use.

1. Place non-conductive samples in gold / palladium sputterer.
2. Sputter all samples on all side for 30 seconds each at the recommended pressure and current.
3. Place

samples in the scanning electron microscope chamber and view each set of holes from the top and profile view. Photograph representative a set, features, etc. 4. Assess HAZ (heat affected zone) and thermal damage such as cracking or spalling.

Experimental Conditions

A basic general start up procedure was followed to assess the condition and power of the Control Laser unit. This is done to check non-variance in the laser operating characteristics or to account for differences, if any, in the results. The procedure is as follows:

1. Start up the laser per start up procedure.
2. Turn on He-Ne laser beam by inputting command into the LaserBrain console.
3. Place low reflectivity black photo paper on a graphite block at a fixed distance (8 to 12 inches) below the focal point.
4. Set laser voltage to 1000 volts, single 0.65 ms pulse, 25 pulses before shutter opens. This is done to qualitatively determine beam power and profile. This procedure is performed once before each set of experiments and once after.

Also, to quantitatively determine the power output of the laser the Digital Power Probe was used before and after a set of experiment to determine the stability of the laser. The procedure was similar to the basic start up procedure:

1. Start up laser per start up procedure.
2. Turn on He-Ne alignment beam.
3. Place power probe head at distance from the focal point so that the beam diameter covers approximately 3/4ths of the surface area of the probe head.
4. Set the

Nd:YAG laser to the required test parameters and pulse the beam for the set time as specified by the power probe head. 5. Measure and record the average beam power.

The general procedure for a set of experiments was as follows:

Two square samples of the material to be drilled were placed in the acrylic jig such that the side faces were butted up against each other flush. The He-Ne laser was positioned on the top face along the center line where the two pieces met. This was done so that the profile of the hole could be observed without the difficulty of cutting and preparing the material in a conventional manner. The z-axis was then adjusted so that the focal point of the laser was on the surface of the material. (With the focal length of the optics used at 150 mm, the distance between the nozzle tip and the workpiece was 6.25 mm.) The required laser parameters were then inputted to the Laserbrain console. The gas was turned on, in this case, helium, and then the laser fired for a single pulse. Four holes were drilled per face starting from the lowest voltage to the highest and beginning at the shortest pulse width.

The holes drilled were then inspected for basic characteristics such as hole depth, hole diameter, hole shape/taper, surface damage, recast depth, and qualitative appearance. This information was gathered with the stereoscope/micrometer x-y table and the scanning electron microscope.

CHAPTER 8

OPERATING CHARACTERISTICS OF THE CONTROL LASER (480-16 ND:YAG LASER)

To determine the operating characteristics of the laser with respect to power versus pulse time interval, drift in operational characteristics due to time (aging, dust, pests, etc.), the average power of the beam was measured over the range of conditions tested.

To determine the energy per pulse for the three time intervals of 0.65, 1.50, and 4.00 ms, the average power was taken over 19.6 seconds, the time period require by the Digital Power Probe. The number of pulses per second was the maximum number of pulses that the laser could provide at a particular pulse width setting. The following table illustrates the operating characteristics with respect to power and time:

Table 6 Operating characteristics. HY-2 Head for Digital Power Probe (100-1100 watt range)

Voltage	Power		
	Pulse duration		
	0.65ms	1.50ms	4.00ms
700	25W	26W	24W
1200	128W	127W	123W
1700	263W	263W	252W
No. pulse/sec	12	6	3

In order to provide better resolution in the lower power range and to verify the previous results, a probe (HY-1 Head for Digital Power Probe, 20-200 watt range) was used that would provide more resolution using the same method as before.

Table 7 Operational characteristics using HY-1 power probe.

	Power		
VOLTAGE	Pulse duration		
	0.65ms	1.50ms	4.00ms
700	25.9W	25.8W	26.7W
1200	125.3W	129.1W	125.9W
Pulses/sec	12	6	3

The operating characteristics of the laser with the pulse width held constant at 3 pulses per second was measured. This was chosen since this was the lowest value encountered in the previous test.

Table 8 Operational characteristics at constant pulse rate. HY-2 Head for Digital Power Probe (100-1100 watt range)

	Power		
Voltage	Pulse duration		
	0.65ms	1.50ms	4.00ms
700	4	10	26
1200	27	59	123
1700	55	122	257
No. pulse/sec	3	3	3

This was then repeated using the smaller probe to obtain better resolution in the lower power range and to verify the previous result.

Table 9 Operational characteristics at constant repetition rate using lower range probe HY-1 Head for Digital Power Probe(20-200 watt range)

VOLTAGE	Power		
	Pulse duration		
	0.65ms	1.50ms	4.00ms
700	4.5	10.8	26.8
1200	27.3	59.1	126.2
1700	58.9	126.1	over range
No. pulse/sec	3	3	3

CHAPTER 9

EXPERIMENTAL RESULTS AND DISCUSSION

Several advanced ceramics and cemented carbides (both coated and uncoated) materials were used in the single pulse drilling studies. They represent many of the advanced materials used today in the metal cutting and metal forming industries. Such materials may find increased demand for specific engineering applications, as designs demand their superior properties. The cutting tool inserts were obtained from several cutting tool manufacturers in the U. S., including, Kennametal, Carboloy, Valenite, and Greenleaf. Table 10 gives a summary of the specific tool material and the source for convenient reference. Single pulse laser drilling tests were conducted on various materials at different energies using three pulse durations (0.65, 1.5 and 4.0 ms) on these materials. Two inserts were held one against the other in an acrylic vise and the holes were drilled at the interface. By this method, the cross sections of the holes can be obtained without the need for making a cross section mechanically with a diamond blade which can be expensive and time consuming. The hole depths and diameters at the inlet were measured using an optical microscope and the cross sections were examined in a scanning electron microscope. In the following, the results of the drilling tests will be presented along with brief discussion.

Table 10 Tool Materials, Their grades and Specific Manufacturer

Manufacturer	Grade	Material
Kennametal	K060	Al ₂ O ₃
	K090	Al ₂ O ₃ / TiC
	KY2100	SiAlON, medium grade
	KY4000	Al ₂ O ₃ / ZrO ₂ / SiC whiskers
	KT175	Cermet- TiC/ TiN base. tougher grade
	KD200	Cubic boron nitride (c-BN)
Carboloy	GR883	WC-Co 6%
Valenite	SNMG433	WC-Co 6%, TiN coated tool
Greenleaf	CNGC-433T	Si ₃ N ₄

Results and Discussion

1. Cemented Tungsten Carbide - 6% Co

Figure 22 shows the variation of hole depth and hole diameter with pulse energy levels for three different pulse durations for a 6 % Co-cemented tungsten carbide base material. It can be seen that with increasing pulse energy the hole diameter increases almost linearly. However, the depth drilled does not increase linearly but begins to saturate at higher energy levels with increasing pulse energy. Figure 23 is an SEM

micrograph of the cross sections of the holes drilled at a) 0.65, b). 1.5, and c). 4.00 ms pulse duration. It may be noted that in all the SEM micrographs of the cross sections of the holes drilled on various materials to be presented and discussed in the following, the top micrograph is for 0.65 ms, the center is for the 1.5 ms, and the bottom one is for 4.00 ms pulse duration. Figure 24 are micrograph close-ups of holes drilled. A heat affected zoned (HAZ) exists which increases in thickness generally with increasing pulse width and increasing pulse energy. Also, cracks extend into the work material due to thermal stresses encountered by the material.

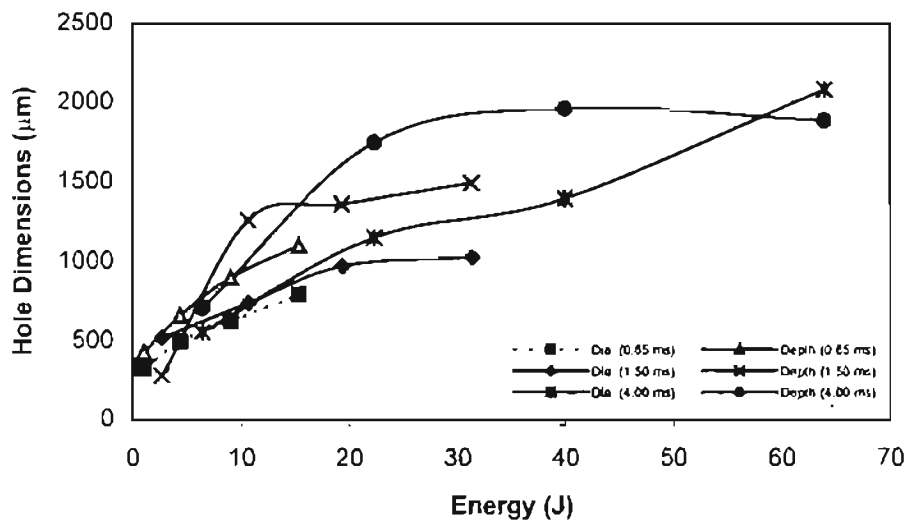


Figure 22 Variation of the hole diameter and hole depth with pulse energy for three pulse durations, namely, shortest (0.65 ms), medium (1.5 ms), and longest (4.0 ms) for a straight cemented tungsten carbide with 6 % Co

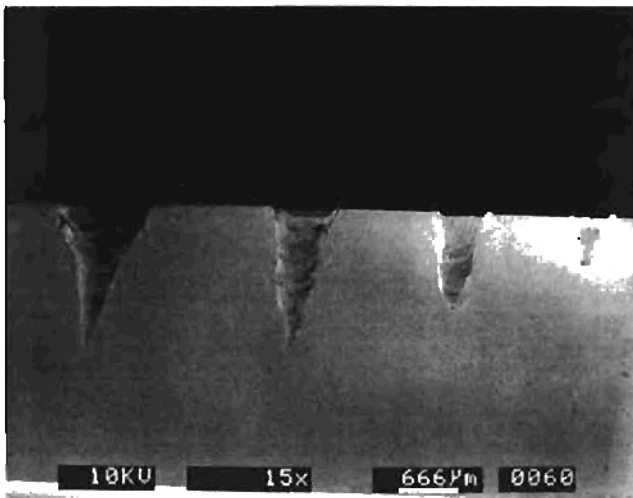
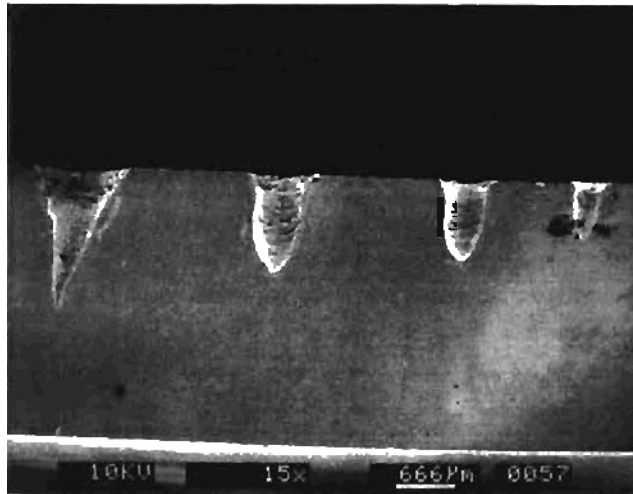
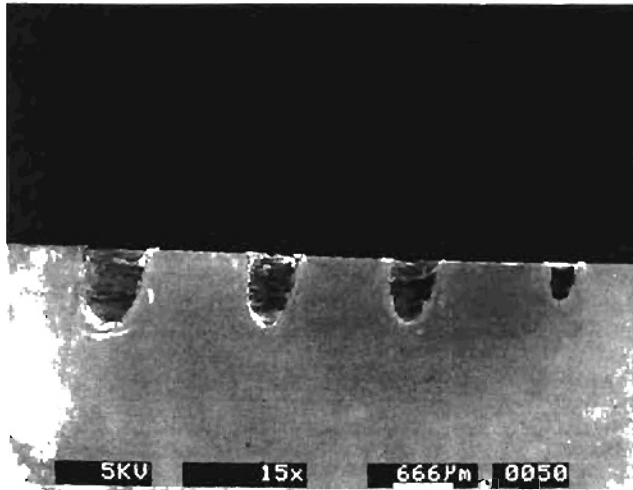


Figure 23 WC-Co 6% Cross-sections of holes drilled at 0.65, 1.50, and 4.00 ms pulse width.

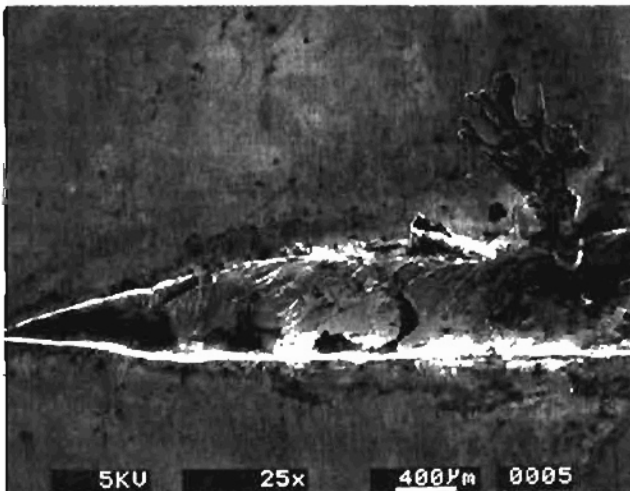
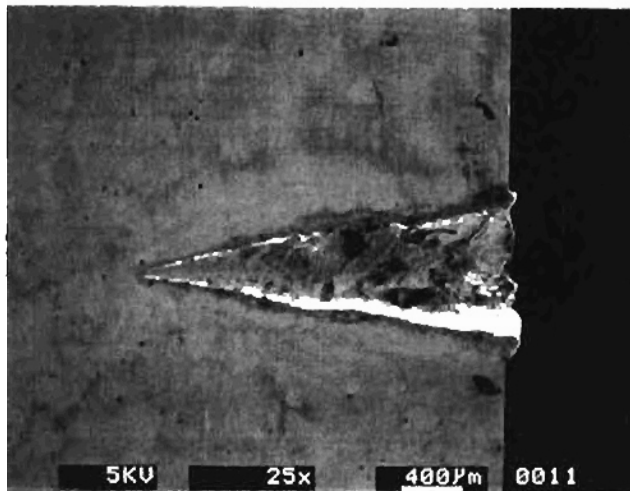
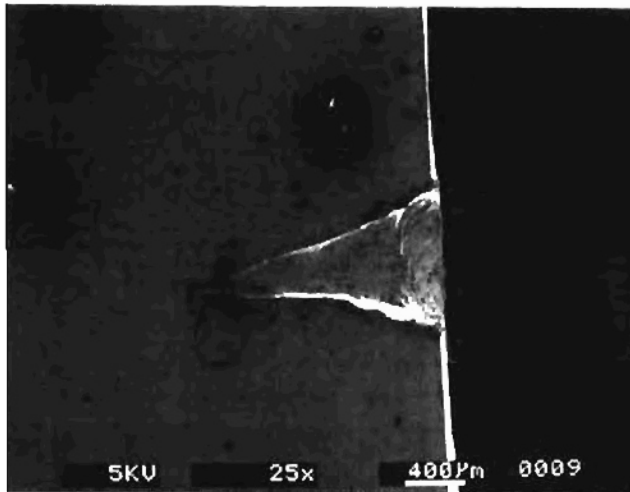


Figure 24 WC- Co 6% HAZ for increasing pulse width

2. Cemented Tungsten Carbide - 6% Co with a 5 μm Titanium Nitride (TiN) Coating

To improve friction and wear resistance, a thin layer (5 μm) of titanium nitride (TiN) is deposited on top of cemented tungsten carbide by chemical vapor deposition (CVD). Figure 25 shows the variation of hole depth and hole diameter with pulse energy level for three different pulse durations for a TiN coated 6 % Co-cemented tungsten carbide base material. It can be seen that the addition of this thin layer has a dramatic effect on the drilling characteristics of cemented tungsten carbide base material. Although the melting point of titanium nitride is slightly less than tungsten carbide, it tends to produce smaller hole diameters for similar conditions. Between the various pulse widths tested, the hole diameter versus pulse energy input did not vary with change in pulse width. With respect to the hole depth versus pulse energy input, the drilling behavior was similar to uncoated cemented tungsten carbide with 6% Co tool at 4.00 ms pulse width conditions. However, at the shortest pulse width of 0.65 ms, saturation occurs at approximately 9 joules. At the pulse width of 1.50 ms, there is a tendency of the material to produce the deepest holes due to multiple internal reflections of the laser beam (approximately 11 joules). Figures 26 (a) to (c) are SEM micrographs of the cross sections of the holes drilled at 0.65 ms, 1.5 ms, and 4 ms pulse durations, respectively for a TiN coated 6 % Co-cemented tungsten carbide base material. They show a significant recast layer at all conditions tested. Figures 27 (a) to (c) are SEM micrographs at higher magnification. They show a recast layer exhibiting cracks in the circumferential and longitudinal directions with the cracks extending into the workpiece. At the longest pulse

width of 4.00 ms, these cracks develop early enough in the drilling process to allow the recast material to flow out of these cracks.

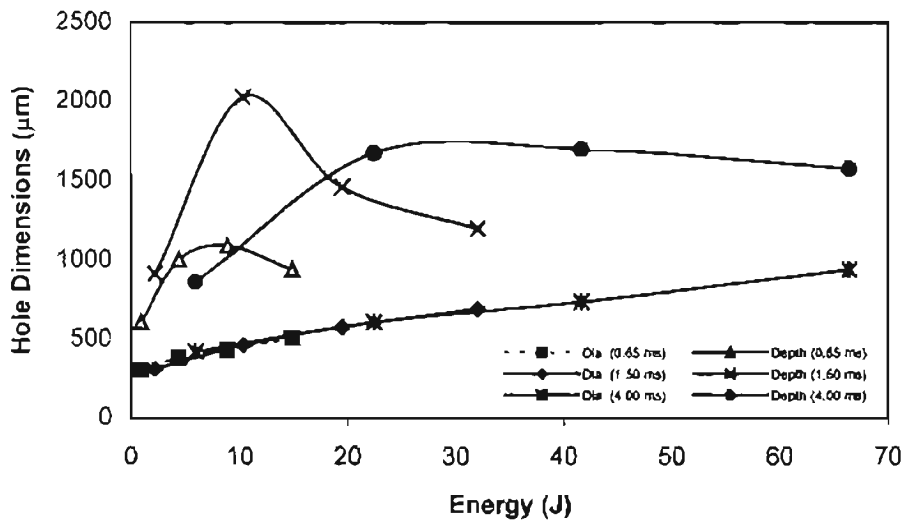


Figure 25 Variation of the hole diameter and hole depth with pulse energy for three pulse durations, namely, shortest (0.65 ms), medium (1.5 ms), and longest (4.0 ms) for a TiN coated straight cemented tungsten carbide with 6 % Co

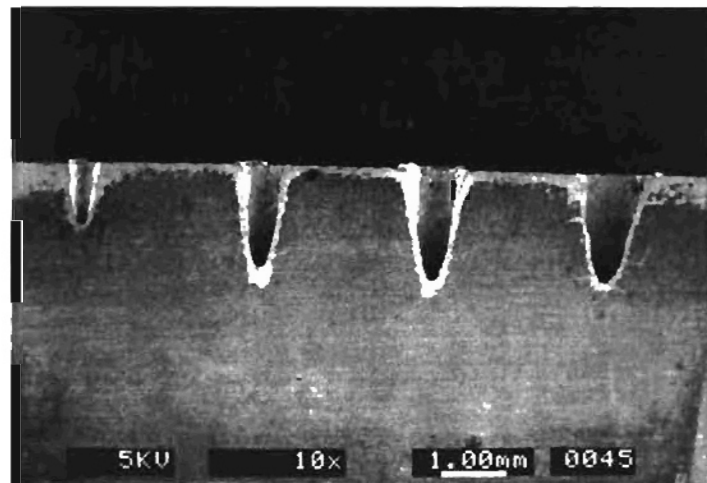
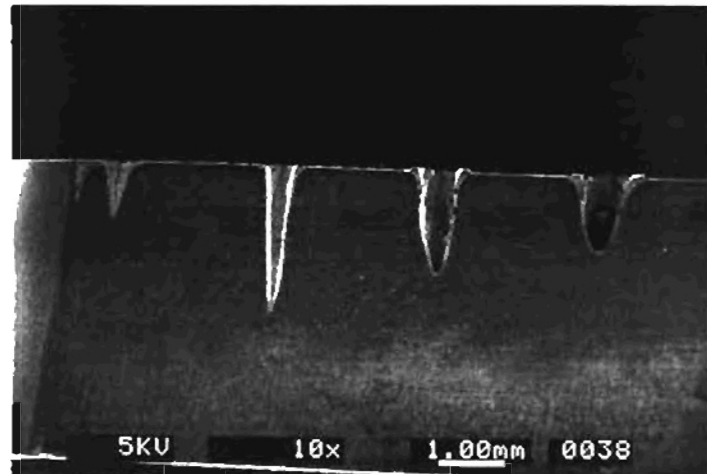
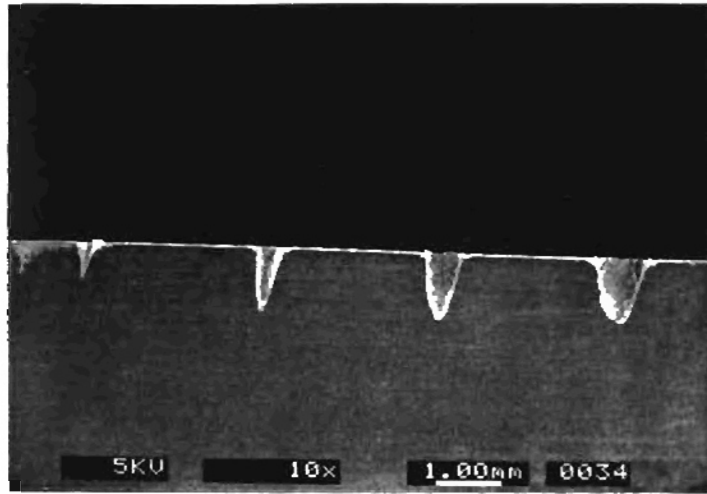


Figure 26 WC- Co 6 wt % TiN coating. Cross sections of the holes drilled at 0.65 ms, 1.5 ms, and 4 ms pulse durations

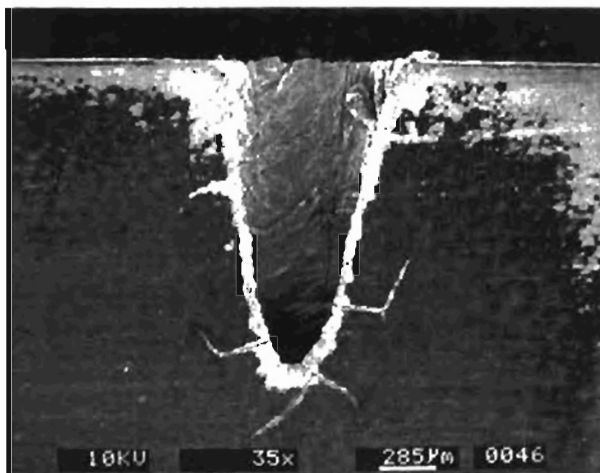
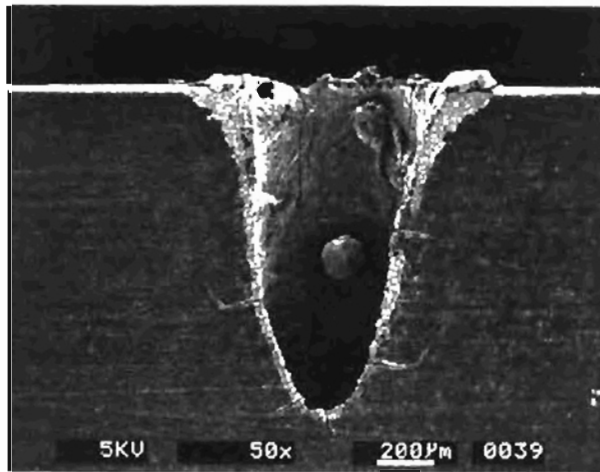
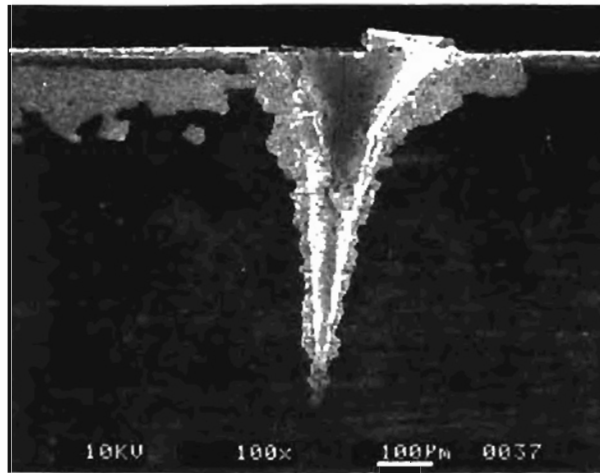


Figure 27 WC- Co6% w/ TiN coating. Cross sections of the holes drilled at: a. 0.65 ms (1 J), b. 1.5 ms (32 J), c. 4 ms (66 J) pulse durations

3. Silicon Nitride Ceramic

Silicon nitride is a reasonably tough material and is used for high-speed machining of cast iron in the automotive industry. Single-phase silicon nitride is a highly covalent compound that exists in two hexagonal polymorphic crystalline forms, the alpha and the more stable beta forms. This type of bonding imparts several desirable engineering properties including high strength, thermal stability up to 1850 C, low coefficient of thermal expansion, reasonably good toughness, and a modulus of elasticity greater than many metals. The predominant impurity in silicon nitride powder is SiO_2 , which is present on the surface of the powder form and in greater quantity on the alpha form. In order to achieve maximum densification during sintering, densification aids, such as alumina, yttria, or magnesia or other oxides are added.

Figure 28 shows the variation of the hole diameter and the hole depth with pulse energy for three pulse durations for the silicon nitride material. It can be seen that the hole diameter increases slightly with increasing pulse energy. Similar to WC-Co6% material, the hole depth saturates at higher powers. However, it appears that there is a minimum threshold to reach saturation, which occurs between 10 to 20 joules. Figures 29 (a) to (c) are SEM micrographs of the cross sections of the holes drilled at 0.65 ms, 1.5 ms, and 4 ms pulse durations, respectively, on silicon nitride material. They show that under all conditions tested no radial cracks extending into the work piece can be observed. However, the SEM cross-sectional examination reveals a molten phase that has recrystallized on the inside diameter of the hole [Figure 30 (a) and (b)]. Notably absent is

a significant recast layer on the inside diameter and at the entrance of the hole. It may be noted that at 1850 °C that silicon nitride decomposes into silicon and nitrogen.(Whitney)

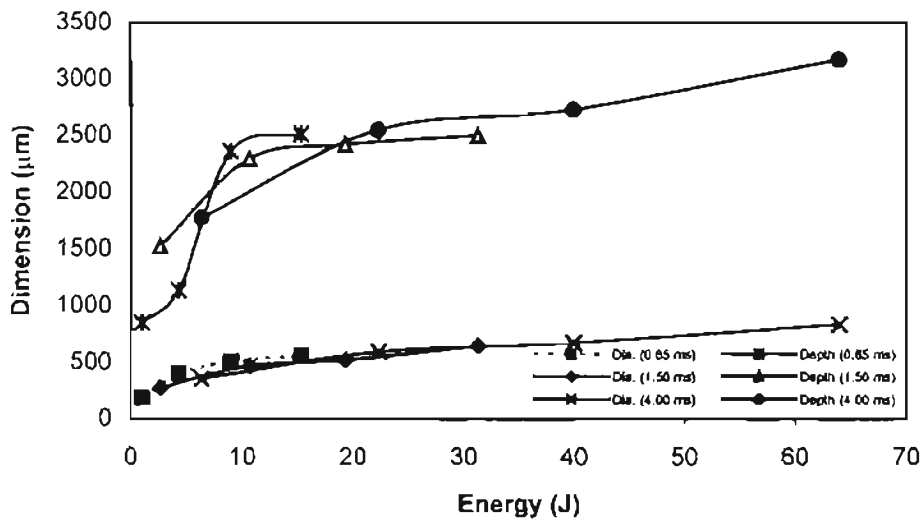


Figure 28 Variation of the hole diameter and hole depth with pulse energy for three pulse durations, namely, shortest (0.65 ms), medium (1.5 ms), and longest (4.0 ms) silicon nitride

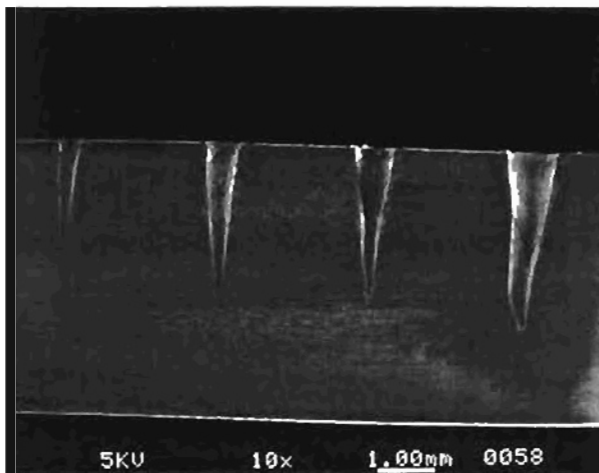
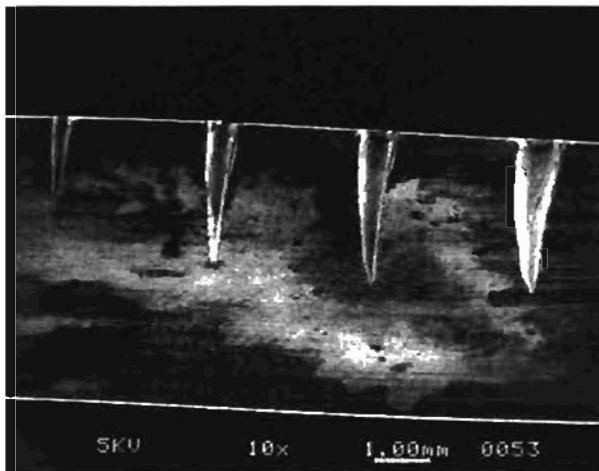
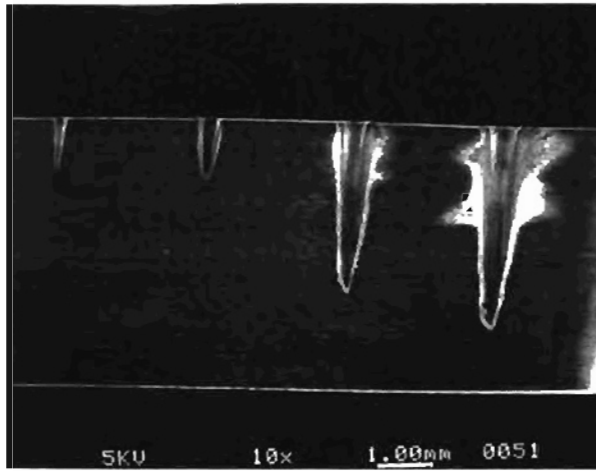


Figure 29 Cross sections of the holes drilled at 0.65 ms, 1.5 ms, and 4 ms pulse durations, respectively on silicon nitride material

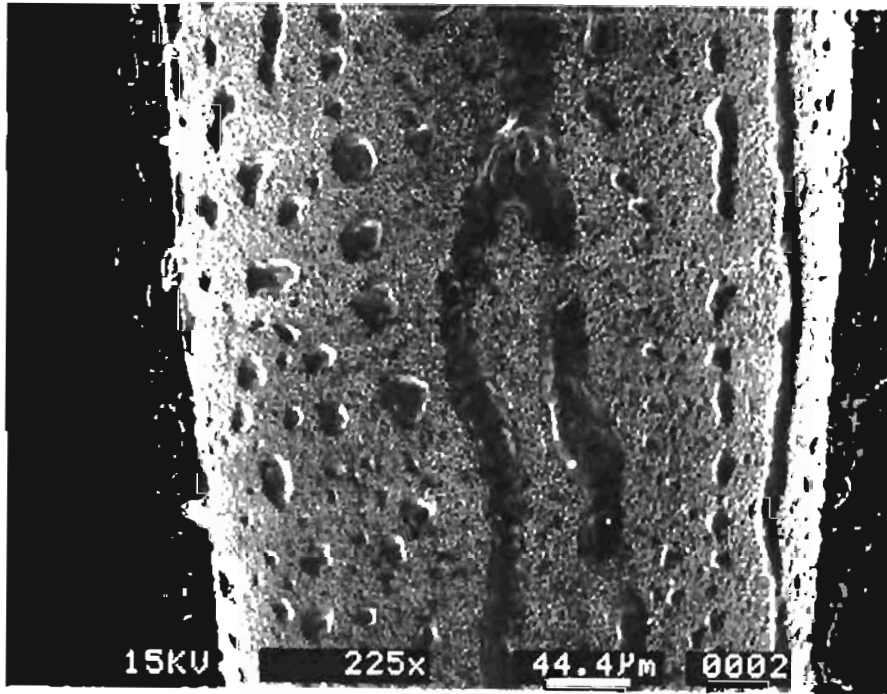
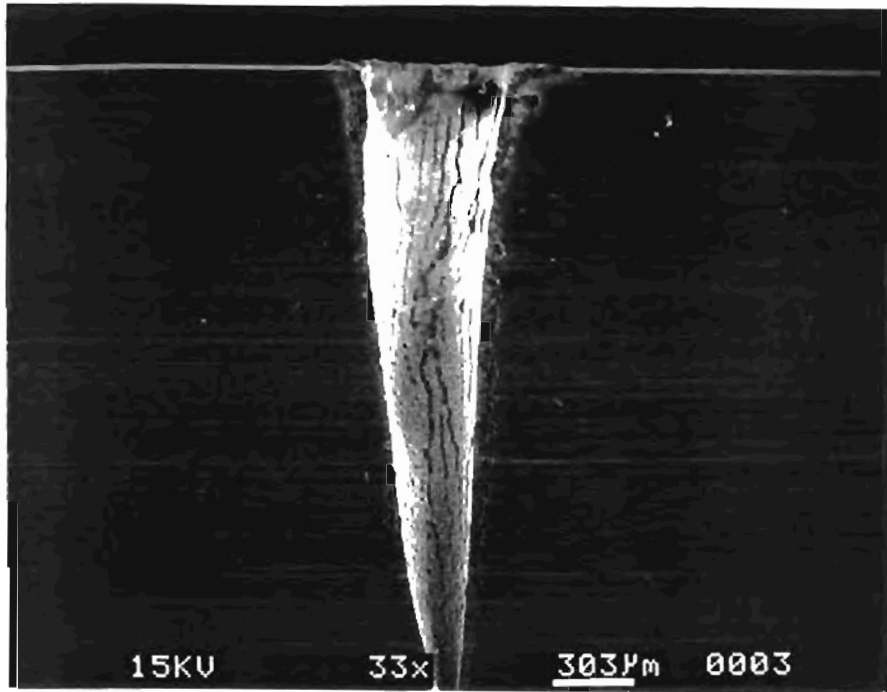


Figure 30 Silicon nitride material. Close-up view.

4. SiAlON Ceramic

Developed in the late 1970's, ceramic research showed that aluminum and oxygen could be substituted for silicon and nitrogen, respectively in the silicon nitride lattice. The general composition is $\text{Si}_{6-Z} \text{Al}_Z \text{O}_Z \text{N}_{8-Z}$, where Z denotes the number of oxygen atoms substituted for nitrogen and has a limiting value of 4.2 at 1700 °C and 2.0 at 1400°C. To fabricate into dense material, sintering aids such as yttria are added.

Figure 31 shows the variation of the hole diameter and the hole depth with pulse energy for three pulse durations for the SiAlON material. It shows that the hole diameter increases with increase in pulse duration, similar to the silicon nitride material. However, hole depth is greater and reaches a slope change around 5 to 10 joules.

Figures 32 (a) to (c) are SEM micrographs of the cross sections of the holes drilled at 0.65 ms, 1.5 ms, and 4 ms pulse durations, respectively on silicon nitride at three power levels. They show that a recrystallized phase exists on the inner surface of the drilled hole but that no cracks extend into the workpiece. No molten material exists on the outer diameter of the hole entrance except for some droplets of the recrystallized material.

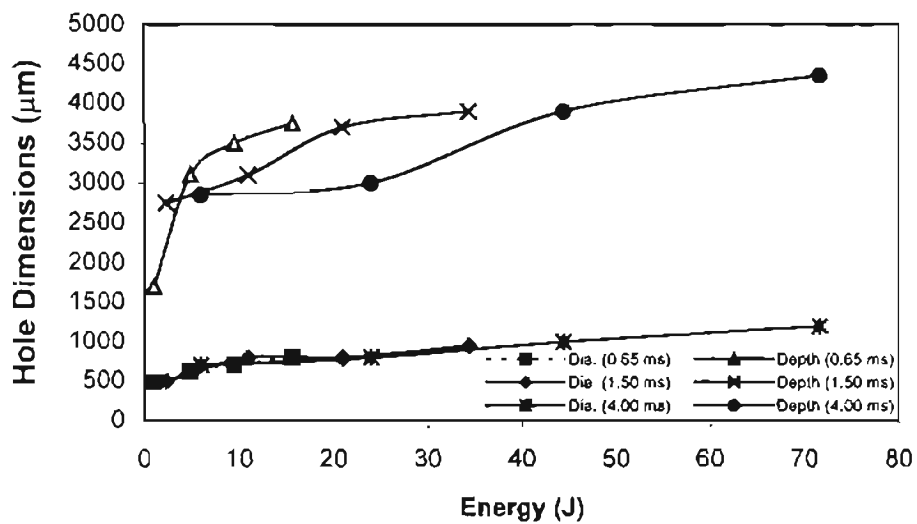


Figure 31 Variation of the hole diameter and hole depth with pulse energy for three pulse durations, namely, shortest (0.65 ms), medium (1.5 ms), and longest (4.0 ms) for SiAlON.

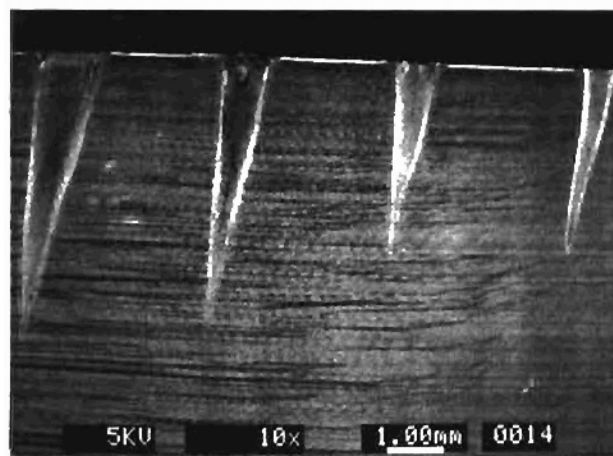
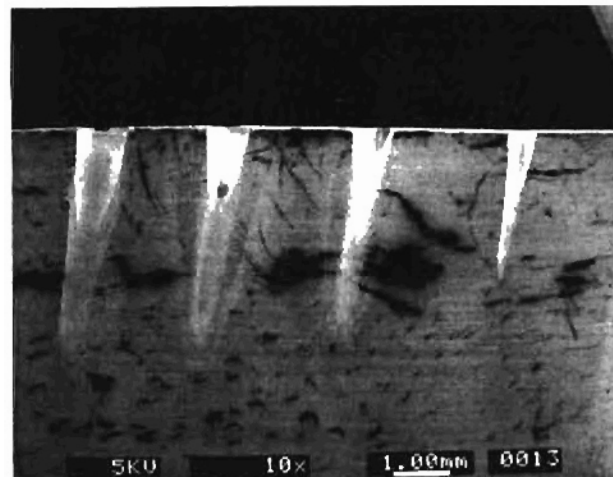
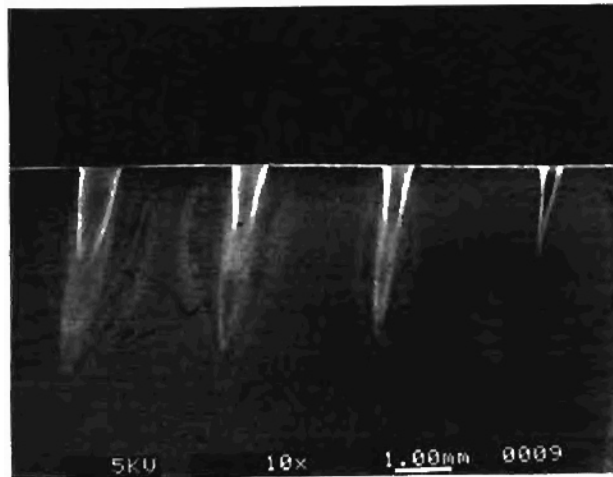


Figure 32 Cross sections of the holes drilled at 0.65 ms, 1.5 ms, and 4 ms pulse durations, respectively on SiAlON material

5. Alumina Ceramic

Figure 33 shows the variation of the hole diameter and hole depth with pulse energy for three pulse durations, namely, shortest (0.65 ms), medium (1.5 ms), and longest (4.0 ms) for aluminum oxide tool material. As the pulse energy is increased, the hole diameter increases as well. However, the hole depth has marked variation, especially at the highest pulse width. At this pulse width and higher pulse energies, the alumina workpiece has a tendency to fracture as shown in Figure 34. Such fracturing may eject large particles that interfere with the beam/ hole interaction. Figure 35 (a) to (c) are SEM micrographs of the cross sections of the holes drilled at 0.65 ms, 1.5 ms, and 4 ms pulse durations, respectively on aluminum oxide tool material at three power levels. It can be seen that this material has a tendency to produce holes with high aspect ratios. This is due to, in part, to the reflectivity of the alumina at high angles of incidence.

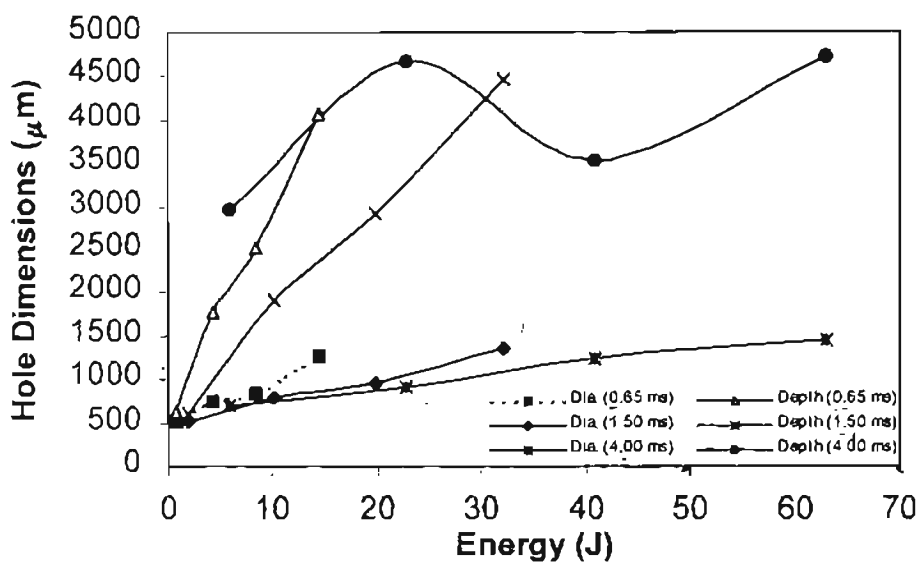


Figure 33 Variation of the hole diameter and hole depth with pulse energy for three pulse durations, namely, shortest (0.65 ms), medium (1.5 ms), and longest (4.0 ms) for aluminum oxide tool material.

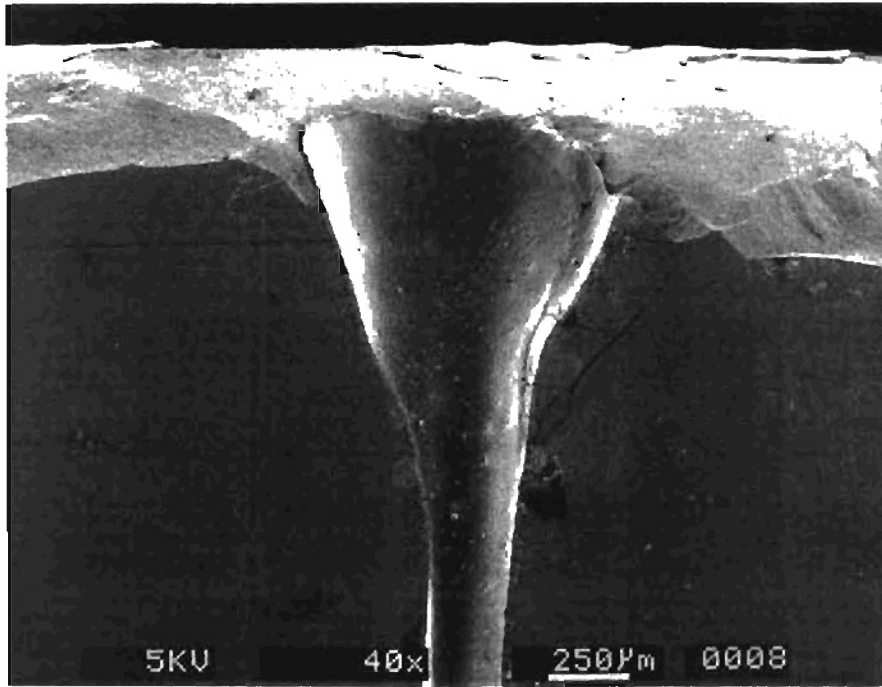


Figure 34 Fracturing of alumina sample at higher energy density

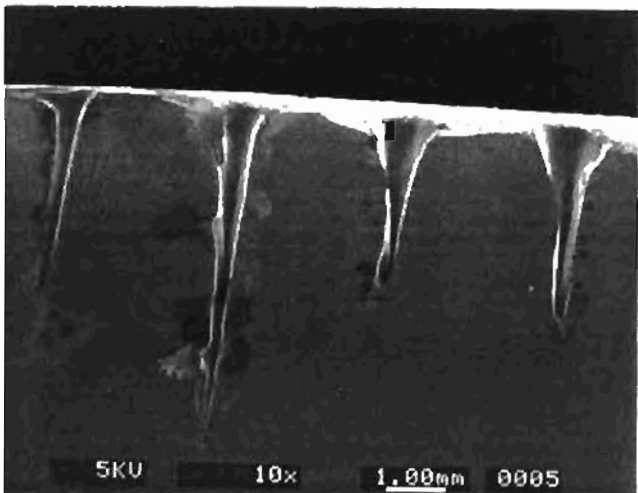
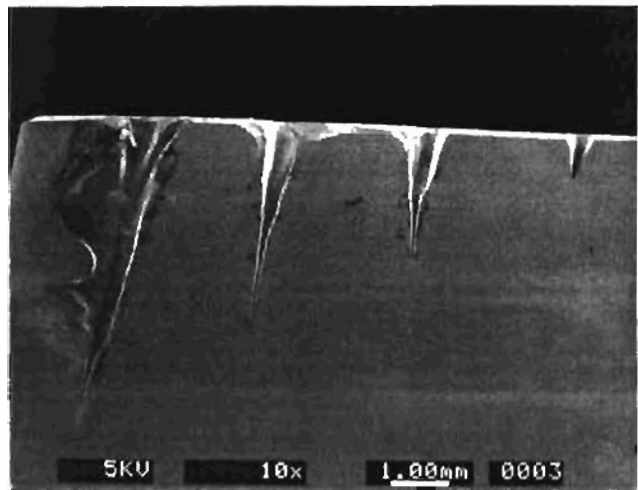
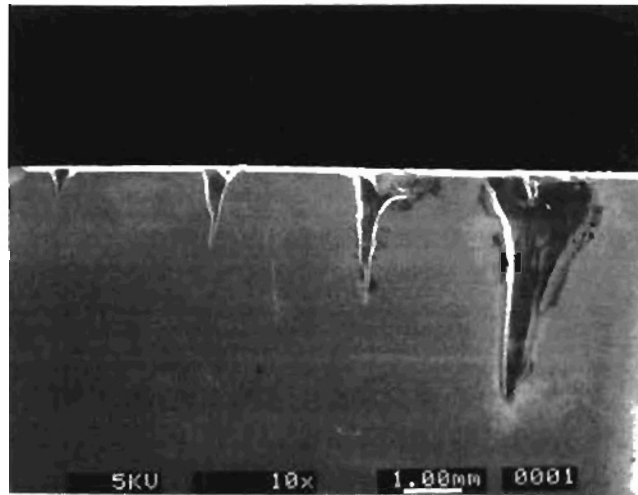


Figure 35 Cross sections of the holes drilled at 0.65 ms, 1.5 ms, and 4 ms pulse durations, respectively on alumina material

6. Alumina plus TiC Ceramic

This material consists of aluminum oxide with the addition of 30 to 40 % titanium carbide particles hot pressed together. The addition of TiC to Al_2O_3 improves the tool material properties, including fracture toughness, bend strength, and resistance to abrasion and erosion wear due to higher hardness. Thermal conductivity and thermal shock cycling are also improved as compared to Al_2O_3 .

Figure 36 shows the variation of the hole diameter and hole depth with pulse energy for three pulse durations, namely, shortest (0.65 ms), medium (1.5 ms), and longest (4.0 ms) for aluminum oxide plus TiC tool material. It shows the hole diameter to increase with increase in pulse energy, similarly to the alumina work material but the hole depth is not as great at the same conditions. However, laser machinability is improved and more predictable especially at the 4.00 ms pulse width conditions. Figures 37 (a) to (c) are SEM micrographs of the cross sections of the holes drilled at 0.65 ms, 1.5 ms, and 4 ms pulse durations, respectively on aluminum oxide plus TiC at three power levels. They show no material fracturing or cracking for this material. What is observed is a molten phase of the alumina and titanium carbide. The aspect ratio is reduced due to the addition of titanium carbide.

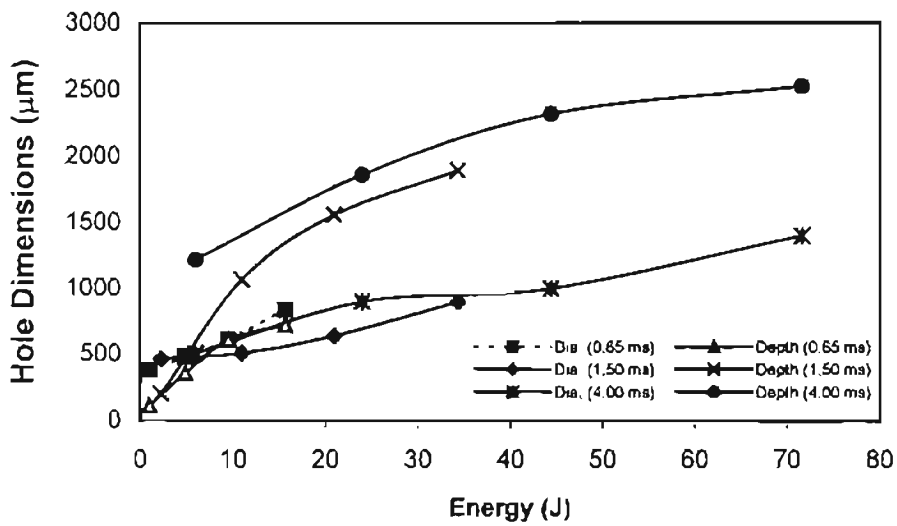


Figure 36 Variation of the hole diameter and hole depth with pulse energy for three pulse durations, namely, shortest (0.65 ms), medium (1.5 ms), and longest (4.0 ms) for aluminum oxide plus TiC tool material.

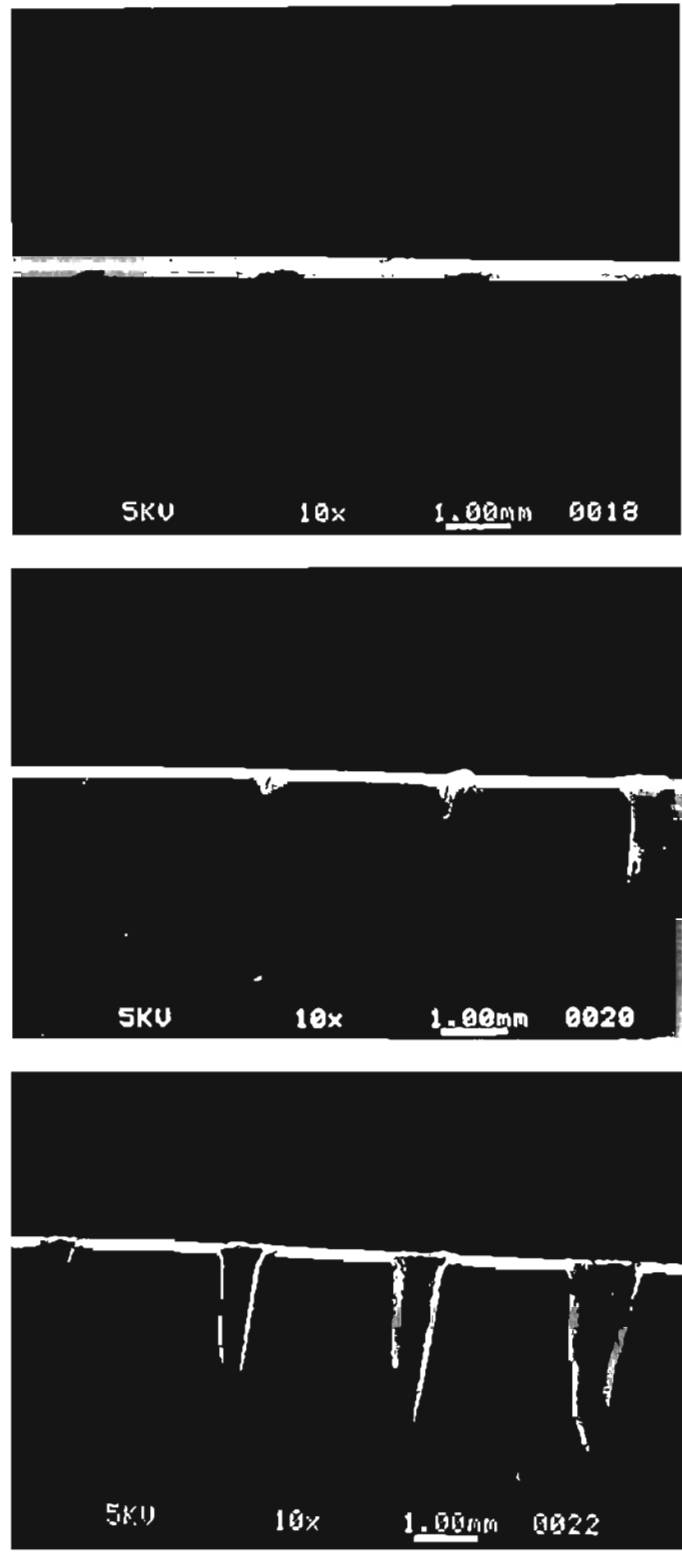


Figure 37 Cross sections of the holes drilled at 0.65 ms, 1.5 ms, and 4 ms pulse durations, respectively on alumina plus TiC material

7. Silicon Carbide Whisker Reinforced Alumina-Zirconia Ceramic

Although aluminum oxide has been used as a cutting tool for years its low resistance to fracture has limited its use to all but high-speed finishing of steels. In an effort to improve the toughness of alumina, two toughening mechanisms have been developed. They are zirconia transformation toughening and whisker/fiber reinforced toughening.

Whiskers of silicon carbide are of the beta or alpha or a combination of alpha and beta forms. Depending on the supplier, they range from 0.05 to 1.0 μm in diameter and 5 to 125 μm in length. Percent addition of silicon carbide whiskers can be up to 45 %. The addition of zirconia further toughens the alumina by a polymorphic transformation of the tetragonal phase to the monoclinic phase. The process of such materials is complex and many different type of oxides can be used to produce this class of engineered materials.

Figure 38 shows the variation of the hole diameter and hole depth with pulse energy for three pulse durations, namely, shortest (0.65 ms), medium (1.5 ms), and longest (4.0 ms) for SiC whisker reinforced alumina-zirconia tool material. It shows that hole diameter increases, similar to that of the aluminum oxide material, with increase in pulse energy. Hole depth is nearly proportional to the input energy and a saturation level or slope change in the curve is not readily apparent. Figures 39 (a) to (c) are SEM micrographs of the cross sections of the holes drilled at 0.65 ms, 1.5 ms, and 4 ms pulse durations, for SiC whisker reinforced alumina-zirconia tool material. They show that the drilling behavior is predictable but that at higher energy levels the effect of internal reflection produces holes with higher aspect ratios but is not as pronounced as seen in the

pure alumina sample. What is readily apparent at all conditions tested is a recast layer whose morphology is distinct from the substrate material as seen in Figures 40 (a) and (b). The thickness ranges from 5 to 20 μm and has a mosaic-like pattern. Cracking or fractures that extend into the workmaterial were observed, as well.

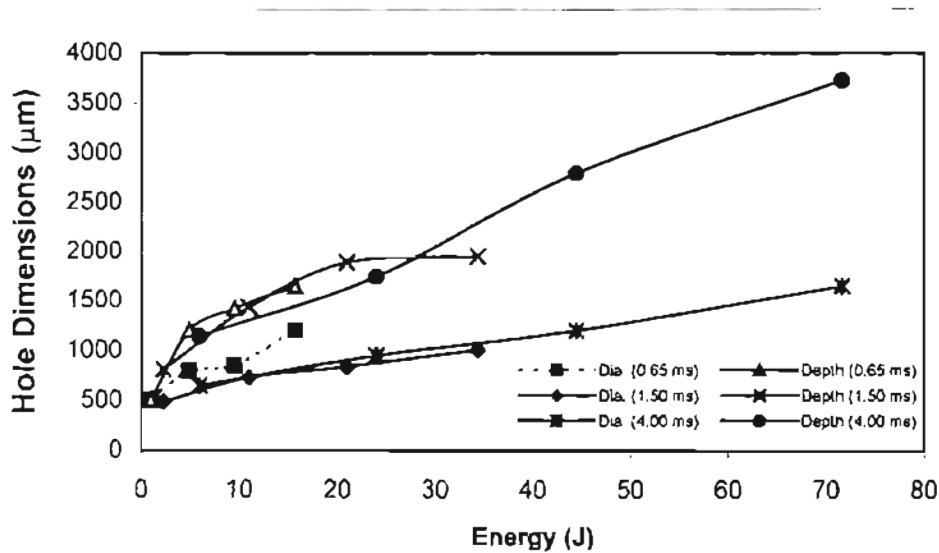


Figure 38 Variation of the hole diameter and hole depth with pulse energy for three pulse durations, namely, shortest (0.65 ms), medium (1.5 ms), and longest (4.0 ms) for SiC whisker reinforced alumina-zirconia tool material.

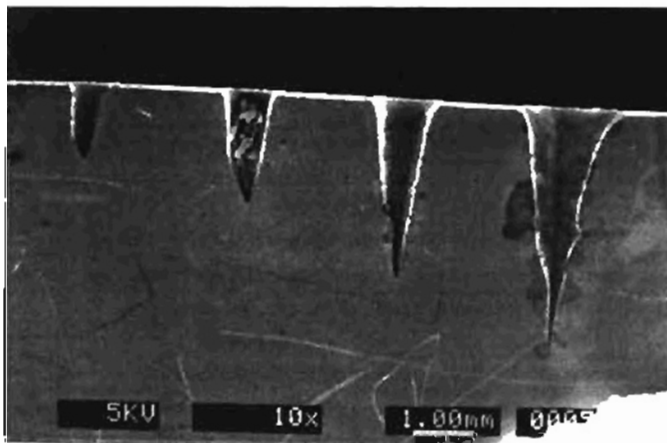
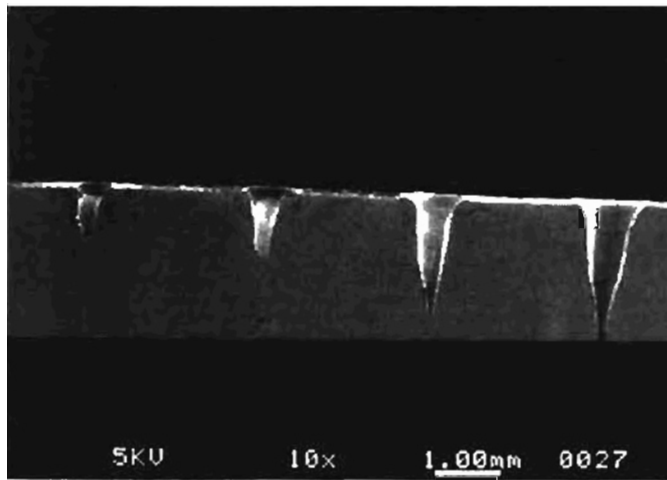
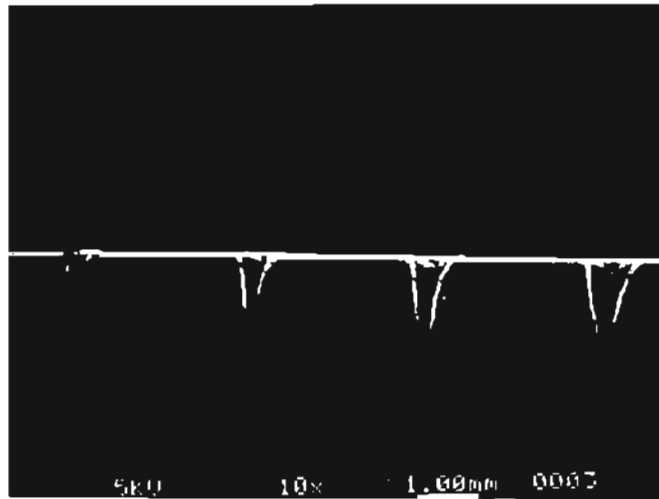


Figure 39 Cross sections of the holes drilled at 0.65 ms, 1.5 ms, and 4 ms pulse durations, respectively on silicon carbide whisker reinforced alumina - zirconia material

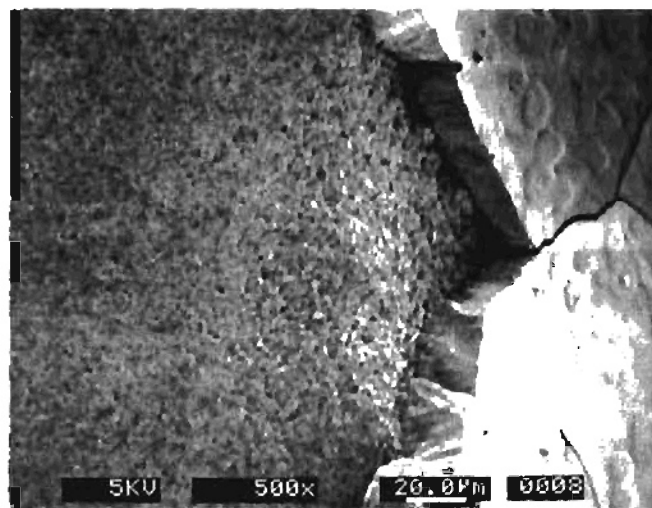
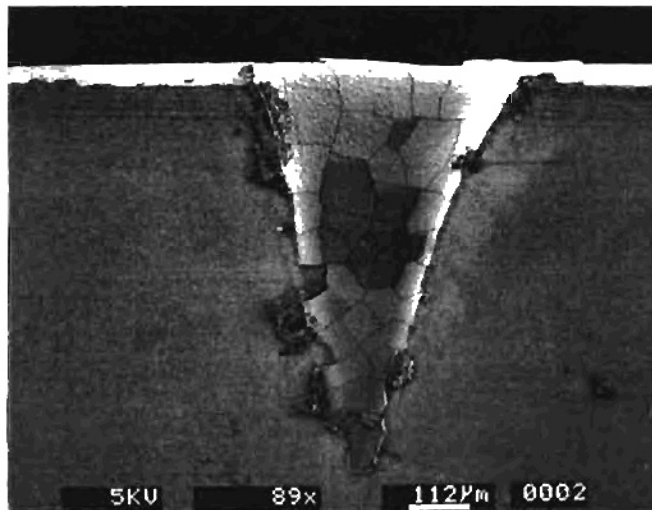
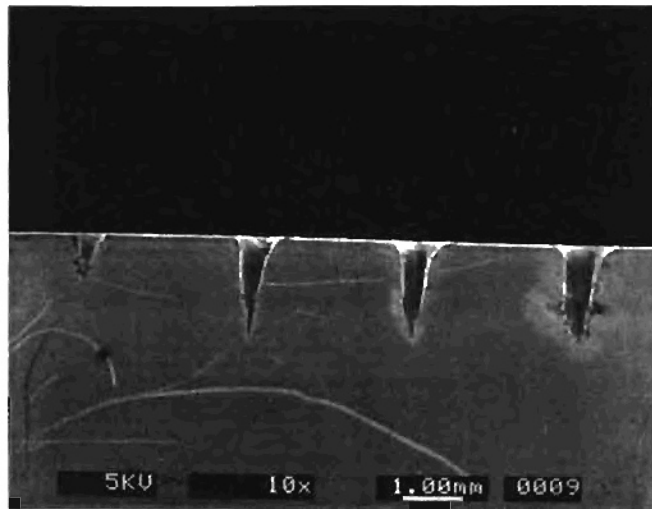


Figure 40 Recast layer on whisker reinforced alumina- zirconia

8. TiC plus TiN Cermet

Cermet, which is an acronym derived from the constituents ceramic and metal. The ceramic phase consists of titanium nitride (TiN) and titanium carbide (TiC). The metallic binder phase is composed of nickel with the addition of a small amount of molybdenum to improve wettability of the binder. They are manufactured using powder metallurgy techniques and liquid phase sintering similar to that used in the manufacture of conventional carbides. Originally developed by Ford Motor Company, TiC cermet with a Ni-Mo binder is used for the high speed finish machining of steels in the automotive industry. To improve the toughness at the expense of some hardness, a TiC-TiN cermet with a similar binder was recently developed to extend the application to semi-roughing and interrupted cutting.

Figure 41 shows the variation of the hole diameter and hole depth with pulse energy for three pulse durations, namely, shortest (0.65 ms), medium (1.5 ms), and longest (4.0 ms) for TiC-TiN cermet tool material. It indicates that the drilling behavior is different from that of pure ceramics. For example, the hole diameter tends to be greater for the shorter pulse width for a given energy level. This tendency is due to the recast layer and the redeposition of ablated material. Hole depth is similarly affected and a leveling or downward saturation trend is observed in the 1.50 ms and 4.00ms pulse width curves. Figures 42 (a) to (c) are SEM micrographs of the cross sections of the holes drilled at 0.65 ms, 1.5 ms, and 4 ms pulse durations for TiC-TiN cermet tool material. They show that for all conditions tested solidified material exists on the inside diameter of the drilled holes which varies from 5 to 10 μm and a heat affect zone beneath. Cracks

exist both circumferentially and longitudinally in the recast layer. These fractures extend into the work piece material indicating the sensitivity to thermal damage of this material.

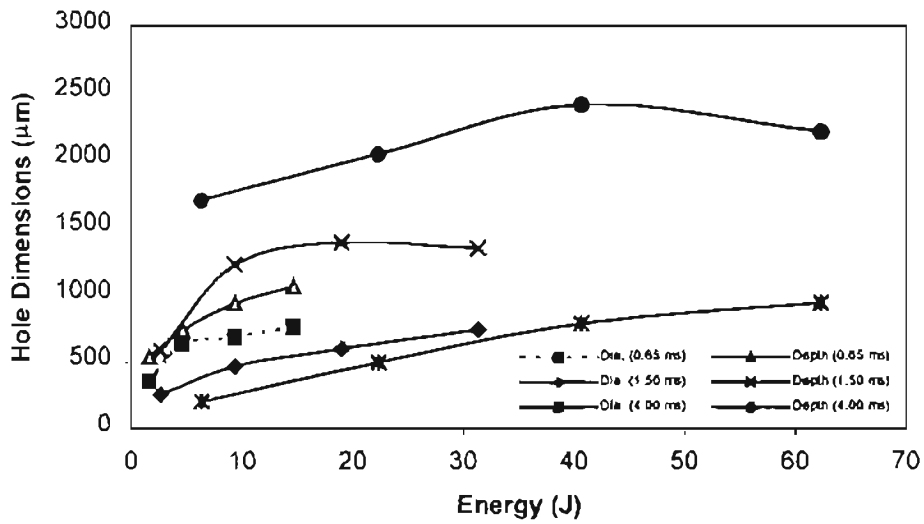


Figure 41 Variation of the hole diameter and hole depth with pulse energy for three pulse durations, namely, shortest (0.65 ms), medium (1.5 ms), and longest (4.0 ms) for TiC-TiN cermet tool material

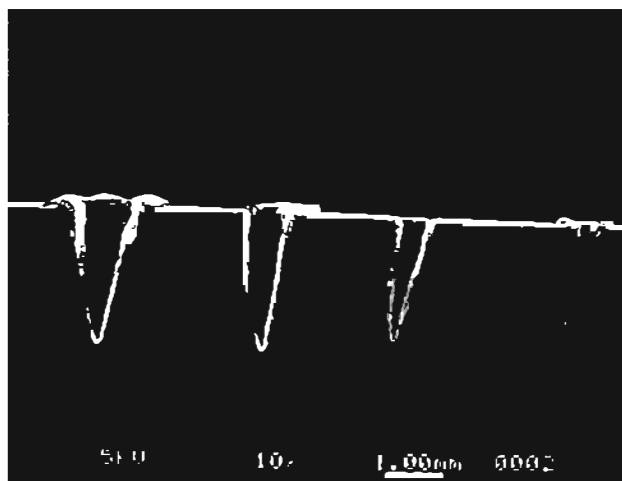
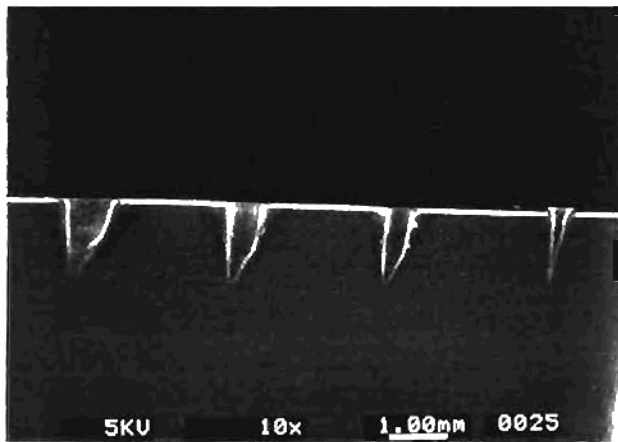
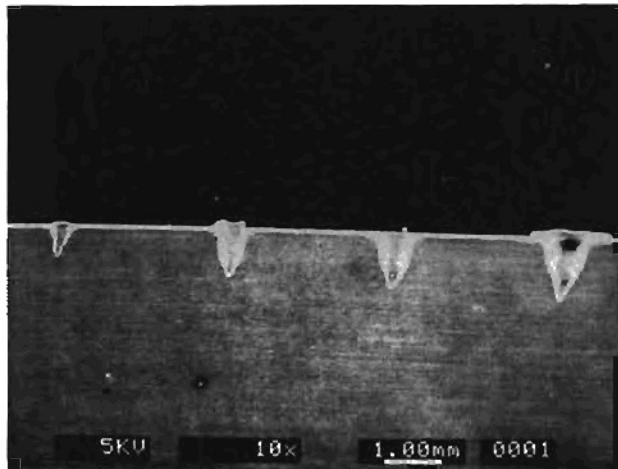


Figure 42 Cross sections of the holes drilled at 0.65 ms, 1.5 ms, and 4 ms pulse durations, respectively on TiC / TiN cermet material

9. Polycrystalline Cubic Boron Nitride (c-BN)

Developed in the late 1960's by Robert Wentorf, Jr., a research scientist at the General Electric Corporate Research in Schenectady, NY. , this material is a diamond analogue with a boron and nitrogen group and with properties similar to that of diamond. This material does not occur naturally. It is the second hardest material (4700 Kg/mm^2), next only to diamond (8000 Kg/mm^2) in hardness. This synthetic material is produced by high-pressure - high temperature methods similar to that of polycrystalline diamond. Monolithic polycrystalline bodies such as that used in this investigation are produced using similar methods. Though not as hard as diamond it has properties that make it well suited to certain applications where diamond is unsuitable, for example in the machining of hardened alloys steels (Rc 55 and above). Because of its greater resistance to oxidation and less reactivity with ferrous workmaterials that react with carbon, it is used to machine such alloys as nickel, cobalt and iron based superalloys and hardened steels.

Figure 43 shows the variation of the hole diameter and hole depth with pulse energy for three pulse durations, namely, shortest (0.65 ms), medium (1.5 ms), and longest (4.0 ms) for polycrystalline cBN tool material. It shows that the hole diameter as well as the hole depth increases nearly proportionally to energy input for all pulse widths. In general, the drilling characteristic of cubic boron nitride is the most uniform of all the materials tested in this investigation. This is primarily due to the absence of a liquid phase at atmospheric pressure for cubic boron nitride. Figures 44 (a) to (c) are SEM micrographs of the cross sections of the holes drilled at 0.65 ms, 1.5 ms, and 4 ms pulse durations polycrystalline cBN tool material. They show that no recast layer exists nor

does a HAZ (heat affected zone). Although material tends to fracture at the hole entrance, which may be a limitation of the two piece method of drilling, no cracks or fracturing is observed within the drilled hole nor extending into the work piece.

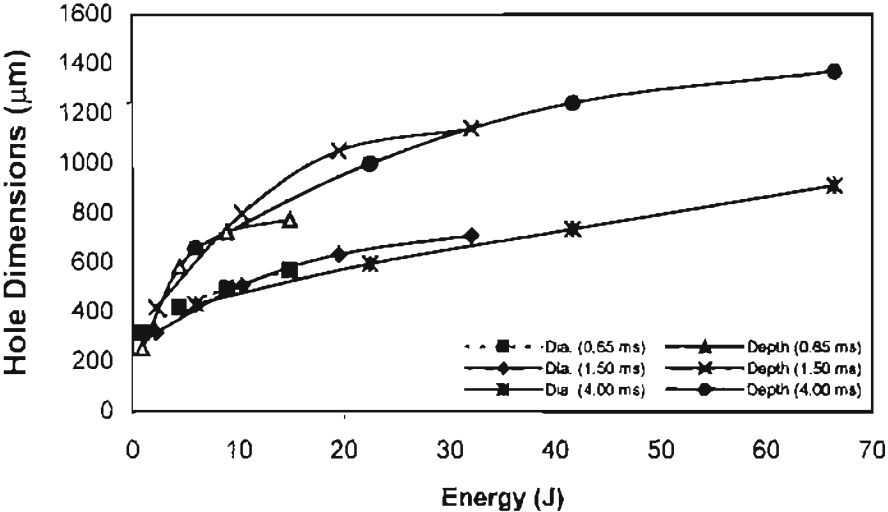


Figure 43 Variation of the hole diameter and hole depth with pulse energy for three pulse durations, namely, shortest (0.65 ms), medium (1.5 ms), and longest (4.0 ms) for polycrystalline c-BN tool material.

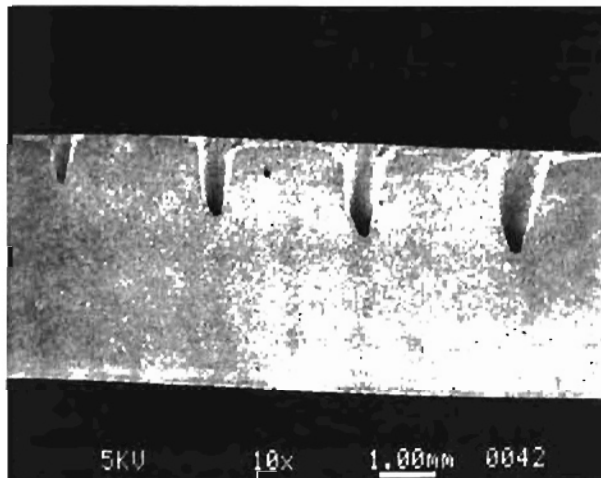
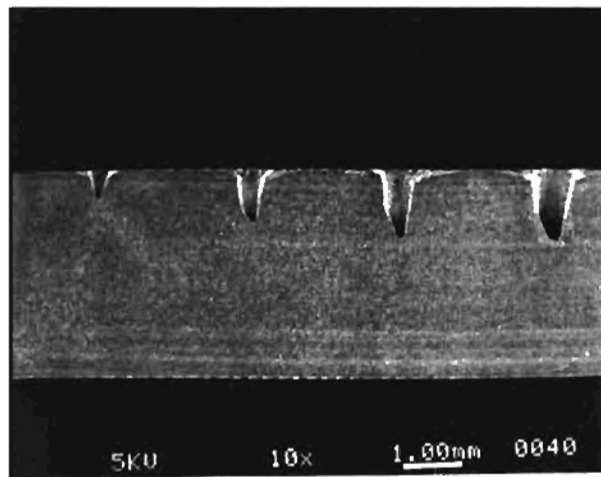
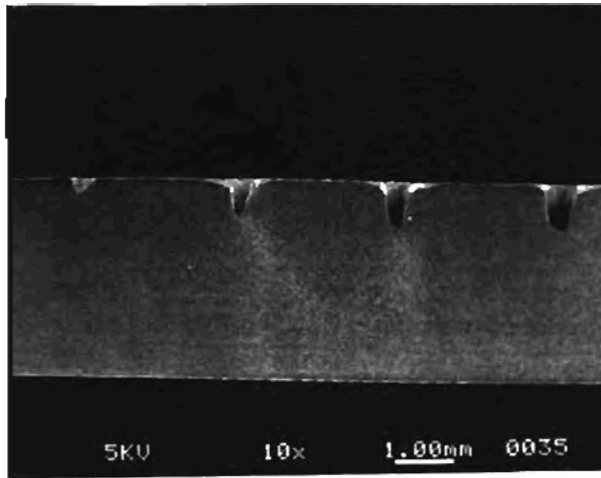


Figure 44 Cross sections of the holes drilled at 0.65 ms, 1.5 ms, and 4 ms pulse durations, respectively on cubic boron nitride material

CHAPTER 10

CONCLUSIONS

In this investigation a Nd:YAG laser machining system was set up to conduct experimental research in laser machining. Initial work involved acquiring the laser, setting up of the laser system in the Laser Assisted Machining Laboratory of the Mechanical Aerospace Engineering Research Labs at Oklahoma State University, alignment of optical components of the laser, design and assembly of computer numeric computer (CNC) 3-axis motion control system, integrated with control of the laser system and gas delivery system. Also, safety systems were installed and safety equipment acquired for personnel working around the laser system. Other research students were trained in the use of the laser equipment.

Research was conducted on the single pulse drilling of advanced materials with the Nd:YAG laser. The materials used in this investigation were advanced ceramic materials and cemented carbides that are difficult to process by conventional methods. A parametric study was conducted to investigate the correlation of hole depth and hole diameter with respect to total laser energy input and pulse duration. This correlation was chosen to be the focus of this study rather than hole dimension versus instantaneous power since it was assumed that conduction effects would be minimal across the materials tested and would provide fundamental information on the amount of material removed per unit energy. However, it is conceivable that if conduction effects are significant in the workpiece tested, then investigating the correlation between material removed versus power may provide more useful information. This may be the case for the TiC/ TiN cermet material tested in this investigation as we see a divergence of the

hole diameter curves between the differing pulse widths. However, as the pulse width of the laser beam is decreased, conduction effects are minimized and using the material removed versus energy correlation will prove more accurate.

Conclusions that can be drawn from this study are the following:

- Concerning hole diameter with respect to energy input, hole diameter increased with increasing energy input. With respect to increasing pulse width, this did not affect the hole diameter except for alumina and the TiC -TiN cermet which exhibited a significant recast layer. This produced larger diameter holes per unit energy input for the shorter pulse widths.
- Concerning hole depth with respect to energy input, in general, increasing the pulse energy increased the hole depth especially at lower energy levels. However, certain materials exhibited non-linear behavior due to fracturing, such as alumina, or saturation at higher energy levels, such as WC-Co6%, WC-Co6% plus TiN, and the TiC-TiN cermet. With respect to the various pulse widths, those materials which have liquid and gas phases produced during drilling exhibited depth versus energy characteristics that were not collinear, indicating that rate of energy input, i.e. power, affects the drilling characteristics. The exceptions were the Silicon Carbide whicker reinforced alumina-zirconia material and the polycrystalline cubic boron nitride material due to the gas only phase of a major constituent.
- Most materials in this investigation showed a recast layer or deposition of decomposition material on the inner walls of the drilled hole with the exception of polycrystalline cubic boron nitride (PCBN).

- The materials with a metallic binder (WC -Co 6%, WC-Co 6%plus TiN coating, TiC-TiN cermet) exhibited susceptibility to cracking due to thermal effects.
- Alumina and PCBN were susceptible to fracturing at the hole entrance due to thermal and ablation effects.

CHAPTER 11

FUTURE RECOMMENDATIONS

In this investigation, the Nd:YAG laser was installed and used in the drilling of some of the difficult-to-machine materials. Because of the considerable time and effort involved in the installation, alignment of the beam and operation of this high power laser only a limited amount of testing was conducted. Future work should include detailed investigation of this process including multiple pulses and different aspect ratios of the holes. The holes made should be characterized for their size, parallelism, surface integrity such as thermal cracks, recast layer etc. In addition, optimal conditions should be developed for good quality holes by this process. The process should also be extended not only for drilling but also for producing 2-dimensional contour geometries on the work piece. In addition, much of the experimental work on the machining of ceramics was using a CO₂ laser. It would be interesting to conduct a comparative evaluation of the performance of both types of lasers that are available at OSU in the machining ceramics and cemented carbides. Thermal modeling of the laser drilling process should be conducted and compared with the experimental results. Some work is already in progress at OSU and this should be continued take a fundamental contribution towards an understanding of the laser-material interactions.

References

- "Laser Assist for Machining," *Manufacturing Engineering*, (Nov 1995) 26-27.
- "A laser is born," *IEEE Spectrum*, May 1992.
- Abakians, H., and M. F. Modest, "Evaporative Cutting of a Semi-Transparent Body with a Moving CW Laser," *ASME Journal of Heat Transfer*, 110, (1988) 924-930.
- Affolter, P., and H. G. Schmid, "Processing of New Ceramic Materials with Solid State Laser Radiation," In *High Power Lasers*, 801, SPIE, (1987) 120-129.
- Allcock, G., Dyer, P. E., Elliner, G., and H. V. Snelling, "Experimental Observations and Analysis of CO₂ Laser Induced Microcracking of Glass," *J. Appl. Phys.*, 78(12), (1995) 7295-7303.
- Arata, Y., Abe, N., and N. Tsujii, "Fundamental Phenomena during Vacuum Laser Welding," In *Proceedings of the Materials Processing Symposium ICALEO '84*, (1984) 1-7.
- Amot, R. S., and C. E. Albright, "Plasma Plume Effects in Pulsed Carbon Dioxide Laser Spot Welding," In *Proceedings of ICALEO '83*, 38,(1983) 51-58.
- Atanasov, P. A., and S. I. Gendjov, "Laser Cutting of Glass Tubing- A Theoretical Model," *J. Phys. D: Appl. Phys.*, 20, (1987) 597-601.
- Baird, J. D., and A. Taylor, "Reaction Between Silica and Carbon and the Activity of Silica in Slag Solution," *Transactions of the Faraday Society*, 54, (1958) 526-539.

Bang, S. Y., and M. F. Modest, "Evaporative Cutting with a Moving CW Laser- Effects of Specular Reflections," In Fundamentals of Radiation Heat Transfer, HTD-160, ASME, (1991) 69-78.

Bang, S. Y., and M. F. Modest, "Evaporative Scribing with a Moving CW Laser - Effects of Multiple Reflections and Beam Polarization," In Proceedings of ICALEO '91, Laser Materials Processing, 74, (1992) 288-304.

Bang, S. Y., and M. F. Modest, "Multiple Reflection Effects on Evaporative Cutting with a Moving CW Laser," ASME Journal of Heat Transfer, 113(3), (1991) 663-669.

Bar-Isaac, and C., U. Korn, "Moving Heat Source Dynamics in Laser Drilling Processes," Applied Physics, 3, (1974) 45-54.

Batanov, V. A., Bunkin, F. V., Prokhorov, A. M., and V. B. Fedorov, "Evaporation of Metallic Targets caused by Intense Optical Radiation," Soviet Phys- JETP, 36, (1973) 311-322.

Batha, H. D., and E. D. Whitney, "Kinetics and Mechanism of the thermal Decomposition of Si_3N_4 ," Journal of the American Ceramic Society, 56, (1973) 365-369.

Biyikli, S., and M. F. Modest, "Beam Expansion and Focusing Effects on Evaporative Laser Cutting," ASME Journal of Heat Transfer, 110, (1988), 529-532.

Borkin, A. G., Drobyazko, S. V., Levchenko, E. B., Senatorov, Y. M., and A. Y. Turygin. "Self focusing and Waveguide Propagation of Radiation in the case of Deep Penetration of a Metal by a Laser Beam," Soviet Journal of Quantum Electronics, 15, (1985) 1515-1523.

Borsch-Supan, W., Hunter, L. W., and J. R. Kutter, "Endothermic Gasification of a Solid by Thermal Radiation Absorbed in Depth," *International Journal of Heat and Mass Transfer*, 27, (1984) 1171-1182.

Brugger, K., "Exact Solutions for the Temperature Rise in a Laser Heated Slab", *Journal of Applied Physics*, Vol. 43, 1972, pp. 577-583.

Carslaw, H.S. and J.C. Jaeger, *Conduction of Heat in Solids*, Oxford University Press, 2nd ed., 1959.

Chen, X., Lotshaw, W. T., Ortiz, A. L., Staver, P. R., Erikson, C. E., McLaughlin, M. H., and T. J. Rockstroh, "Laser Drilling of Advanced Materials: Effects of Peak Power, Pulse Format, and Wavelength," *Journal of Laser Applications*, 8, (1996) 233-239.

Chen, X., A.L. Ortiz, P.R. Stave, W.T. Lotshaw, T.J. Rockstroh, M. H. McLaughlin, "Improved hole drilling using a high peak power Nd:YAG laser at the second harmonic wavelength", *Journal of Laser Applications*. 9: (6), Dec. 1997, 287-290.

Chryssolouris, George, Laser Machining: Theory and Practice, Springer-Verlag, New York, Inc., 1991

Chun, M. K., and K. Rose, "Interaction of High Intensity Laser Beams with Metals," *Journal of Applied Physics*, 41(2), (1970) 614-620.

Dabby, F. W. and Paiek, U.-C., "High-Intensity Laser-Induced Vaporization and Explosion of Solid Material", *IEEE Journal of Quantum Electronics*, Vol. QE-8, 1972, pp. 106-111.

DeBastiani, D., Modest, M. F., and V. S. Stubican, "Mechanisms of Reactions during CO₂ Laser Processing of Silicon Carbide," *Journal of the American Ceramic Society*, 73(7), (1990) 1947-1952.

Dobrovolskii, I. P., and A. A. Uglov, "Analysis of the Heating of Solids by Laser Radiation Allowing for the Temperature Dependence of the Absorptivity," *Soviet Journal of Quantum Electronics*, 4, (1974) 788-790.

Drowart, J., De Maria, G., and M. G. Inghram, "Thermodynamic Study of SiC Utilizing a Mass Spectrometer," *Journal of Chemical Physics*, 29, (1958) 1015-1021.

Duley, W. W., and J. N. Gonsalves, "CO₂ Laser Cutting of Thin Metal Sheets with gas Jet Assist," *Optics and Laser Technology*, 6, (1974) 78-81..

Duley, W. W., "Laser Processing and Analysis of Materials," Plenum Press, New York, (1983).

Duley, W.W., CO₂ Lasers: Effects and Applications. Academic Press, Inc., 1976.

Durand, C., Ramulu, M., Pierre, R., and J. Machan, "An Experimental Analysis of a Nd-YAG Laser Cutting Process for Machining Silicon Nitride," *International Journal of Prod. Res.*, 34(5), (1996) 1417-1428.

Eberl, G., Hildebrand, P., Kuhl, M., Sutor, and U., P. Wrba, "New Developments in the LASERCAV Technology," in the Proceedings of ICALEO '91, Laser Materials Processing, 74, San Jose, CA, (1992) 1-14.

Engin, D., and K. W. Kirby, "Development of an Analytical Model for the Laser Machining of Ceramic and Glass-Ceramic Materials," *J. Appl. Phys.*, 80(2), (1996) 681-690.

Fieret, J., Terry, M. J., and B. A. Ward, "Overview of Flow Dynamics in Gas-Assisted Laser Cutting," In *High Power Lasers*, 801, SPIE, (1987) 243-250.

Finucane, M. A., and I. Black, "CO₂ Laser Cutting of Stained Glass," *Int. J. of Adv. Manuf. Technology*, 12, (1996) 47-59.

Ghosh, S., B.P. Badgajar, G.L. Goswami, "Parametric Studies of Cutting Zircaloy-2 Sheets with a Laser Beam", *Journal of Laser Application*, V0008 N3, June 1996, pp. 143-148.

Gonsalves, J. N., and W. W. Duley, "Cutting thin Metal Sheets with the CW CO₂ Laser," *Journal of Applied Physics*, 43, (1972) 4684-4687.

Gonsalves, J. N., and W. W. Duley, "Interaction of CO₂ laser radiation with Solids I. Drilling of Thin Metallic Sheets," *Canadian Journal of Physics*, 49, (1971) 1708-1713.

Gregersen, O., and F. O. Olsen, "Beam Analyzing System for CO₂ Lasers." In *Proceedings of Laser Materials Processing*, ICALEO, (1990) 27-35.

Grigoryants, A. G. "Basics of Laser Material Processing," Mir Publishers, 1994.

Grum, J., and D. Zuljan, "Analysis of Heat Effects in Laser Cutting of Steels," *Journal of Materials Processing and Performance*, 5(4), (1996) 526-537.

Hachfeld, K. D., "Laser Beam Quality and Brightness Impacts Industrial Applications," in *The Industrial*

Hecht, J., "Laser Guidebook," Optical and Electro-Optical Series, 2nd Edition, (1992).

Hecht, J., "Understanding Lasers: An Entry Level Guide," IEEE Press Understanding Science and Technology Series, 2nd Edition, (1992).

Hecht, Jeff, "Excimer lasers produce powerful ultraviolet pulses," Laser Focus World, June 1992, pg. 63-72.

Herziger, G., Beyer, E., Kramer, R., Loosen, and P., F. Ruhl, "Diagnostic System for Measurement of the Focus Diameter of High Power CO₂ Lasers," In International Conference on Laser Advanced Materials Processing-Science and Applications, High Temperature Society of Japan, Japan Laser Processing Society, Japan,(1987) 37-41.

Ilavarasan, P. M., and P. A. Molian, "Laser Cutting of Thick Sectioned Steels Using Gas Flow Impingement on the Erosion Front," *Journal of Laser Applications*, 7, (1995) 199-209.

Iyer, Ragesh, "Material Processing using a CO₂ Laser", (1997) MS Thesis, Oklahoma State University, Stillwater, OK

Jones, M. G., Georgalas, G., and Brutus, A., "Basic Computer Model of the Pulsed Laser Drilling Process with a Neodymium Laser", *Industrial Laser Handbook*, 1983, pp.159-164.

Kirichenko, N. A., and B. S. Luk'yanchuk, "Laser Activation of Oxidizing Reactions on the Surfaces of Metals," *Soviet Journal of Quantum Electronics*, 13, (1983) 508-511.

Kocher, E., Tshudi, L., Steffen, and J., G. Herziger, "Dynamics of Laser Processing in Transparent Media," *IEEE Journal of Quantum Electronics*, QE-8, (1972) 120-125.

Kunz, T. D., Menefee, R. F., Krenk, B. D., Fredin, L. G., and M. J. Berry, "Laser Probe Absorption Spectroscopy Measurements on Laser Induced Plumes," *High Temperature Science*, 27, (1990) 459-472.

Lax, M., "Temperature Rise Induced by a Laser Beam," *Journal of Applied Physics*, 50, (1971) 1761-1789.

Lim, G. C., and W. M. Steen, "Measurement of the Temporal and Spatial Power Distribution of a High Power CO₂ Laser Beam," *Optics and Laser Technology*, (1982) 149-153.

Longfellow, J, "High Speed Drilling in Alumina Substrates with a CO₂ Laser," *Ceramic Bulletin*, 50(3), (1971) 251-253.

Lukacs, M., Sayer, and M., H. Bisset, "Copper Vapour Laser Machining of Ceramics." *Canadian Ceramics Quarterly*, (1995) 148-151.

Lunau, F. W., Paine, E. W., Richardson, M., and M. D. Wijetunge, "High Power Laser Cutting using a Gas Jet," *Optics Technology*, 1, (1969) 255-258.

Lusquiños, F, J. Pou. R Soto, and M. Pérez-Amor, "The drilling of slate tiles by a Nd:YAG laser", *Journal of Laser Applications*, (1997) 9, 211-214.

Manes, K.R., L.E. Zapata, "Towards High Brightness Multi-Kilowatt Solid State Lasers." *ICALEO 1990*, pg. 100-122.

Maydan, D. "Micromachining and Image Recording on Thin Films by Laser Beams," *Bell System Technical Journal*, 50, (1971) 1761-1789.

- Mazumder, M., and W. M. Steen, "Heat Transfer Model for CW Laser Material Processing," J. Appl. Phys., 51(2), (1980) 941-947.
- Modest M. F., and H. Abakians, "Heat Conduction in a Moving Semi-Infinite Solid Subjected to Pulsed Laser Irradiation," ASME Journal of Heat Transfer, 108, (1986) 597-601.
- Modest, M. F., "Laser Processing of Ceramics", IN Waidelich, W., ed., Laser in Engineering- Proceedings of the 11th International Congress laser '93. Munich, Germany, 1993, pp. 360-371.
- Modest, M. F., and H. Abakians, "Evaporative Cutting of a Semi-Infinite Body with a Moving CW Laser," ASME Journal of Heat Transfer, 108, (1986) 602-607.
- Modest, M. F., and S. Ramanathan, "Laser Machining of Ablating Materials-Overlapped Grooves and Entrance/Exit Effects," ICALEO, (1994) 303-312.
- Modest, M. F., "Laser Processing of Materials-The Present and Future," In Proceedings of the XXII ICHMT International Symposium on Manufacturing and Materials Processing, Dubrovnik, Yugoslavia, 1990.
- Molian, P. A, "Dual-Beam CO₂ Laser Cutting of Thick Metallic Materials," Journal of Materials Science, 28, (1993) 1738-1748.
- Nissim. Y. I., Lietoila, A., Gold, R. B., and J. F. Gibbons, "Temperature Distributions Produced in Semiconductors by a Scanning Elliptical or Circular CW Laser Beam," Journal of Applied Physics, 51, (1980) 274-279.

Paek, U. C. , and Gagliano, F. P.. "Thermal Analysis of Laser Drilling Processes", *IEEE Journal of Quantum Electronics*, Vol. QE-8, 1972, pp. 112-119.

Paek, U. C., and V. J. Zaleckas, "Scribing of Alumina Material by YAG and CO₂ Lasers." *The American Ceramic Bulletin*. 54, (1975), 585-588.

Powell, J., King, T. G., and I. A. Menzies, "Cut Edge Quality Improvement by Laser Pulsing." In 2nd International Conference of Lasers in Manufacturing. Birmingham, UK, (1985) 37-45.

Ramanathan, S., and M. F. Modest, "High Speed Photographic Studies of Laser Drilling of Ceramics and Ceramic Composites." *Journal of Laser Applications*. 7, (1995) 75-82.

Ready, J. F. "Development of Plume of Material Vaporized by Giant Pulse Laser," *Applied Physics Letters*, 3(1), (1963) 11-13.

Ready, J. F. "Effects Due to Absorption of Laser Radiation," *Journal of Applied Physics*. 36(2). (1965) 462-468.

Risch, T. K., and B. Laub. "General Model for Thermochemical Ablation into a Vacuum." *Journal of Thermophysics and Heat Transfer*, 4(3), (1990) 278-284.

Roy, S., and M. F. Modest, "Three-Dimensional Conduction Effects During Evaporative Scribing with a CW Laser." *Journal of Thermophysics and Heat Transfer*. 4(2), (1990) 199-203.

Roy, S., Bang, S. Y., Modest, M. F., and V. S. Stubican, "Measurement of Spectral Directional Reflectivities of Solids at High Temperatures Between 9 and 11 mm," In *Proceedings of the ASME/JSME Engineering Joint Conference*, 4, (1991) 19-26.

Rykalin, N. N., Uglov, A. A., and I. Y. Smurov, "Nonlinearities of Laser Heating of Metals," *Soviet Physics-Doklady*, 27, (1982) 970-972.

Saifi, M. A., and R. Borutta, "Optimization of Pulsed CO₂ Laser Parameters for Al₂O₃ Scribing," *Ceramic Bulletin*, 54(11), (1975) 986-989.

Sami, M., and B. S. Yilbas, "A Kinetic Theory Approach for Laser Pulse Heating Process," *Optics and Lasers in Engineering*, 24, (1996) 319-337.

Schawlow, A. and R. Townes, "Infrared and Optical Masers," *Physical Review*, vol. 112, 1958, pg. 1940-49.

Schellhorn, M., Nowack, and R., G. Roth, "Optical Diagnostics of Laser-Metal Interaction during Welding," In 3rd International Conference of Lasers in Manufacturing. Paris, France, (1986) 97-105.

Schuocker, D, "Theoretical Model of Reactive Gas Assisted Laser Cutting including Dynamic Effects," In *High Power Lasers and Their Industrial Applications*, 560, SPIE, (1986), 210-219.

Sheng, P. S., and Ko-Wang Liu, "Laser Machining for Secondary Finishing Applications," *Journal of Engineering for Industry*, 117, (1995) 629-636.

Singhal, S. C, "Thermodynamic Analysis of the High-Temperature Stability of Silicon Nitride and Silicon Carbide," *Ceramurgia International*, 2, (1976) 123-130.

Steen, W. M. "Laser Materials Processing," Springer Verlag, 1991.

Sturmer, E., and M. Von Allmen, "Influence of Laser Supported Detonation Waves on Metal Drilling with Pulsed CO₂ lasers," *Journal of Applied Physics*, 49, (1978) 5648-5654.

Todd, J.A., S.M. Copely, "Development of a Prototype Laser Processing System for Shaping Advanced Ceramic Materials", *Journal of Manufacturing Science and Engineering*, Vol. 119, Feb. 1997, 55-67.

Thomassen, F. B., and F. O. Olsen, "Experimental Studies in Nozzle Design for Laser Cutting," In 1st International Conference of Lasers in Manufacturing, Brighton, UK, (1983) 169-180.

Trubelja, M. F., Ramanathan, S., Modest, M. F., and V. S. Stubican, "Carbon Dioxide Laser Cutting of a Carbon-Fiber-Silicon Carbide-Matrix Composite," *Journal of American Ceramic Society*, 77(1), (1994) 89-96.

Trubelja, M. F., Ramanathan, S., Modest, M. F., and V. S. Stubican, "Carbon-Dioxide Laser Cutting on Laser Advanced Materials Processing- Science and Applications." Nagaoka, Japan. (1992) 633-638.

Tuersley, I. P., Hout, A. P., and I. R. Pashby, "Nd-YAG laser machining of SiC Fibre/borosilicate glass composites. Part I. Optimisation of laser pulse parameters", *Composites Part A – applied Science and Manufacturing*, 29: (8), (1998) 947-954.

Tuersley, I. P., Hout, A. P., and I. R. Pashby, "Nd-YAG laser machining of SiC Fibre/borosilicate glass composites. Part II. The effect of process variables", *Composites Part A – applied Science and Manufacturing*, 29A: (8), (1998) 955-964.

Tuersley, I. P., Hoult, A. P., and I. R. Pashby, "The Processing of a Magnesium-Alumino-Silicate Matrix, SiC Fibre Glass-Ceramic Matrix Composite Using a Pulsed Nd-YAG Laser," Chapman and Hall, (1996) 4111-4119.

Uglov, A. A., and A. N. Kokora, "Thermophysical and Hydrodynamic Effects in Laser Beam Processes of Materials (Review)," Soviet Journal of Quantum Electronics, 7, (1977) 671-678.

Uglov, A. A., Smurov, I. Y., and A. A. Volkov, "Calculation of Heating of Metals by Continuous Laser Radiation in an Oxidizing Atmosphere," Soviet Journal of Quantum Electronics, 13, (1983) 154-156.

Umehara, N, R. Komanduri, "Magnetic Fluid Grinding of HIP-Si₃N₄ Rollers", Wear, V. 192 N1-2, Mar. 1996, 85-93.

von Allmen, M., Blaser, P., Affolter, and K., E. Sturmer, "Absorption Phenomena in Metal Drilling with Nd-YAG lasers," IEEE Journal of Quantum Electronics, QE-14, (1978) 85-88.

Von Allmen, M." Drilling Velocity in Metals," Journal of Applied Physics, 47, (1976) 5460-5463.

Von Allmen, M., "Laser-Beam Interactions with Materials," Springer Series in Materials Science, 2, Springer Verlag, Berlin, (1987).

Wallace, R. J., Bass, M., and S. M. Copley, "Curvature of Laser Machined Grooves in Si₃N₄," Journal of Applied Physics, 59, (1986) 3555-3560.

Wallace, R. J., "A Study of the Shaping of Hot Pressed Silicon Nitride With a High Power CO₂ laser," PhD Thesis, University of Southern California, Los Angeles, CA.(1983).

Watanabe, T., Yoshida, and Y., T. Arai, "Reflectivity and Meltability of Aluminum Alloys with YAG laser beams," In International Conference on Laser Advanced Materials Processing-Science and Applications, Japan, (1992) 505-510.

Wei, P. S., and J. Y. Ho, "Energy Considerations in High-Energy Beam Drilling," International Journal of Heat and Mass Transfer, 33(10), (1990) 2207-2216.

Whitehouse, David R., Introduction to Laser Technology and Material Processing," *The Fabricator*, June 1992.

Yagi, Shigenori, K. Kuba, N. Junichi, T. Yamamoto, "Solid laser device", U.S. Patent No. 5125001, June 23, 1992.

Yakovlev, E. B, "Changes in the Properties of Glass Heated by a Laser." J. Opt. Technology, 63(2), (1996) 105-108.

Yamamoto, J., and Y. Yamamoto, "Laser Machining of Silicon Nitride," In International Conference on Laser Advanced Materials Processing- Science and Applications," High Temperature Society of Japan, Japan Laser Processing Society, Osaka, Japan, (1987) 297-302.

Yilbas, B. S., and A. Z. Al-Garni, "Some Aspects of Laser Heating of Engineering Materials." Journal of Laser Applications, 8, (1996) 197-204.

Yilbas, B. S., "Laser Heating Process and Experimental Validation," Int. J. Heat Mass Transfer, 40(5), (1997) 1131-1143.

Yilbas, B. S., "Parametric Study to Improve Laser Hole Drilling Process", *Journal of materials Processing Technology*, 70: (1-3), Oct. 1997, 264-273.

Yue, T. M., Jiang, C. Y., Xu, J. H., and W. S. Lau, "Laser Fantasy: From Machining to Welding," *Journal of Materials Processing Technology*, 57, (1996) 316-319.

Zhang, Z., M.F. Modest, "Temperature-Dependent Absorptances of Ceramics for Nd:YAG and CO₂ Laser Processing Applications", *Journal of Heat Transfer*, Vol. 120, May 1998, 322-327.

Zhang, Z., M.F. Modest, "Energy requirements for ablation or decomposition of ceramics during CO₂ and Nd:YAG laser machining", *Journal of Laser Applications*, 10: (5), Oct. 1998, 212-218.

APPENDIX A

LASER SAFETY

1. Introduction

Laser poses an unfamiliar but potentially hazardous situation in the form of a coherent high-energy optical beam, which may not be in the visual spectrum and hence cannot be seen by the eye. Use of controls, adjustments, or use of operating procedures other than those specified in the instructional manuals or without adequate training may result in hazardous radiation exposure. Fortunately, to date, the accident record with lasers industry-wide has been remarkably good due to stringent enforcement of safety rules. But there have been some accidents. The risk can be reduced if the danger is perceived. The main dangers from a laser beam are:

1. Damage to the eye,
2. Damage to the skin,
3. Electrical hazards, and
4. Hazards from the fume.

These will be considered in the following, which are based heavily on Reference 1 as well as References 2 and 3 that deal exclusively with laser safety.

In the U.S., the safety considerations involving the use of lasers are mainly guided by the American National Standard Institute [ANSI z 136.1 (1986)]. It provides standards (rules

and regulations) concerning the application of laser, such as engineering controls, recommendations regarding protective equipment for the personnel involved in the use of lasers, administrative and procedural controls and special controls. Class 4 lasers, which are generally the type used in material processing systems, should also have a laser safety officer (LSO) who should see that these guidelines are observed. Safety limits were set for each of the above category. Much of the material in this Appendix is a standard material taken directly from the Standards [1,2]. In the following the following issues will be briefly covered: safety limits, namely, damage to the eye and the skin, laser classification, typical Class 4 laser safety arrangements, potential risks in a properly set up facility, and electrical and fume hazards.

2. Safety Limits

1. Damage to the Eye

The ocular fluid has its own spectral transmissivity as shown in Table A1. It indicates that there are two types of problems with radiation falling on the eye. There is potential damage to the retina at the back of the eye and potential damage to the cornea at the front of the eye. The radiation that falls on the retina will be focussed by the eye's lens to give an amplification of the power density by a factor of around 10^5 . This means that lasers with wavelengths in the visible or near visible wave band (Ar, He/Ne, ND-YAG, Nd-glass) are far more dangerous than those outside that band (CO₂ Excimer). The nature of the threat from different lasers is listed in Table A1.

Safe exposure limits were established by experiment and they are listed as the Maximum Permissible Exposure levels (MPE levels). These levels are indicated in Tables

A2 and A3 for retinal and corneal damage. At power density and times greater than these safe limits damage may occur due to boiling or at higher levels to explosive evaporation. The boiling limit is the reason for the very low levels of power that the eye can tolerate. For example a 1 mW He/Ne laser with a 3 mm diameter beam would have a power density in the beam of $(0.001 \times 4) / (3.14 \times 0.3 \times 0.3) = 0.014 \text{ W/cm}^2$. On the retina, this would be $0.014 \times 10^5 \text{ W.cm}^2$. A blink reflex at this level would only allow a 0.25s exposure, which is the MPE level for a Class 2 laser.

Table A 1 Basic Biological Hazards with Lasers

Laser Type	Wavelength μm	Biological Effects	Skin	Cornea	Lens	Retina
CO2 laser	10.6	Thermal	X	X		
Nd-YAG laser	1.06	Thermal	X			X
Excimer laser	0.351	Photo-chemical	X	X	X	

Notice that the calculation assumes that all the radiation can enter the pupil of the eye. Thus it is common practice to ensure that working areas around lasers are painted with light colors and are brightly illuminated.

The hazard zone around a laser is that in which radiant intensities exceed the MPE levels. These zones are known as the Nominal Hazard Zone (1). The size of the zone can be calculated based upon the beam expansion from the cavity, or lens, or fiber, or from diffuse or specular reflection from a workpiece. For example, considers 2 kW CO₂ laser beam with a 1 mrad divergence. The MPE level for safe direct continuous viewing

of the beam (not that much would be seen with IR radiation!) is when the level falls to 0.01 W/cm^2 . This would occur when the beam has expanded to 504 cm diameter - a distance of 5020 m away, around 3 miles! This means that precautions must be taken to avoid the beam escaping from the area of the laser by installing proper beam stops, screens for exits and enclosed beam paths. Similar calculations for a 500 W CO_2 laser give a Nominal, Hazard Zone for diffuse reflections of 0.4 m. Therefore it is necessary to wear goggles when near a working laser. As a rule, never look at a laser beam directly for it is like looking into a loaded gun barrel ready to be fired anytime.

Laser goggles which block 1,064nm laser radiation must be worn when operating a Class III or IV Nd:YAG laser. Instant and permanent damage can occur when the naked eye is exposed to laser radiation. Insure that personnel are not exposed, either physically or visually, to direct or scattered laser radiation.

2. Damage to the Skin

There are also MPE levels for skin damage. These are far less severe than for the eye and so are essentially irrelevant. The laser is capable of penetrating the body at speeds as fast as that for steel and so the focussed beam needs to be seriously respected. The damage done to the skin is usually blistering or cutting but the wound is clean and will heal - unlike some eye damage. Incidentally a vein or artery cut by laser will bleed even though it is cauterized! As a general rule never let any part of your body come in the path of a laser beam. If an adjustment has to be made to the beam path do it by holding the edges of mirrors etc.

3. Laser Classification

Lasers are classified according to their relative hazard. Most lasers of interest to material processing are classified as Class 4 except for some which are totally built into a machine in which there is no human access possible without the machine being switched off.

Table A2 is a summary of the classification:

Table A 2 Classification of Lasers

Class	Definition
1	Intrinsically safe <0.2 μ J in 1 ns pulse or <0.7 mJ in a 1s pulse
2	Eye protection achieved by blink reflex (0.25 sec) <1 mW CW laser
3A	Protection by blink and beam size <5mW with 25W/m ² (e. g. an 16 mm beam diameter from a 5 mW laser)
3B	Possible to view diffuse reflection <2.4 mJ for 1 ns pulse or <0.5 W CW visible
4	All lasers of higher power Unsafe to view directly, or by diffuse reflection May cause fire Standard safety precautions must be observed

4. Class 4 Laser Safety Precautions

The following safety precautions are recommended:

All beam paths must be terminated with material capable of withstanding the beam for several minutes.

- * Stray specular reflections must be contained.
- * All personnel in Nominal Hazard Zone must wear safety goggles.
- * For CO₂ radiation they can be made of glass or perspex, in fact normal spectacles may do, if the lenses are large enough.
- * Personnel not involved in the use of the laser must have approval for entry.
- * There should be warning lights and hazard notices so that it is difficult (impossible) to enter the area without realizing that it is being entered.
- * Extra care should be taken when aligning the beam.
- * There should be a Laser Safety Officer to check that these guidelines are followed.

These guidelines are summarized in Figure A4 of a typical laser material processing arrangement.

5. Potential Risks Even in a Properly Set Up Facility

If the facility is properly designed then the beam is enclosed and its path terminates such that it can not escape to cause damage. A standard set up would have the beam focussed and pointing downward. As the beam expands after the lens, the NHZ is considerably reduced. Such a system is generally safe except in certain unlikely events that can be classified in a risk analysis tree. This would include breaking of the lens and total removal with loss of the nozzle, failure of a mirror mount and the mirror swinging free etc. The essence of such an analysis is to devise a system for rapidly identifying an

errant beam. This can be achieved by monitoring the beam and/or the enclosure. If the beam is monitored as leaving the laser but not arriving at the expected target then the system should immediately be shut down. If a hot spot appears within the enclosure then again the system should be shut down.

6. Electrical Hazards

Nearly all the serious or fatal accidents with lasers have been associated with the electrical supply. A typical Co₂ laser may have a power supply capable of firing the tubes with a voltage of 30 kV and a current of 400 mA. This is a dangerous power supply and when working on it the standard procedures for electric supplies should be followed. The smoothing circuits contain large capacitors and so even when the power is switched off a fatal charge is still available and proper precautions to earth the system before working on it are essential. Panic buttons must be available at the laser and at the main exit. Access to the high tension circuit should be protected by interlocks. As a rule do not enter the high voltage supplies without first carefully earthing the system.

7. Fume Hazards

The very high temperatures associated with laser volatilize most materials and thus form a fine fume, some of which can be poisonous. With organic materials, in particular, the plasma acts as a sort of dice shaker and a variety of radical groups may reform into new chemicals. Some of these chemicals are highly dangerous, such as the cyanides and some are potential carcinogens. It is necessary, as a general rule, to have an adequately ventilated area around the laser processing position as for standard welding. Some of the

problems with cutting nonmetallic materials have been identified by Ball et al [2]. These are shown in Table A3, but it should be realized that these volumes are not significant and represent a hazard only if much work is carried out over an extended period.

Table A 3 Volume of Gases Released During Laser Machining of Some Plastics

Decomposition Products	Polyester	Leather	PVC	Kevlar	Kevlar/Epox
Acetylene	0.3-0.9	4.0	0.1-0.2	0.5	1.0
Carbon monoxide	1.4-4.8	6.7	0.5-0.6	3.7	5.0
Hydrogen chloride			9.7-10.9		
Hydrogen cyanide				1.0	1.3
Benzene	3.0-7.2	2.2	1.0-1.5	4.8	1.8
Nitric dioxide				0.6	0.5
Phenyl acetylene	0.2-0.4			0.1	
Styrene	0.1-1.1	0.3	0.05	0.3	
Toluene	0.3-0.9	0.1	0.06	0.2	0.2

As a rule, the laser processing zone should be adequately ventilated.

8. Conclusions

The laser is as risky as any other high energy beam except that it often is invisible. Hence, it should be properly handled. It is the responsibility of the operator to learn how to handle it correctly and that of the institution that owns the laser to provide proper safety procedures and to ensure that proper training of the personnel involved is given.

References

1. Steen, W. M., "Laser Material Processing," Springer-Verlag, London, U.K. (1991)
2. Rockwell, R.J. "Fundamentals of Industrial Laser Safety" Industrial Laser Annual Handbook, published by Penwell Books, Tulsa, OK, (1990) pp 131-148.
3. Ball et al., "Industrial Laser Annual Handbook," published by the Penwell Books, Tulsa, OK, (1989) p 23

APPENDIX B

Raw Data

The following is raw data for the measurements taken for each material tested

Table 11 Dimensional data for WC-Co6%

Pulse width (ms)	Run 1		Run 2		Run 3		Run 4		Energy, J
	Dia. μm	Depth μm	Dia. μm	Depth μm	Dia. μm	Depth μm	Dia. μm	Depth μm	
0.65	420	93	328	560	236	433	291	628	1.00
	644	299	419	563	431	900	485	883	4.33
	713	353	460	773	672	1420	649	1047	9.00
	750	271	645	843	905	1778	860	1522	15.33
1.50	470	102	368	178	394	1207	445	178	2.67
	660	1969	610	1791	622	2019	673	1334	10.67
	838	2096	622	1829	749	1892	775	2235	19.33
	991	2477	864	1638	978	2451	876	2629	31.33
4.00	520	876	520	1956	305	660	292	699	6.37
	750	3505	730	3477	483	991	546	965	22.33
	914	3823	1028	4013	622	1181	673	1219	40.00
	1016	4343	1041	3200	953	1715	940	1740	64.00

Table 12 Dimensional data for WC-Co 6% + TiN coating

Pulse width (ms)	Run 1		Run 2		Run 3		Run 4		Energy, J
	Dia. μm	Depth μm	Dia. μm	Depth μm	Dia. μm	Depth μm	Dia. μm	Depth μm	
0.65	304.8	609.6	228.6	635					0.93
	381	1003.3	342.9	1092.2					4.43
	431.8	1092.2	508	1104.9					8.90
	508	939.8	673.1	1066.8					14.87
1.50	304.8	812.8	317.5	1016					2.23
	457.2	2336.8	469.9	1714.5					10.33
	571.5	1485.9	584.2	1435.1					19.50
	660.4	1054.1	723.9	1346.2					32.03
4.00	419.1	863.6	406.4	965.2					5.97
	609.6	1676.4	622.3	1752.6					22.47
	736.6	1701.8	800.1	1841.5					41.63
	939.8	1574.8	1054.1	1803.4					66.43

Table 13 Dimensional data for alumina

Pulse width (ms)	Run 1		Run 2		Run 3		Run 4		Energy, J
	Dia. μm	Depth μm	Dia. μm	Depth μm	Dia. μm	Depth μm	Dia. μm	Depth μm	
0.65	559	559	483	813	500	500			0.77
	711	1346	813	2515	700	1500			4.23
	965	1562	800	3810	750	2200			8.43
	1600	4000	1000	4100	1200	4100			14.47
1.50	445	406	600	800	711	838			1.93
	681	1422	900	2400	787	2515			10.20
	900	2134	1000	3700	800	3785			19.80
	1715	3810	1000	5100	889	5512			32.10
4.00	800	3391	650	3700	648	1778			5.87
	991	5398	800	6100	953	2553			22.67
	1321	2896	1000	3200	1372	4483			40.83
	1448	3277	1400	3950	1524	6960			62.93

Table 14 Dimensional data for alumina + TiC

Pulse width (ms)	Run 1		Run 2		Run 3		Run 4		Energy, J
	Dia. μm	Depth μm	Dia. μm	Depth μm	Dia. μm	Depth μm	Dia. μm	Depth μm	
0.65	381	114	305	241					1.00
	483	356	521	457					4.87
	610	610	572	508					9.50
	838	724	597	737					15.67
1.50	470	203	394	279					2.27
	508	1067	521	940					10.97
	639	1562	813	1270					20.97
	900	1898	889	1524					34.37
4.00	508	1219	483	927					5.97
	900	1867	660	1156					24.00
	1000	2324	660	1410					44.43
	1400	2527	762	1753					71.63

Table 15 Dimensional data for SiC whisker reinforced, zirconia toughened alumina

	Run 1		Run 2		Run 3		Run 4		
Pulse width (ms)	Dia. μm	Depth μm	Dia. μm	Depth μm	Dia. μm	Depth μm	Dia. μm	Depth μm	Energy, J
0.65	508	508	457	559					1.00
	800	1200	610	1054					4.87
	850	1425	686	1346					9.50
	1200	1650	787	1321					15.67
1.50	550	750	432	876					2.27
	875	1800	584	1080					10.97
	950	1700	724	2083					20.97
	1100	1700	914	2210					34.37
4.00	650	1150	572	1105					5.97
	950	1750	965	1613					24.00
	1200	2800	1016	2680					44.43
	1650	3734	1257	3556					71.63

Table 16 Dimensional data for silicon nitride

Pulse width (ms)	Run 1		Run 2		Run 3		Run 4		Energy, J
	Dia. μm	Depth μm	Dia. μm	Depth μm	Dia. μm	Depth μm	Dia. μm	Depth μm	
0.65	203	965	178	737					1.00
	330	927	470	1346					4.33
	521	2743	495	1981					9.00
	572	3467	546	1562					15.33
1.50	279	1524	330	1397					2.67
	470	2299	470	2337					10.67
	521	2426	584	2489					19.33
	648	2502	699	2477					31.33
4.00	356	1778	368	1753					6.37
	597	2553	584	2515					22.33
	673	2731	711	2667					40.00
	838	3175	927	3162					64.00

Table 17 Dimensional data for SiAlON

Pulse width (ms)	Run 1		Run 2		Run 3		Run 4		Energy, J
	Dia. μm	Depth μm	Dia. μm	Depth μm	Dia. μm	Depth μm	Dia. μm	Depth μm	
0.65	490	1700	406	1715					1.00
	620	3100	521	3099					4.87
	700	3500	648	3366					9.50
	800	3750	737	3810					15.67
1.50	500	2750	457	2769					2.27
	800	3100	660	3289					10.97
	800	3700	724	4001					20.97
	950	3900	889	4013					34.37
4.00	700	2850	483	2565					5.97
	800	3000	622	2680					24.00
	1000	3900	787	3480					44.43
	1200	4350	902	3810					71.63

Table 18 Dimensional data for TiC/ TiN cermet

Pulse width (ms)	Run 1		Run 2		Run 3		Run 4		Energy, J
	Dia. μm	Depth μm	Dia. μm	Depth μm	Dia. μm	Depth μm	Dia. μm	Depth μm	
0.65	381	610	330	457					1.67
	635	800	635	673					4.67
	737	1041	635	826					9.33
	889	1181	635	940					14.67
1.50	254	51	254	1118					2.67
	521	1245	419	1207					9.33
	584	1397	610	1384					19.00
	686	1397	800	1295					31.33
4.00	203	1702	432	1715					6.33
	495	2045	572	2070					22.33
	787	2413	762	2362					40.67
	940	2210	1003	2350					62.33

Table 19 Dimensional data for polycrystalline cubic boron nitride

Pulse width (ms)	Run 1		Run 2		Run 3		Run 4		Energy, J
	Dia. μm	Depth μm	Dia. μm	Depth μm	Dia. μm	Depth μm	Dia. μm	Depth μm	
0.65	318	254	178	279					0.93
	419	584	254	635					4.43
	495	724	368	775					8.90
	572	775	432	851					14.87
1.50	318	419	216	406					2.23
	508	800	406	889					10.33
	635	1054	533	1143					19.50
	711	1143	635	1245					32.03
4.00	432	660	368	673					5.97
	597	1003	572	1168					22.47
	737	1245	749	1346					41.63
	914	1372	889	1549					66.43

VITA

Johnnie Lee Hixson

Candidate for the Degree of

Master of Science

Thesis: INSTALLATION OF A ND:YAG LASER FACILITY AND INITIAL SINGLE PULSE LASER DRILLING OF SOME ADVANCED MATERIALS

Major Field: Mechanical Engineering

Biographical:

Education: Graduated from Geronimo High School, Geronimo, Oklahoma in May 1985; received Bachelor of Science degree in Mechanical Engineering from Oklahoma State University, Stillwater, Oklahoma in May 1992. Completed the Requirements for the Master of Science in Mechanical Engineering degree at Oklahoma State University in December, 1998.

Professional Memberships: American Society of Mechanical Engineers (ASME)